2023

Journal of JART

—English edition—

2023

The Japan Association of Radiological Technologists

Journal of
JART
—English edition—
2023
The Japan Association of
Radiological Technologists

CONTENTS

Note: The contents of this magazine are those that have been published in JART magazine.

Overview of the Japan Association of Radiological Technologists

The Japan Association of Radiological Technologists, a public interest incorporated association under the jurisdiction of the Ministry of Health, Labour and Welfare, was established in 1947 with the purpose of contributing to the health of citizens through raising the professional ethics of members, improving and furthering the study of medical radiology and medical radiological technology, and enhancing public health.

In light of the startling progress being made in the fields of image diagnostics and radiation therapy where radiological technologists work, it is necessary to stay constantly aware of the latest know-how and technology. JART collaborates with other certification agencies to enhance the capacity of all radiological technologists in general through providing lifelong learning seminars, short courses, academic conferences and numerous other learning opportunities. We believe that such activities constitute our obligation as medical professionals to the general public.

As the only medical profession that has “radiological” in its name, we strive to limit medical exposure, to raise the standing of our profession, and to realize a profession of specialist technologists that can be advertised. And we are committed to promoting services with you all for the provision of safe and secure medical care.

general principles

We will render our services to those in need of health care.

We will act as individual members of a health care team.

We will perform our duties in our field of specialty.

We will continue to study for the benefit of mankind.

We will respect and practice the policy of informed consent.

Regarding Publication of the English Edition

UEDA Katsuhiko (President)

The journal of the JART English version issues every year. It has a favorable reception for we members of the world and general people. As well as this issue, 8 articles to be useful for radiological technologists are issued.

We will feature clinical, educational, and research-based achievements by radiological technologists in the monthly issues of the JART journal, and continually work to improve the magazine. I truly hope that this English edition will benefit radiological technicians worldwide.

To give our radiological technologists from across the globe an insight into our business, I will briefly explain the history of the JART. In March 1896, we succeeded in taking the first X-ray image in Japan. In 1897, Shimadzu Corporation released an X-ray generator for educational use. In 1925, there were approximately 1,500 X-ray technicians. In 1927, the first Shimadzu X-ray Technician Training Institute was established, and evidence-based education was put in place. The JART was founded in 1947 to make “radiological technologist” a national qualification. Since its establishment, we have worked towards broad acceptance of this national qualification, in collaboration with the government, the Diet, the Japanese Medical Association, and occupational military authorities.

As a result in June 1951, we were finally able to see the promulgation of the Radiology X-ray Technicians Act, Act No.226 of 1951. Since then, we have responded to the changing needs of the society, revising the original act to get the Radiology X-ray Technicians Act of 1968 passed, and partially revising that to get the Radiology Technicians Act and Radiology X-ray Technicians Act of 1983 passed, and finally getting the Radiology Technicians Act, which is in place currently, passed. Back then, the scope of work was limited to general X-ray testing, television X-ray testing, angiography, X-ray computed tomography scanning, RI scanning, and radiation therapy. In 1993, the Radiology Technicians Act was further revised, and MRI scanning, ultrasonic testing, and non-mydriatic fundus camera examination were added to the list. In 2010, image interpretation assistance, radiation examination explanation, and consultation work were added. In April 2015, intravenous contrast agent injection using automated contrast injectors, needle removal and hemostasis, lower digestive tract examination (anal catheter insertion and administration of contrast medium), anal catheter insertion, and oxygen inhalation during radiation therapy were added as operations that could be performed by radiological technologists.

In October 2021, the needle insertion for examinations of contrasting of the examination for CT, MRI, Ultrasound and Radioisotope are added as the new operation that can be performed by radiological technologists.

The JART will continue to respond to the needs of the medical industry, and we hope to broaden the operational scope of radiological technologists based on our foundation in scientific evidence.

History of The Japan Association of Radiological Technologists (JART)

1947
- Establishment of JART (July 13)

1951
- Promulgation of the Act on Medical Radiographers (June 11)
- Authorization for Establishment of the Japan Association of Radiographers (June 13)

1954
- First national examination for Medical Radiographers (May 30)

1956
- Event to commemorate the 10th anniversary of founding, attended by Her Imperial Highness Princess Chichibunomiya

1962
- Event to commemorate the 15th anniversary of founding and 10th anniversary of enactment of the Act on Medical Radiographers, attended by Her Imperial Highness Princess Chichibunomiya

1968
- Promulgation of the Act to Partially Revise the Act on Medical Radiographers (establishment of two professions) (May 23)
- First national examination for radiological technologists

1969
- Renaming as the JART
- Staging of the 4th International Society of Radiographers & Radiological Technologist (ISRRT) World Congress at Tokyo Palace Hotel, attended by Her Imperial Highness Princess Chichibunomiya

1975
- Event to commemorate the 80th anniversary of the discovery of X-rays, attended by Her Imperial Highness Princess Chichibunomiya

1979
- Completion of the Education Center for JART

1983
- Partial revision of the Act on Medical Radiographers and the Act on Radiological Technologists (unification of the professions)

1985
- Event to commemorate the 90th anniversary of the discovery of X-rays, attended by Her Imperial Highness Princess Chichibunomiya
- Staging of the 1st Japan Conference of Radiological Technologists

1987
- General assembly resolution for establishment of the New Education Center and a four-year university

1989
- Completion of the New Education Center (Suzuka City)

1991
- Opening of Suzuka University of Medical Science

1993
- The Act to Partially Revise the Act on Radiological Technologists, and Ministerial Ordinance to Partially Revise the Enforcement Orders (April 28)

1994
- Appointment of the President of JART as the 11th President of ISRRT

1995
- Event to commemorate the 100th anniversary of the discovery of X-ray, attended by Her Imperial Highness Prince Akishinomiya

1996
- Start of the Medical Imaging and Radiologic Systems Manager certification system

1998
- Staging of the 11th ISRRT World Congress at Makuhari

1999
- Start of the Radiation Safety Manager certification system

2000

- "Presentation of the Medical Exposure Guidelines (Reduction Targets)" for patients

2001

- Start of the Radiological Technologists Liability Insurance System

2003

- Enactment of X-Ray Week

2004

- Relocation of offices to the World Trade Center Building in Tokyo

2005

- Start of the Medical Imaging Information Administrator certification system

2006

- Staging of a joint academic conference between Japan, South Korea, and Taiwan
- Revision of the Medical Exposure Guidelines

2008

- Establishment of the committee on Autopsy imaging (Ai)

2009

- Revision to the national examination for radiological technologists
- Launch of the Team Medicine Promotion Conference, with the President of JART as its representative
- Appointment of the President of JART as chairperson of the Central Social Insurance Medical Council specialist committee

2010

- Health Policy Bureau Director's notification concerning promotion of team medicine

2011

- Support activities following the Great East Japan Earthquake
- Staging of an extraordinary general meeting concerning transition to a public interest incorporated association

2012

- Registration of transition to a public interest incorporated association (April 1)
- Event to mark the 65th anniversary of founding and transition to a public interest incorporated association (June 2)
- Renaming as public interest incorporated association JART
- Launch of the Radiological Technologists Liability Insurance System with participation by all members

2013

- Signing of the Comprehensive Mutual Cooperation Agreement on Prevention of Radiation Exposure (September 21)

2014

- Consignment of work to measure personal exposure of residents
- Revision of the Act on Radiological Technologists, Government Ordinance to Partially Revise the Enforcement Orders, and Revision of the Enforcement Regulations (June 25)
- Launch of the radiation exposure advisor certification system

2015

- Event to commemorate the 120th anniversary of the discovery of X-rays

2017

- Event to mark the 70th anniversary of founding (June 2)

2018

- Notice from the Regional Medical Care Planning Division Director, Health Policy Bureau, Ministry of Health, Labour and Welfare, and Director of the Economic Affairs Division regarding Operational Considerations for Securing a System for Safety Management pertaining to Medical Equipment

2019

- Notice from the Health Policy Bureau on a Safety Management System for Medicinal Use of Radiation

2020

- Partial revision of the Ordinance on Prevention of Ionizing Radiation Hazards

2021

- Relocation of offices to the Mita Kokusai Building in Tokyo
- Partial revision of the designation regulation for radiological technologist training school
- Holding the 23th AACRT with 37th JCRT in Tokyo

2022

- Event to mark the 75th anniversary of founding (July 16)

Received April 7, 2021; accepted June 30, 2021

Supraspinatus Outlet View Accuracy comparison between the conventional method rotated 100 degrees in X-ray photography and the Horio method using the central X-rays

TAKAI Natsuki[1)], SUZUKI Yoshiaki[2)], KATO Kyoichi[3)]

1) Medical examination center, Mitsubishi-kobe hospital
2) Department of Radiology, Shimoda medical center
3) Showa University Graduate School of Health Sciences

Note: This paper is secondary publication, the first paper was published in the JART, vol. 69 no. 831: 32-39, 2022.

Key words: Supraspinatus Outlet View, Y-View, Scapula, Reference line, Radiography

【Abstract】
This study examined which, between the conventional method of rotating the scapula 100 degrees and Horio's method of using the central X-ray connecting the root of spine of scapula (the scapular spine triangle) and the center of the glenoid cavity, satisfied the visualization conditions of the Supraspinatus Outlet View.

The conventional method and the Horio method were reproduced by 3D-CT of 40 cases of scapula, and the tangentiality of the scapula body in the left-right rotation direction was compared. For the upward and downward rotation directions, the parallelism with the central X-ray indicated by Horio was evaluated using the base of the supraspinatus fossa as an index.

As a result, the tangentiality of the scapular body in the left-right rotation direction was 9.39 mm ± 3.81 mm in the conventional method and 2.22 mm ± 2.34 mm in the Horio method, which was significantly higher with the Horio method.

When the Horio method was used, the parallelism in the upward and downward rotation directions was − 0.15° ± 1.55°.

It was proved that the Horio method satisfies the drawing condition of Supraspinatus Outlet View, in comparison with the conventional method.

1. Introduction

In the Y-view on X-ray imaging, the center of the glenoid cavity of the scapula and humeral head overlap, with the sides formed by the acromion, scapular spine, and supraspinatus; the superior angle and coracoid process; and the body of the scapula forming a Y-shape [1)]. The Y-view is used to observe changes to the bony elements of the shoulder joint and their relative positions, as well as the subacromial joint, and separates the scapula from the ribs.

There are two ways to take images in the Y-view: the trans-scapular lateral view [2, 3)] and the supraspinatus outlet view [3–7)]. The majority of Japanese documents on X-ray imaging techniques describe the supraspinatus outlet view (hereinafter, Y-view). In this method, the subacromial joint space can be visualized by obliquely shooting the X-ray craniocaudally, which effectively captures osteophyte formation under the acromion, shape of the undersurface of the acromion, and calcification of the rotator cuff stop (Acromio-Humeral interval: AHI) [5, 8, 9)]. In addition, X-ray in the Y-view is effective for its main purpose, which is the observation of the shoulder joint; e.g., dislocation of the humeral heads and acromioclavicular joint, fracture of the clavicle, scapula, and humerus, osteophyte under the acromion, tumor of the scapula and humeral neck, and snapping scapula syndrome [5, 8, 9, 10)].

An X-ray in the Y-view is taken correctly under the following conditions: overlap of a) the

lateral border of the body of the scapula, which is the axillary fossa side, and b) the medial border of the body of the scapula, which is the spinal [10]. The tangential imaging of the anterior surface of the scapula [6] also reveals that the body of the scapula is separated from the ribs [2, 3, 10–12]. Furthermore, a wide view of the subacromial joint formed by the acromion and humeral head [13] and X-rays taken at an angle tangential to the supraspinatus must be obtained [11], i.e., the subacromial region must be observed tangentially. Images that do not fulfill these conditions will not allow visualization of the components of the shoulder joint in the Y-shape. In other words, the relationship between the scapula and humeral head will be distorted, hindering the diagnosis of fractures, dislocations, and ligament injuries, which is detrimental to ensuring reproducibility during follow-up.

Specifically, the method involves the straight segment of the posterior border of the scapular spine (which can be palpated from the body surface) being rotated horizontally 100° to the image-receiving area [12, 14-16]. This method (henceforth, the conventional method) is extensively documented. However, different documents describe the angle of incidence of the X-rays in the upward direction as 0°, 10°, 15°, and 20° with the angle being applicable to all patients [1, 3, 14, 16]. Additionally, X-rays taken in the Y-view in clinical practice have required many reexaminations due to differences between patient position and scapular anatomy, which result in distortions of the scapular Y-view in lateral, upper, or lower rotations. In particular, for patients with rounded backs, the Y-view of the X-rays is taken in the recumbent position, which requires further adjustments to achieve appropriate visualization of the scapula.

It is necessary to use not only a single indicator, as in the conventional method, but also to identify the central X-ray that connects the point of incidence and point of exit of the X-ray for the body of the scapula. However, to the best of our knowledge, Horio's (1971) study is the only one that described the central X-ray in the Y-view as the scapular spine triangle and glenoid cavity [17], and this expression has not been used in any of Horio's subsequent studies. In addition, no studies have examined the validity of the two points presented by Horio for the Y-view. It is necessary to reexamine the body surface index because stable imaging cannot be achieved with the body surface index in Y-view as described in the current literature, and the incidence angle varies between references. In this case, it is important to use the central X-ray of the patient's scapula as a reference in Y-view. This and other imaging methods result in changes in the patient's position according to their posture and shoulder movement.

Here we report our experience using three-dimensional (3D) computed tomography (CT) in the conventional method and an alternative method that uses the scapular spine triangle and glenoid cavity that form the central X-rays (hereinafter, the Horio method) to determine which method meets the conditions of visualization in Y-view more effectively.

2. Methods

2-1. Ethical considerations

The data from this retrospective study was anonymized. The ethics committee of our institution approved this study.

2-2. Devices and subjects

A 64-row CT scanner (Optima CT660 Pro 15HW25.2, GE Healthcare Japan Co., Ltd.) and workstation (SYNAPSE VINCENT Ver.5.4, Fujifilm Medical Co., Ltd.) were used for constructing 3D images. The CT was acquired with a rotation time of 0.5 s, 64 × 0.625 mm optical sight, 5.0 mm section thickness, 0.984 mm beam pitch, 78.75 mm/s table feed speed, 500 mm scan range, 120 kV tube voltage, 100–500 mA tube current. The images were reconstructed at 350

mm image reconstruction and 500 mm reconstruction field of view. Chest CT obtained 40 scapular images of 22 patients from May 2018 to October 2019 for a diagnostic purpose different from this study, in which the entire scapula (21 right, 19 left; 13 males, 9 females; ages 33–88 years; mean age 61.3 ± 16.0 years) were analyzed.

2-3. Method of determining central X-ray as a reference point concerning the scapula

Fig.1 depicts the point of the scapular spine triangle, which is the point of incidence of the X-ray with respect to the scapula in Y-view imaging, and the X-ray exit point, i.e., the glenoid cavity. Fig.1-a represents the 3D scapular image of the point of incidence in Y-view, i.e., the root of the spine of the scapula (scapula spine triangle), which is defined as the point of intersection (●) between the line that extends from the superior border of the scapular spine to the medial border of the scapula (solid line) and the line originating at the inferior angle extending to the base of the supraspinatus (broken line) [8]. As shown in Fig.1-b, the glenoid cavity's point of exit corresponds to the point (×) where 1) the longitudinal axis (broken line) connecting the uppermost and lowest points of the glenoid cavity (supraglenoid and infraglenoid tubercle), and 2) the line connecting the most anterior and posterior borders of the glenoid cavity (solid line) cross perpendicularly (hereinafter, center of the glenoid cavity) on the view that allows its frontal observation [17]. Next, as shown in Fig.1-c, the line connecting these two reference points, i.e., the root of the spine of the scapula (scapula spine triangle) and center of the glenoid cavity, is defined as the Y-view central axis.

2-4. Evaluation of left–right rotation on Y-view

The left–right rotation direction of the scapula is indicated by the overlap between the lateral and medial borders of the body of the scapula, which is required for an effective Y-view [10] indicates. As depicted in Fig.2, reference points for evaluation were placed on the medial and lateral borders to find if the conditions are met for an effective Y-view., the tangentiality of the lateral and medial lines in the Y-view in the conventional method and the Horio method, which relies on the scapular spine triangle and the glenoid cavity, were assessed. The percentage of overlap between the

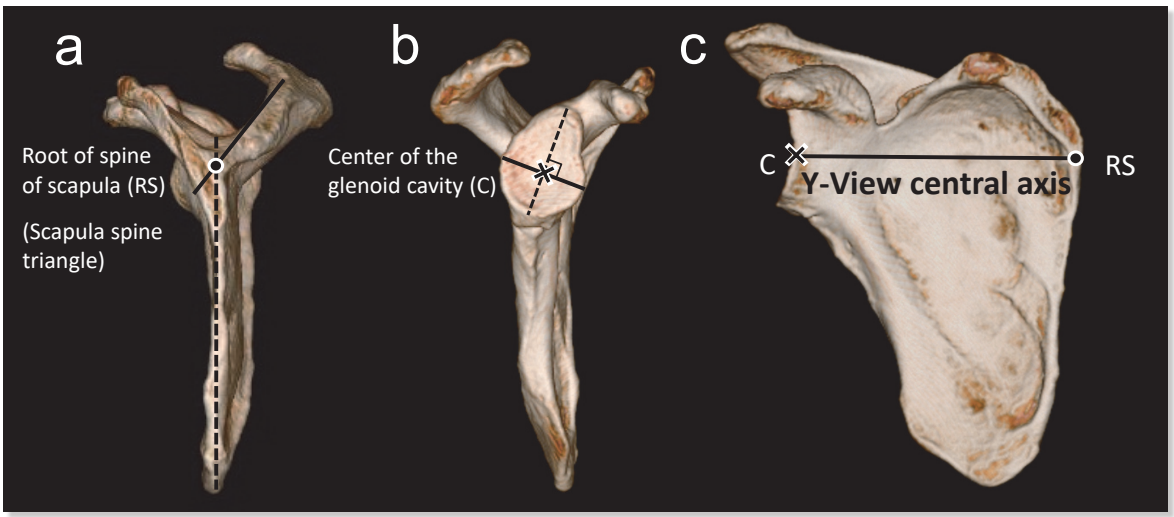

Fig.1 Position of point of incidence of the X-ray (root point of the spine of the scapula) and the point of injection (center of the glenoid cavity) and The Y-View central axis

a. The root point of the spine of the scapula (The scapular spine triangle) (●)
b. Center of the glenoid cavity (×)
c. The Y-View central axis (solid line)

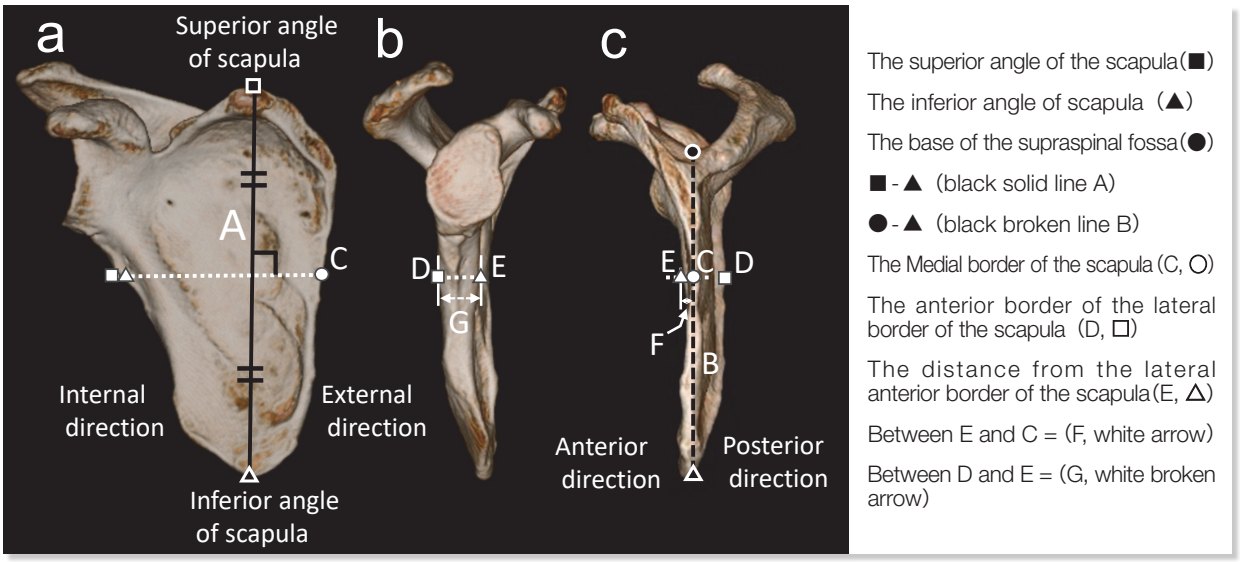

Fig.2 Positions of the medial and lateral borders for evaluating tangency in the lateral rotation

a. Anterior view image of scapula by 3D-CT VR processing
b. Image viewed from the external direction
c. Image viewed from the internal direction

medial and lateral borders and the distance between them were evaluated as indicators of tangentiality using the methods described below:

The Y-view was generated from a 3D CT image and was rotated laterally 90° so that the image could be viewed from the front. The horizontal line (white broken line) that perpendicularly crossed the line between the superior angle (■) and inferior angle (▲) of the scapula at the height of the midpoint was defined as the point of intersection on the lateral border, and its posterior and anterior borders were denoted as points D (□) and E (△), respectively The point of intersection at the midpoint of the medial border (■－▲) was defined as the center of the medial border (C). In addition, to evaluate the degree to which the medial border of the scapula is more anterior to the lateral border and tangential to the anterior surface of the scapula, "tangential condition" was defined as the overlap of the medial border on the anterior half of the thickness of the lateral border to measure the distance between the anterior lateral border and the medial border. The distance from the anterior lateral border (point E △) to the medial border (point C, ○) (segment E－C = F, white arrow) was measured and compared to the distance from the lateral posterior border (point D, □) to the thickness of the anterior lateral border (point E, △) (segment D－E = G, white broken line arrow).

2-5. Upward and downward rotation on Y-view

Previous studies have described the use of Y-view imaging to obtain a wide view of the subacromial joint formed by the acromion and humeral head [13] and to shoot the X-ray tangentially to the supraspinatus [11]. In other words, this represents the coronal alignment of the upward and downward rotation of the scapula. Aoki et al.[8] reported that X-ray incidence parallel to the inclination of the supraspinatus was used as a surrogate reference for the subacromial inclination to draw an appropriate Y-view image, as the subacromial inclination in the coronal direction of the body tends to be obscured by subacromial osteophyte formation. Therefore, tangential visualization of the supraspinatus should be useful for adjusting the rotation of the Y-view upwards and down-

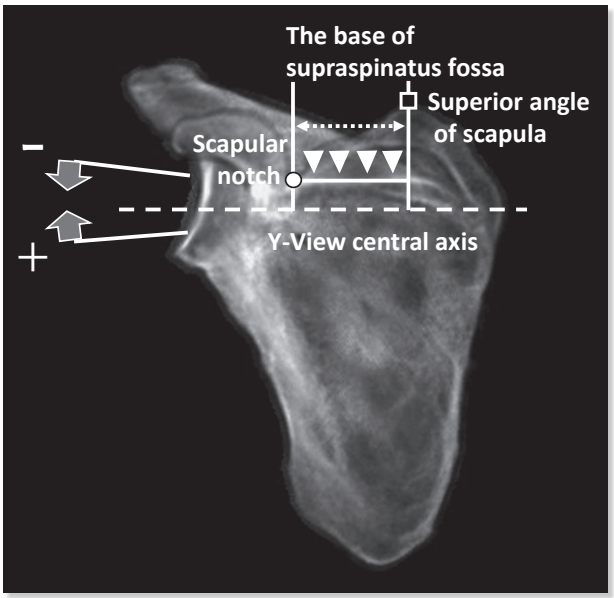

Fig.3 Relationship between the setting of the base of the supraspinatus fossa and the Y-View central axis in the anterior view image of the scapula in 3D-CT Raysum display

The scapular notch (○)
The superior angle of scapula (■)
Linear section of the base of the supraspinatus fossa (▼)
Y-View central axis (dashed line)

wards. Using this as a reference, we determined whether the Y-view generated the Horio method also fulfilled the criteria of a Y-view image. As depicted in Fig.3, the angle formed by the Y-view central axis and the straight segment of the supraspinatus base was measured on an image of the scapula observed frontally in a 3D CT Raysum view. The base of the supraspinatus was defined as the straight segment visible in the frontal Raysum view between the scapular notch (lateral) (○) and the superior angle (medial) (■) indicated by the dotted arrow. A rotational correction in the upward direction of the tilt of the straight segment of the supraspinatus base to the Y-view central axis in the upward direction was defined as + (positive), and a rotational correction in the downward direction was defined as a − (negative).

2-6. Statistical analysis

For consistency evaluation of left–right rotation, Welch's t-test was performed with two control groups, the Horio method (n = 40) and the conventional method (n = 40), excluding outliers. To evaluate the consistency of upward or downward rotation, outliers were eliminated using the Smirnov–Grubbs test, and one-sample t-test with the population mean set to 0° (n = 40) was performed. The one-sample Kolmogorov–Smirnov test was, and the Smirnov–Grubbs test used to assess normality and exclude outliers, respectively. $P < 0.01$ was considered statistically significant.

3. Results

3-1. Assessment of left–right rotation on Y-view

Fig.4 depicts the distance between the anterior lateral border and the medial border in the Y-view measured as measured by the Horio method and the conventional method. The distances were 2.22 ± 2.34 mm and 9.39 ± 3.81 mm according to the Horio method and the conventional method, respectively. No outliers were produced by either method, and there was a significant difference between them ($p < 0.01$).

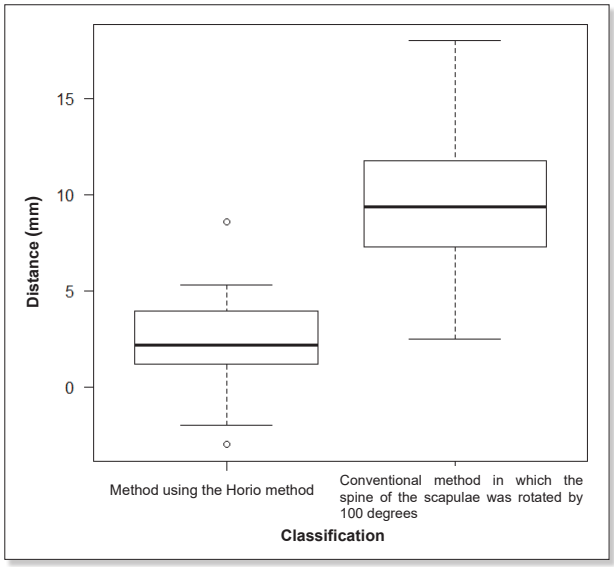

Fig.4 Positions of the medial border with respect to the lateral borders of the scapula when using the Horio method and the conventional method (box plot)

Fig.5 illustrates the position of the medial border relative to the thickness of the lateral border in the Y-view as determined by the Horio method and the conventional method. The thickness of the lateral border as represented by the D–E distance (●) was 13.88 ± 1.66 mm and 12 ± 2.13 mm measured by the Horio method and the conventional method, respectively (Fig.5-A, B). Using the Horio method, the medial border overlapped with the thickness of the lateral border in 90.0% (36/40) of the scapulae. Of these, the lateral anterior and medial borders were visualized completely tangentially in four scapulae, whereas they did

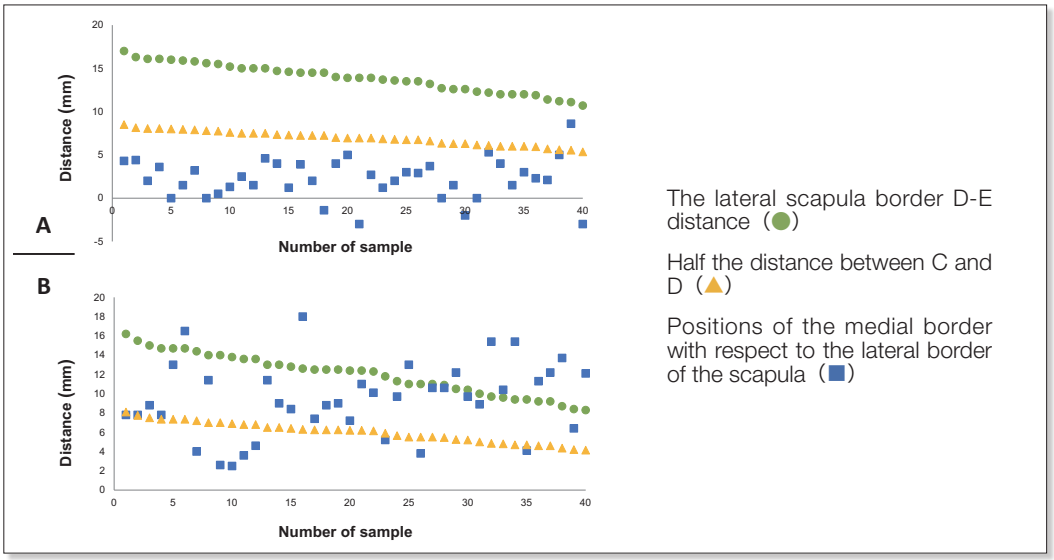

Fig.5-A Positions of medial border with respect to the lateral border of the scapula when using the Horio method (scatter diagram)

Fig.5-B Positions of the medial border with respect to the lateral border of the scapula using the conventional method (scatter diagram)

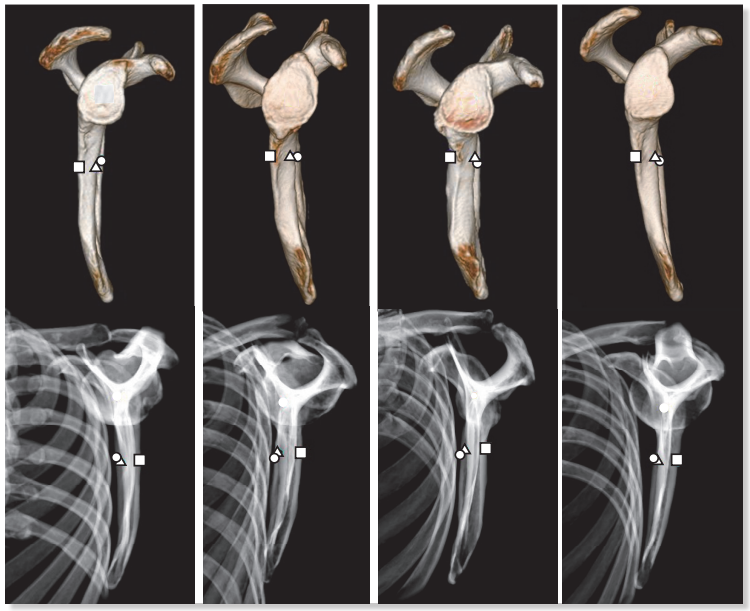

Fig.6 Four scapulae where the medial border did not overlap with the lateral border

The Medial border of the scapula (○)
The anterior border of the lateral border of the scapula (□)
The distance from the lateral anterior border of the scapula (△)

not overlap in four scapulae. Fig.6 depicts the 3D CT and Raysum images of the four scapulae in which the lateral anterior and medial borders did not overlap. As illustrated in Fig.6, the medial border was anterior to the lateral border in all four scapulae. As depicted in Fig.5-A, in 97.2% (35/36) of the 36 scapulae in which the medial border overlapped with the thickness of the lateral border in the Horio method, the medial border was closer to the anterior border than the midpoint of the width of the lateral border, which corresponds to 87.5% (35/40) of all cases.

In contrast, the medial border overlapped with the thickness of the lateral border by 72.5% (29/40) in the conventional method (Fig.5-B). There was no scapula in which the lateral anterior and medial border could be imaged completely tangentially. In the 11 scapulae where they did not overlap, the medial border was more posterior to the body than the lateral border thickness. In the 29 scapulae in which the medial border overlapped with the thickness of the lateral border, the medial border was closer to the anterior than the midpoint of the width of the lateral border in 31.0% (9/29); which corresponded to 22.5% (9/40) of scapulae.

3-2. Assessment of superior and inferior rotation on Y-view

Fig.7 depicts the angles formed by the Y-view central axis and the base of the supraspinatus. Angles ranged from -4° to 3° with the mean angle of -0.15° ± 1.55° and a distribution peak at 0° (42.5%, 17/40).

4. Discussion

In this study, the left–right rotation assessment in the Y-view (Fig.5-B) demonstrates that the medial and lateral borders of the body of the scapula did not overlap in 11 of 40 scapulae imaged using the conventional method and that the medial border was shifted posteriorly

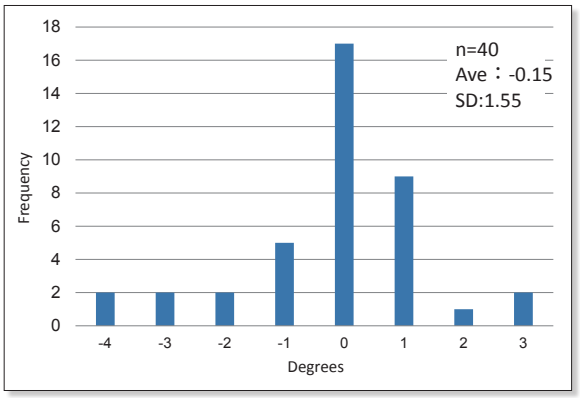

Fig.7 Angles between the Y-View central axis and the base of the supraspinatus fossa

When correction in the upward rotation is needed it is assigned as plus.
When correction in the downward rotation is necessary, it is assigned as minus.

to the posterior surface of the medial border in all 11 scapulae. In 65.5% scapulae in which the medial border overlapped the thickness of the lateral border, the medial border was posterior to the midpoint of the width of the lateral border, corresponding to a 75.0% deviation rate from the tangential condition of the scapular body. In the conventional method, which uses a 100° rotation between the straight segment of the posterior border of the scapular spine and the image reception area as a reference, shows that the body is rotated excessively medially to the ideal position, i.e., with the anterior surface of the scapular body positioned tangentially, which would require the rotation angle to be greater than 100°. However, a simple correction to an angle greater than 100° in the conventional method is ineffective in generating a good Y-view image (Fig.4), as it results in greater spread due to individual anatomical differences than the Y-view obtained using the Horio method. This shift is inevitable as long as the straight segment of the posterior border of the scapular spine is used as the reference point, resulting in an incomplete Y-view image.

In contrast, the Horio method distributed the distance between the anterior lateral border and the medial border in left–right rotation more uniformly than the conventional method.

Additionally, 90% of the scapulae where the medial border overlapped the thickness of the lateral border had the overlap in the anterior half of the thickness of the lateral border. This suggests that the Horio method allows for more accurate imaging and better conformance to the conditions of Y-view imaging in left–right rotation than the conventional method. In four scapulae, the medial border did not overlap with the thickness of the lateral border; however, all four met the other condition of the Y-view described in radiographic documents, which is that the body of the scapula is separated from the ribs [2, 3, 10-12]. Therefore, using the Horio method, the body of the scapula and ribs were found to be separated in all 40 scapulae examined from 22 patients, suggesting that it is a universally valid method of right–left rotation that permits accurate Y-view imaging in all patients.

Next, when evaluating upward and downward rotation in Y-view, the condition of accurate imaging in the Y-view, i.e., the base of the supraspinatus [8, 11] was used as a reference. As depicted in Fig.7, this resulted in a mean angle of -0.15° ± 1.55° between the base of the supraspinatus and Y-view central axis; i.e., it corresponds well with the base of the supraspinatus, indicating good conformance to the condition of accurate visualization inn the Y-view. This suggests that the method proposed by Horio method to reference the central X-rays in a superior Y-view using the scapular spine triangle and glenoid cavity is an effective method. Furthermore, this study demonstrated that the glenoid cavity, as shown by Horio, refers to the cavity's center. Therefore, aligning the angle of incidence of the X-rays to the Y-view central axis, which connects the scapular spine triangle and center of the glenoid cavity, adjusts positioning for both left–right as well as upward and downward rotation of the scapula, serving as a universal reference unaffected by the patient's postural change, scapular movement, or anatomical differences. The Horio method generates a more precise and ideal Y-view X-ray image than the conventional method, in which the angle of incidence of X-rays is adjusted between 0° and 20°.

This study has several limitations. First, this was a single-center, retrospective study, which calls for a multi-center prospective study to increase the level of evidence. Next, no comparison was made between the X-ray images produced by the Horio and conventional methods. This would be unethical as it would expose patients to a higher radiation dose of radiation than is required. Third, for a controlled assessment of the scapular angle, it would be necessary to control the scapula's inclination in the coronal, sagittal, and horizontal directions, which was not possible with the available X-ray images. Fourth, the images of the scapulae in this study were acquired using chest CT, which is performed with the arms raised, as opposed to the normal seated or standing position with the arms lowered. However, this study evaluated the scapula independently as opposed to its relationship with neighboring bones such as the humerus or clavicle and structures such as muscles; therefore, we consider this irrelevant.

Further investigation is necessary for future studies, such as examining body surface references for using the Y-view central axis and new body surface indices for each posture. If this is possible, it is expected that the patient will be able to receive Y-view images that satisfy the imaging conditions even in the hunched posture and the supine position.

5. Conclusions

A simulation using 3D CT images demonstrated the effectiveness of imaging using the central X-ray connecting the two points, the scapular spine triangle and the glenoid cavity, as shown by Horio as the reference for Y-view imaging satisfied the imaging conditions for the Y-view more than the conventional method.

6. Acknowledgments

We would like to express our sincere gratitude to Shimoda Medical Center for their cooperation in this research and to Professor Yasuo Takatsu of Tokushima Bunri University for his assistance in preparing this manuscript. A part of this study was presented at the 32nd Annual Conference of the Japan Association of Radiological Technologists (2016, Gifu).

Conflicts of interests

The corresponding author nor the coauthors have no conflicts of interest to declare.

References

1) Oda Nobuhiro, et al.: Housyasengijyutsugakusirizu Xsensatsueigijyutsugaku (Revised 2nd edition). Tokyou: Ohmsha, p228-229, 2014.
2) Sloane C, et al.: Clark's pocket handbook for radiographers. Hodder education an Hachette uk company, 79-180, 2010.
3) Ballinger PW, et al.: Merrill's Atlas of Radiographic Positions and Radiologic Procedures.1,185-187, 190, 204, 214-215, Mosby, 1999.
4) Liotard JP, et al.: Critical Analysis of the Supraspinatus Outlet View: Rationale for a Standard Scapular Y-view. J Shoulder Elbow Surg, 7(2), 134-139, 1998.
5) Umer M, et al.: Subacromial impingement syndrome. Orthopedic Reviews, 9, 4(2), e18, 2012.
6) Apivatgaroon A, et al.: The acromion in supraspinatus outlet and rockwood caudal tilt views from three-dimensional computed tomography scan of the shoulder. AP-SMART, 20, 12-16, 2020.
7) Duralde XA, et al.: Troubleshooting the supraspinatus outlet view. J Shoulder Elbow Surg, 8(4), 314-319, 1999.
8) Aoki Mitsuhiro, et al.: Kenpou no keisha no rinshoukeisoku to subacromial impingement syndrome to no kankei. Japan Shoulder Society, 14(2), p270-274, 1990.
9) House J, et al.: Evaluation and management of shoulder pain in primary care clinics. South Med J, 103, 1129-1135, 2010.
10) Ogawa Norihisa: Shin・Zusetsu Tanjun Xsensatsueiho Satsueiho to Sindan・Dokuei no Point. Tokyou: Kanehara Shuppan, 2012.
11) Takakura Yoshinori, et al.: Zukai Joshisatsueiho. Tokyou: Ohmsha, p24-29, 2011.
12) Kanamori Isao, et al.: Shinryogazokensaho Xsensatsueiho. Iryokagakusha, p209, 2010.
13) Wu G, et al.: ISB recommendation on definitions of joint coordinate systems of various joints for the reporting of human joint motion-Part II : shoulder, elbow, wrist and hand. J Biomech, 38(5): 981-992, 2005.
14) Japanese Society of Radiological Technology, Satsueibunkakai: Houshaseniryogijutugakusosho(21) Sports Gaisho・Shogai no tameno Satsueigijutsu. Japanese Society of Radiological Technology, p80, 2003.
15) Kumagai Sadayoshi: Kotsu Xsensatsueigijutsu. Tokyou: Ishiyaku Shuppan, p79, 1969.
16) Horio Shigeharu: Kotsu・Kansetsu Xsenshashin no Torikata to Mikata. Tokyou: Igakushoin, p15-16, 2010.
17) Horio Shigeharu: Kotsutanjunsatsueiho to Xsenkaibozufu. Tokyou: Igakushoin, p242-245, 1971.

Received March 7, 2021; accepted October 16, 2021

3D T_2-weighted turbo field echo (3D T_2 TFE) sequences for evaluation of cervical nerve roots

KAWAKAMI Koji[1], KITSUKAWA Kaoru[2], KIMURA Yusuke[2], YONEYAMA Masami[3], FUKUCHI Hirofumi[1], YOSHIKAWA Tatsuo[1]

1) Imaging Center, St. Marianna University School of Medicine Hospital
2) Department of Radiology, St. Marianna University School of Medicine
3) Philips Japan

Note: This paper is secondary publication, the first paper was published in the JART, vol. 69 no. 833: 19-24, 2022.

Key words: MRI, cervical spine, nerve root, neurography, 3D T_2 TFE

【Abstract】
Evaluation of cervical nerve root abnormalities using magnetic resonance imaging is less straightforward for cervical spondylosis than for spinal cord compression. For better visualization of cervical nerve roots, a three-dimensional T_2-weighted turbo field echo (3D T_2 TFE) sequence may be useful, due to the increased signal intensity of nerve bundles, as well as the rapid black blood imaging. In this study, 3D T_2 TFE and 3D T_2 volume isotropic turbo spin echo acquisition (3D T_2 VISTA) sequences were compared for visualization of nerve roots. Images from 10 volunteers were visually evaluated and statistically analyzed. The 3D T_2 TFE sequence was able to show nerve roots with a significantly higher signal than the surrounding structures. In statistical analysis, 3D T_2 TFE provided significantly higher nerve root visualization in C3–C7 vertebrae than did 3D T_2 VISTA. Concordance between observers was high. 3D T_2 TFE may be helpful in diagnosing nerve root compression in patients with cervical radiculopathy.

Introduction

Cervical radiculopathy is caused by the compression of the cervical nerve at the level of the intervertebral foramen due to disc bulging or osteophytes in Luschka's joints or intervertebral joints. Cases that develop spinal canal stenosis and lumbar disc herniation in the lumbar spine undergo magnetic resonance imaging (MRI) to visualize how the nerve roots are compressed. However, only a few studies have sought to visualize cervical nerve root and morphological changes within the intervertebral foramen using MRI [1)-5)]. Conventional MRI imaging methods may have difficulty identifying which nerve root is injured and the responsible lesion [6)]. The intervertebral foramen is anatomically smaller than the lumbar spine and is located obliquely to the body axis [5), 7)]. During diagnostic imaging of cervical spondylotic radiculopathy, accurate identification of the lesion is important for selecting surgical treatment. For this purpose, three-dimensional (3D) imaging methods with thin slices and no gaps between slices have been considered advantageous [6)]. MR Neurography as the MR Imaging methods for the cervical nerve, includes 3D Volume Isotropic Turbo Spin Echo Acquisition (3D T_2 VISTA) sequences [8)], and especially when the peripheral nerves are needed to visualize outside the intervertebral foramen, diffusion-weighted imaging and High-Resolution 3D Volumetric Nerve-Sheath Weighted RARE Imaging (3D SHINKEI) have been reported in the literature and applied clinically [9)-13)]. The 3D T_2 VISTA sequences described above is basically a T_2-weighted imaging method that delineates cerebrospinal fluid (CSF) and adipose tissues with a high signal and normal nerve roots, degenerated intervertebral discs, and yellow ligaments with a low signal [8)]. However, no significant difference in the ability to visualize nerve roots in the intervertebral foramen was observed between the aforementioned modalities and two-dimensional methods, making it difficult to observe the nerve roots in

the intervertebral foramen, which are important in cervical spondylotic radiculopathy. In order to continuously observe a wide area extending from the spinal cord to the anterior and posterior roots, dorsal root ganglia, and extravertebral foramen nerve roots, imaging methods that suppress the signal from blood vessels, CSF, and fatty tissue surrounding the nerve root and emphasize the nerve root itself are considered effective [10]. It has been reported that the 3D T_2 Turbo Field Echo (3D T_2 TFE) sequences is capable of high-signal imaging of nerve fibers, and can obtain three-dimensional T_2-weighted black-blood imaging can be obtained in a short time [13), 14)]. This method is a gradient echo (GRE) method that collects spin echo (SE) signals, which require two RF pulses to generate. In principle, when the echo time (TE) is longer than the repetition time (TR), and the longer TR and TE are, the more sensitive to motion and the lower the fluid tissue signal can be captured. The current study aimed to compare the nerve root imaging performance of the 3D T_2 TFE sequences and the 3D T_2 VISTA sequences, which allows for a freely reconstructable in a 3D sequence.

1 Methods

1.1 Validation of the 3D T_2 TFE sequences

We performed 3D T_2 TFE imaging in 10 healthy volunteers and verified its ability to visualize cervical nerve roots in the images. This study was approved by the Ethics Committee of our hospital, and all volunteers were informed of the purpose of the study and provided consent (Approval No. 3418). The Achieva 1.5-T (Philips Japan Co., Ltd.) and Neuro Vascular coil were used as the receiver coil. The imaging parameters are shown in Table 1. The 3D T_2 VISTA sequences was based on previous studies [8)]. whereas the 3D T_2 TFE sequences was based on phantom verification. The measurement position was a transverse image at the level of the fifth cervical vertebra.

Table 1 3D T_2 TFE and 3D T_2 VISTA scan parameters for volunteer imaging

	3D T_2 TFE	3D T_2 VISTA
TE (msec)	5.9	150
TR (msec)	12	1200
Flip angle (degree)	35	90
TFE (TSE) factor	30	40
Startup echoes	default	0
Shot interval (msec)	439	
DRIVE		yes
Uniformity	CLEAR	CLEAR
Profile order	Centric	Sequential
Fat sat	ProSet 121	no
Band width [Hz]	271	315
Field of view [FOV] (mm)	180	180
Rectangular FOV (%)	65.9	66.6
Matrix [matrix × phase]	174 × 116	180 × 120
Reconstruction matrix	432 × 432	432 × 432
Number of signals averaged	4	1
Slice thickness (mm)	1	1
Slice	50	50
Scan time (min)	5.37	4.40

ProSet: Principle of Selective Excitation Technique

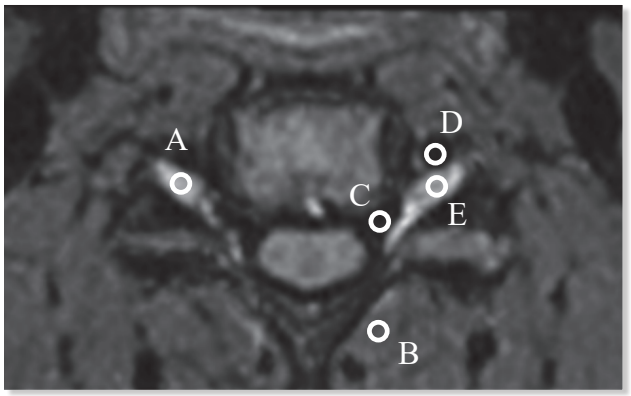

Fig.1 ROI placement for the axial 3D T_2 TFE images

The reformatted axial image of the originally acquired 3D T_2 TFE image shows the locations of the ROIs used for measuring the signal intensity of the right nerve root (A), paraspinal muscle (B), cerebrospinal fluid (C), left vertebral artery (D), and left nerve root (E).

The region of interest (ROI) was set at 4.0 mm, the image was enlarged sufficiently to minimize errors, and the signal intensities of the bilateral nerve roots, paraspinal muscles, CSF, and left vertebral artery were calculated (Fig.1). After one-way analysis of variance, the Steel–

Dwass test was performed for each group to determine significant differences. The confidence interval was set at 99% ($p < 0.001$). Statistical analysis software JMP Pro®13 (SAS Institute Inc.) was used [15].

1.2 Imaging evaluation

A total of 10 healthy volunteers [mean age, 29.4 years (25–40 years); 7 males and 3 females] were imaged using the 3D T_2 TFE and 3D T_2 VISTA methods and visually evaluated for nerve root delineation ability. None of the volunteers had symptoms of cervical nerve root disease. The imaging parameters are shown in Table 1. Two radiologists (with 4 and 30 years of diagnostic radiology experience) independently scored the ability of both methods to visualize the bilateral first cervical to first thoracic nerve roots. The evaluation method was based on a four-point scale, with a score of 3, 2, 1, and 0 indicating that the cervical nerves from inside the dural sac to outside the intervertebral foramen could be clearly observed, were partially obscured but observable, were only partially observable, and were not observable, respectively [16] (Fig.2).

1.3 Statistical evaluation of image evaluation

The Wilcoxon signed-rank test was used to evaluate the nerve root imaging performance of the 3D T_2 TFE and 3D T_2 VISTA sequences in 10 volunteers, after which kappa values were used to analyze the interobserver agreement. Confidence intervals were set at 95% ($p < 0.05$), and tests for significant differences were performed.

2 Results

2.1 Validation of the 3D T_2 TFE sequences

Among the 10 healthy volunteers, signal values at the level of the fifth cervical vertebra were highest in the bilateral nerve roots and were significantly higher than were signal values in fluid tissues such as the left vertebral artery and CSF. No significant differences in signal values were observed between the left and right nerve roots or between the left vertebral artery and CSF (Fig.3).

2.2 Image evaluation

The 3D T_2 TFE sequences revealed that bilateral nerve roots had a high signal, whereas blood vessels and CSF had a low signal. Mean-

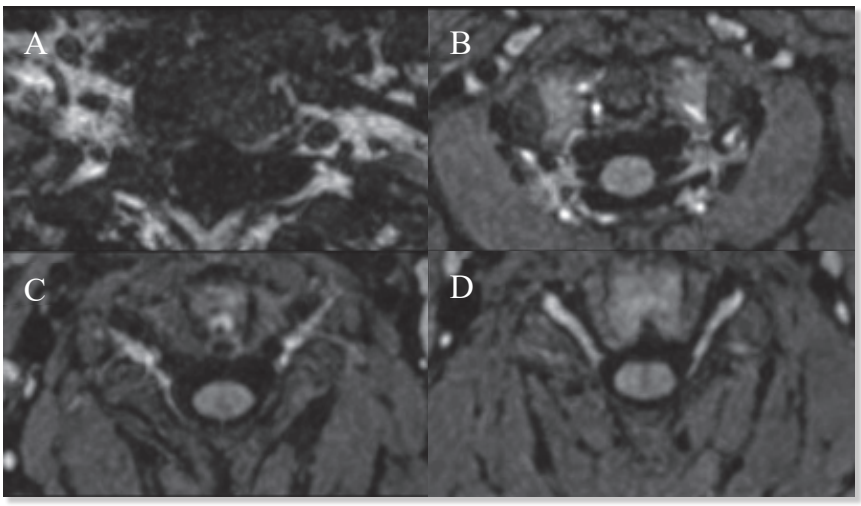

Fig.2 Examples of image quality scoring

MR imaging examples of the 4 grades used for qualitative evaluation of the cervical nerve from the intradural to extraforaminal regions. The reformatted axial images of the originally acquired 3D T_2 TFE image show examples of the following: not visible (score 0; A), partly visible (score 1; B), visible (score 2; C), and clearly visible (score 3; D).

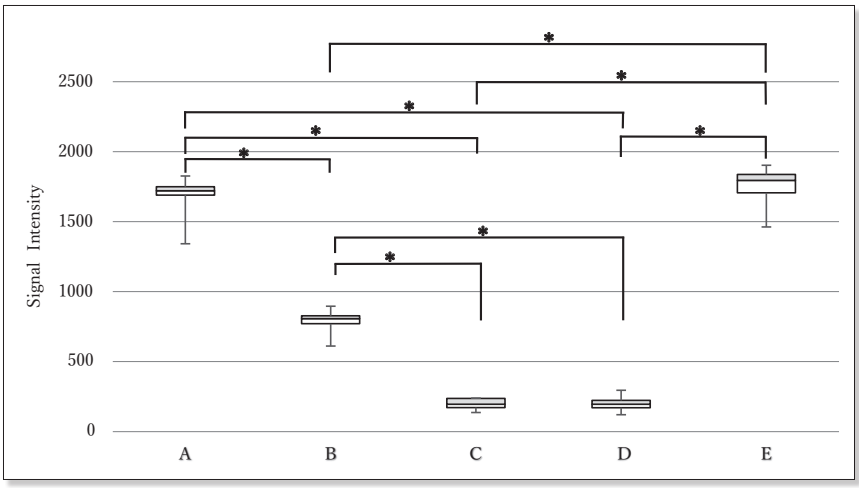

*: $p < 0.001$

Fig.3 Signal intensity of various structures in 3D T_2 TFE images

(A): right nerve root, (B): paraspinal muscle, (C): cerebrospinal fluid, (D): left vertebral artery, (E): left nerve root

The average signal value from 10 healthy volunteers was highest in the bilateral nerve roots, which was significantly higher than the average signal values of the other structures.

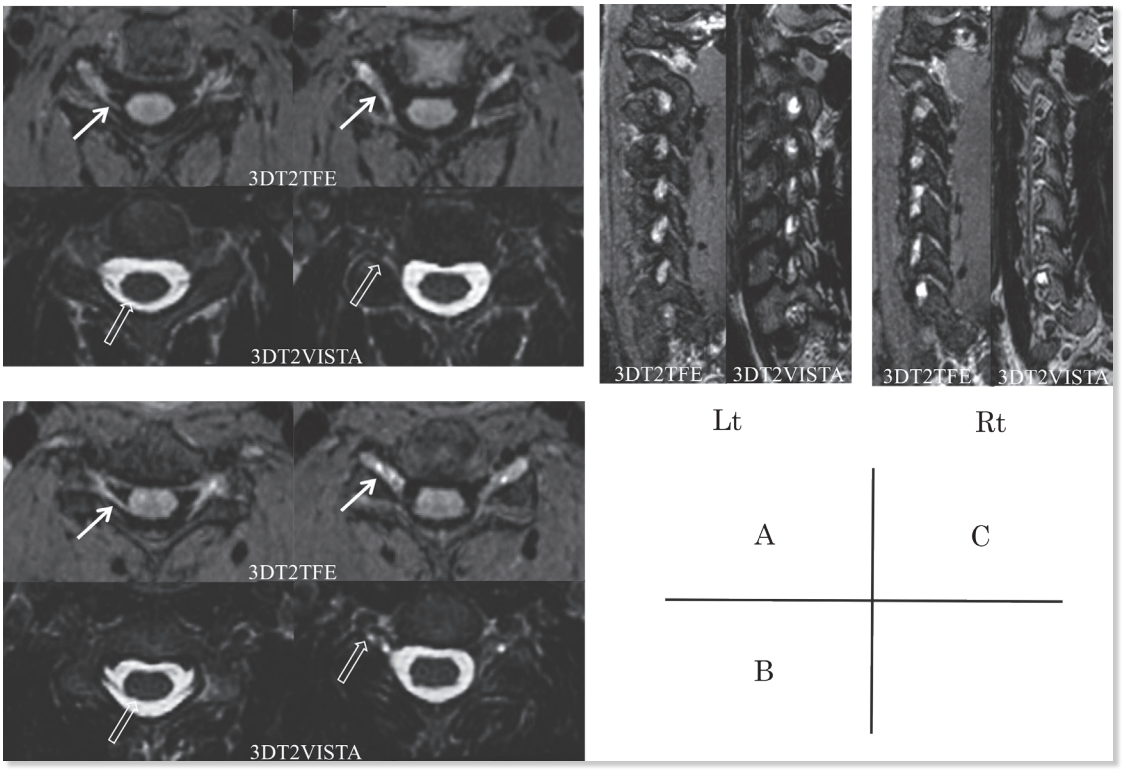

Fig.4 3D T_2 TFE and 3D T_2 VISTA images

(A) 3D T_2 TFE and 3D T_2 VISTA axial reformatted images at the level of C3.
(B) 3D T_2 TFE and 3D T_2 VISTA axial reformatted images at the level of C5.
(C) 3D T_2 TFE and 3D T_2 VISTA oblique sagittal reformatted images.

(A) - (C) Reformatted acquired 3D T_2 TFE images demonstrating that the nerve roots and spinal cord have the highest signal intensity within the thecal sac through the extraforaminal region (white arrow). The structures surrounding the nerve root, such as blood vessels and CSF, are visualized as areas of low signal intensity. Thus, the 3D T_2 TFE sequence provides high contrast images between the cervical nerve root and surrounding structures. In contrast, the 3D T_2 VISTA images show the nerve root and spinal cord as having low signal intensity (open arrow). Moreover, the extradural region of the cervical nerve root is not as well visualized as with the 3D T_2 TFE sequence.

while, the 3D T2 VISTA sequences showed that the CSF and adipose tissue had a high signal, whereas the nerve roots had a low signal (Fig.4). The 3D T2 TFE and 3D T2 VISTA images were obtained from 10 volunteer. Two radiologists evaluated those images according to the visual scale and gave high mark on 3D T2 TFE images at the level of 3 to 7 cervical spine (Table 2).

2.3 Statistical image evaluation

The results of statistical analysis of nerve root delineation performance are shown in Table 2. In visual score of nerve root delineation, the 3D T2 TFE images at the level of the third to seventh cervical vertebrae had significantly higher. The interobserver agreement using kappa values was 0.68 (0.56–0.80) and 0.34 (0.25–0.52) for the 3D T2 TFE and 3D T2 VISTA sequences, respectively, with the 3D T2 TFE sequences showing a greater agreement.

3 Discussion

Among the 10 volunteers imaged using the 3D T2 TFE sequences, the signal intensity in the ROI at the level of the fifth cervical vertebra was significantly higher than that of the left vertebral artery and fluid tissues, such as the CSF, with the highest signal values observed at the bilateral nerve roots. Yoneyama's report states that to selectively delineate nerves on MRI, either enhancing the nerves themselves or suppressing the signal of surrounding tissues can be effective [10]. Moreover, we were able to confirm the difference in signal intensity between cervical nerve roots and surrounding structures with the 3D T2 TFE technique.

Visual evaluation by the radiologist revealed higher scores at the third to seventh cervical vertebra levels and significantly better nerve root delineation with the 3D T2 TFE sequences than with the 3D T2 VISTA sequences. This may have been attributed to the ability of the 3D T2 TFE sequences to reduce the signal around the nerve root, such as CSF, bone, and blood vessels, and image the nerve root itself with a high signal. In contrast, the 3D T2 VISTA sequences delineates the nerve root itself with

Table 2 Nerve root scores and Wilcoxon signed-rank test results for each of the two readers

	Reader 1		p-value	Reader 2		p-value
	3D T2 TFE	3D T2 VISTA		3D T2 TFE	3D T2 VISTA	
	right nerve root (mean ± SD) left nerve root (mean ± SD)			right nerve root (mean ± SD) left nerve root (mean ± SD)		
C1	0.7 ± 0.15 0.7 ± 0.15	0.1 ± 0.10 0.1 ± 0.10	0.015	1.2 ± 0.15 1.2 ± 0.15	1.1 ± 0.10 1.1 ± 0.10	n.s
C2	1.3 ± 0.21 1.3 ± 0.21	2.2 ± 0.29 2.2 ± 0.29	n.s	2.4 ± 0.18 2.6 ± 0.18	1.6 ± 0.24 1.7 ± 0.24	0.009 0.015
C3	2.7 ± 0.15 2.7 ± 0.15	2.1 ± 0.23 2.1 ± 0.23	0.029	2.3 ± 0.16 2.2 ± 0.15	1.8 ± 0.22 1.6 ± 0.24	0.038 0.039
C4	2.7 ± 0.21 2.9 ± 0.10	1.8 ± 0.20 1.8 ± 0.20	0.006	2.6 ± 0.18 2.3 ± 0.17	1.9 ± 0.26 1.8 ± 0.28	0.03
C5	3.0 ± 0 3.0 ± 0	1.8 ± 0.20 1.9 ± 0.18	0.004	2.9 ± 0.10 2.9 ± 0.10	1.9 ± 0.26 1.9 ± 0.30	0.009
C6	3.0 ± 0 3.0 ± 0	1.9 ± 0.18 2.0 ± 0.21	0.004 0.006	3.0 ± 0 3.0 ± 0	1.8 ± 0.20 1.8 ± 0.30	0.006
C7	3.0 ± 0 2.9 ± 0.10	2.2 ± 0.25 2.2 ± 0.25	0.016 0.015	2.9 ± 0.10 2.8 ± 0.15	2.0 ± 0.29 1.9 ± 0.31	0.009
C8	2.3 ± 0.26 2.4 ± 0.34	2.4 ± 0.34 2.4 ± 0.27	n.s	1.9 ± 0.31 2.1 ± 0.28	2.0 ± 0.24 1.9 ± 0.31	n.s
Th1	0.6 ± 0.22 0.6 ± 0.22	2.3 ± 0.26 2.0 ± 0.26	n.s	1.7 ± 0.29 1.9 ± 0.31	1.2 ± 0.15 1.3 ± 0.17	n.s

n.s. : not significant

a low signal. Therefore, while T_2 contrast between the CSF and nerve root allows us to observe the nerve root run in the spinal canal where CSF exists, the contrast decreases outside the spinal canal where the CSF signal disappears, and the visibility of the nerve root becomes poor, making it difficult to adequately follow the run of the nerve root. However, outside the spinal canal, where the CSF signal is lost, the contrast is reduced, leading to the presumption that the nerve roots could not be adequately followed due to poor visibility [8]. Previous studies have shown that diagnostic imaging of cervical spondylotic nerve root disease requires high-resolution imaging using the 3D method with thin slices and no gaps between slices [6]. This study's investigation of 3D T_2 TFE sequences has demonstrated the ability to reconstruct images in any cross-section and produce high-contrast imaging of the spinal cord. As a result, there is potential for improved depiction of nerve root compression in cervical spondylotic nerve root disease, specifically for nerve roots outside the intervertebral foramen.

The 3D T_2 TFE sequences was not superior to the 3D T_2 VISTA sequences for the eighth cervical vertebra and first thoracic vertebra nerve root. This may have been due to the influence of magnetic susceptibility caused by the lungs, phase dispersion caused by respiration and body movement, and signal degradation caused by coil geometry. The T_2 TFE sequences used in the current study is a GRE method that collects SE signals, and gradient spoiling is performed immediately after RF to reduce the signal of the FID component [17]. Moreover, although the multi-shot method cuts off the steady state once and collects data, allowing for further reduction in the signal of flowing tissues, such as the CSF and blood vessels, the effects of body movement and respiration are reflected sensitively, for which we assume the absence of a significant difference at the level of the eighth cervical vertebra or first thoracic vertebra. Since the preferred site of cervical radiculopathy is at the level of the 4th to 7th cervical nerve roots, we believe that 3D T_2 TFE may be useful in most cases for the diagnosis of cervical radiculopathy, even if the findings of the 8th cervical nerve root or the 1st thoracic nerve root are not significantly better than the 3D T_2 VISTA sequences.

The 3D T_2 TFE sequences displayed a higher interobserver agreement rate than did the 3D T_2 VISTA sequences, perhaps due to its the ability to image the nerve roots themselves running from the spinal cord into and out of the intervertebral foramen with high contrast. Conversely, evaluating the entire nerve root running from the spinal cord to outside the intervertebral foramen using the 3D T_2 VISTA sequences proves quite difficult, which may have reduced the interobserver agreement rate [18), 19)].

One limitation of this study is that our study population comprised healthy volunteers and not on patients with cervical spine disease. Future studies will be needed to examine whether nerve root symptoms coincide with the stenosis site in patients with clinical symptoms.

4 Conclusion

The 3D T_2 TFE sequences and the 3D T_2 VISTA sequences, which allows for a freely reconstructable 3D sequence for cervical nerve root delineation, were examined for their ability to delineate nerve roots. Our findings showed that the 3D T_2 TFE sequences was able to delineate nerve roots by presenting them as a significantly higher signal compared to the surrounding structures. Moreover, the 3D T_2 TFE sequences was significantly more effective at the level of the third to seventh cervical vertebrae, from within the spinal canal to outside the intervertebral foramen, than was the 3D T_2 VISTA sequences while showing with a high interobserver agreement rate. We believe that this method will be widely used as a standard imaging technique for nerve root evaluation during cervical spine MRI in the near future.

Conflicts of interest

We have no conflicts of interest to disclose in this study.

Acknowledgments

We would like to express our deepest gratitude to the members of the Imaging Center for their guidance in this study.

A part of this paper was presented at the 45th Annual Meeting of the Japanese Society for Magnetic Resonance Medicine in Utsunomiya, Japan.

References

1) Hiroki Shishido, et al.: Visualization of the Foramen Intervertebral Nerve Root of Cervical Spine with 3.0 Tesla Magnetic Resonance Imaging: A Comparison of Three-dimensional Acquisition Techniques. Japanese Journal of Radiological Technology, 70(7), 670-675, 2014 (in Japanese).
2) Park HJ, et al.: A practical MRI grading system for cervical foraminal stenosis based on oblique sagittal images. Br J Radiol, 86(1025), 20120515, 2013.
3) Park HJ, et al.: The clinical correlation of a new practical MRI method for grading cervical neural foraminal stenosis based on oblique sagittal images. AJR, 203(2), 412-417, 2014.
4) Park HJ, et al.: Clinical correlation of a new practical MRI method for assessing cervical spinal canal compression. AJR, 199: 197-201, 2012.
5) Naoyasu Okamura, et al.: Evaluation of Cervical Spine Lesions by the 3D T2-SPACE Compared with the 2D T2WI. Spinal Surgery, 34(1), 59-65, 2020 (in Japanese).
6) Chikage Inukai, et al.: Usefulness of Curved Coronal MPR Imaging for the Diagnosis of Cervical Radiculopathy. Neurological Surgery, 38(3), 251-257, 2010 (in Japanese).
7) Hisanobu Koga, et al.: 3.0T MR Imaging of the Cervical Nerve Root in the Intervertebral Foramen. Spinal Surgery, 22(2), 80-85, 2008 (in Japanese).
8) Kwon JW, et al.: Three-dimensional isotropic T2-weighted cervical MRI at 3T: Comparison with two-dimensional T2-weighted sequences. Clinical Radiology, 67, 106-113, 2012.
9) Syuji Okinaga, et al.: Delineation of brachial plexus disease by diffusion-weighted MRI. The journal of Japanese Society for Surgery of the Hand, 26(6), 616-621, 2010 (in Japanese).
10) Masami yoneyama: MR Neurography: Novel MR Imaging Techniques for Depiction of Peripheral Nerves. Neurological Therapeutics, 32(2), 201-204, 2015 (in Japanese).
11) Tsuchiya K, et al.: Visualization of cervical nerve roots and their distal nerve fibers by diffusion-weighted scanning using parallel imaging. Acta Radiol, 47, 599-602, 2006.
12) Masami Yoneyama, et al.: Rapid High Resolution MR Neurography with a Diffusion-weighted Pre-pulse. Magn Reson Med, 12, 111-119, 2013.
13) Masami Yoneyama, et al.: Reevaluation of T2-weighted fast field echo (T2FFE): application to rapid volumetric black-blood imaging. Radiol phys Technol, 6(2), 305-312, 2013.
14) Marielle E.P. Philippens, et al.: TRACING THE CRANIAL NERVE PATHWAYS NV AND NVII WITH 3D T2-FFE. Mag. Reson. Med, 20, 1059, 2012.
15) Osamu Uchida, et al.: Medical Data Analysis with JMP. Tokyotosho, 96-99, 2012 (in Japanese).
16) Masahiro Miura, et al.: Latest findings in cerebrospinal fluid. Spine & spinal cord, 28(8), 694-703, 2015 (in Japanese).
17) Masami Yoneyama, et al.: Differentiation of hypointense nodules on gadoxetic acid-enhanced hepatobiliary-phase MRI using T2 enhanced spin-echo imaging with the time-reversed gradient echo sequence: An initial experience. EJR, 95, 325-331, 2017.
18) Harold L Kundel, et al.: Measurement of Observer Agreement. Radiology, 228, 303-308, 2003.
19) Hiroshi Nishiura: A Robust Statistic AC1 for Assessing Inter-observer Agreement in Reliability Studies. Japanese Journal of Radiological Technology, 66(11), 1485-1491, 2010 (in Japanese).

Received June 2, 2021; accepted November 25, 2021

Dosimetry with a custom-made chest radiography dosimeter and radiation dose management from the analysis results

SHINKAI Eishu[1)], OOISHI Tetsuya[1)], TAKAGI Yuu[1)], KATOU Hiroaki[1)], KOMIYA Hiroko[1)], UEDA Kouki[1)], YOSHIKAWA Kumiko[1)], RIKITAKE Sayaka[1)], BABA Ikuko[2)]

1) Roueiken Medical Check Center, Fukuoka Institute of Occupational Health, Radiological Technologist
2) Roueiken Medical Check Center, Fukuoka Institute of Occupational Health, Doctor

Note: This paper is secondary publication, the first paper was published in the JART, vol. 69 no. 835: 39-44, 2022.

Key words: chest radiography, radiation dose management, incident surface dose, body weight

【Abstract】
Chest radiographs in medical examinations usually involve many examinees of different body types. In this study, a method for estimating the exposure dose for each examinee was determined.
First, we made our own radiation dosimeter for chest radiography of the examinee, installed it in one of the chest radiography rooms, confirmed that it could measure with high accuracy, and analyzed the measurement data.
The measured data showed, that the exposure dose correlated well with the weight of the examinee. Therefore, the relationship between the weight of the examinee and his/her exposure dose can be applied for the exposure dose management of the examinee, even in other chest imaging rooms.

1. Introduction

The diagnostic reference levels (DRLs) that were first introduced in June 2015 specified that the incident surface dose to the frontal chest was 0.3 mGy. Subsequently, the DRLs were revised in July 2020 (DRLs 2020), and a new item for the frontal surface of the chest at the time of medical examination was added separately from the frontal surface of the chest and set at 0.2 mGy.

Our institution conducts both facility and traveling medical checkups, and more than 340,000 individual underwent chest imaging in 2019. The large number of people who undergo chest imaging has resulted in a large population effective dose. Thus, we keenly felt the need to manage the dose in examinees during health examinations. We then attempted to manage the dose of the examinees in the chest imaging, including the optimization by DRLs 2020.

In the past, lung field phantoms (standard body shape) were usually taken in using a phototimer in all chest imaging equipment. The values of the examinee's exposure dose under those imaging conditions were posted in each imaging room. However, estimating the radiation doses of many examinees with different body shapes is difficult; therefore, a custom-made dosimeter was installed in one of the chest radiography rooms. We evaluated the characteristics of the dosimeter, confirmed that it can measure doses with high accuracy, analyzed the measured data, and developed a simple method for estimating the chest doses of each examinee.

2. Materials and methods

2.1 Overview of the custom-made dosimeter for chest radiography

A dosimeter for chest radiography was developed because a custom-made dosimeter has comparable performance to commercially available dosimeters [1)] and can be manufactured inexpensively (less than 100,000 yen).

2.1.1 Ionization chamber

Considering the size of the front face of the movable aperture, the ionization chamber [2] is square, with 180 × 180 mm in external dimension and 146 × 146 mm in internal dimension. The frame was made by cutting out a 4-mm thick brass plate. The electrodes were of parallel-plate type and consisted of two layers: current-collecting and high-voltage electrodes. The walls were made of two layers of 100-μm-thick polyester film stretched over the frame at 4-mm intervals. The collector electrode was formed on the upper layer and the high-voltage electrode on the lower layer, using 15-μm-thick aluminum (household aluminum foil, 99.4% purity) and bonded together. The area of the collector electrodes was 20 × 20 mm, and that of the high-voltage electrodes was 30 × 30 mm.

Fig.1 shows an illustration of the cross section of an ionization chamber, and Fig.2 shows the actual appearance of the ionization chamber.

2.1.2 Amplifier

The amplifier was the same in principle as commonly used amplifiers; however, a Model AD549KH (Analog Devices) was used as the direct current amplifier. The ionizing charge at the time of X-ray irradiation was charged to a capacitor of 0.016 μF, and the amount of charge was converted to the absorbed dose at the skin surface of the examinee (20 cm from the top of the imaging plate) and displayed.

The indicated value was obtained by calibrating the custom-made ionization chamber dosimeter (Roueiken type) [3] with Accu Dose+10X6 (Radcal Corporation), measuring the dose (μC/kg) at the target position, and multiplying the backscatter coefficient and absorbed dose conversion factor to obtain the incident surface absorbed dose. To achieve this value, the adjustment resistor shown in Fig.3 was used to display the value in mGy.

A DC voltage of 200 V was applied to the high-voltage electrode using a high-voltage module (Bellnix Co., Ltd.).

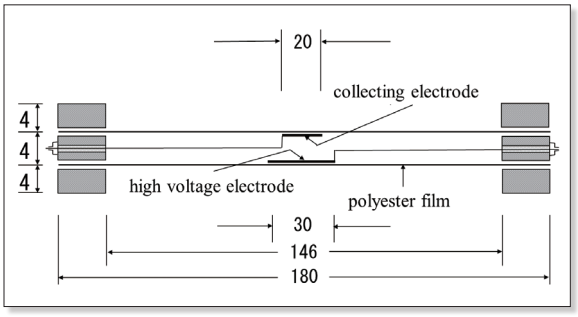

Fig.1 Illustration of the cross section of an ionization chamber

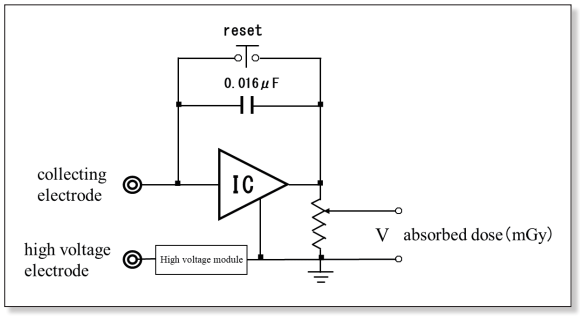

Fig.3 Principle of the measuring circuit of an amplifier

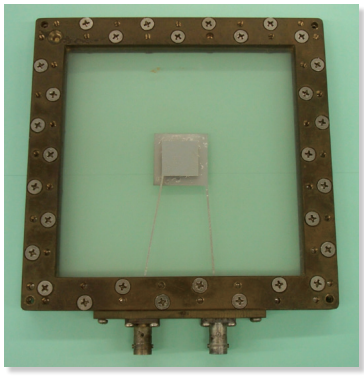

Fig.2 Actual appearance of the ionization chamber

Fig.4 Actual appearance of the amplifier

Fig.3 shows the principle for measuring the circuit of an amplifier, and Fig.4 shows the actual appearance of the amplifier.

2.2 Characterization of the custom-made dosimeter for chest radiography

The following equipment and materials were used to characterize the custom-made dosimeter for chest radiography: high-voltage X-ray equipment, HITACHI DHF-153H4R (Radnext) (total filtration 2.5 mm Al); and digital photography equipment, FUJI FILM DR-ID1200 (CALNEO Smart).

Dose ratios were obtained using the custom-made ionization chamber dosimeter (Roueiken type) [3] as a reference dosimeter.

2.2.1 Beam quality characteristics

The radiation quality characteristics of the custom-made dosimeter for chest radiography were measured at 80, 100, 120, and 130 kV tube voltages. The irradiation field was 43 × 43 cm on the imaging tabletop. The ionization chamber of the chest radiography dosimeter was mounted in front of the movable aperture, and the custom-made ionization chamber dosimeter (Roueiken type) [3] was simultaneously measured at 179 cm, 20 cm away from the thoracic imaging tabletop.

2.2.2 Dose-rate characteristics

The dose rate characteristics of the custom-made dosimeter for chest radiography were measured at a tube voltage of 120 kV in the same arrangement as for the measurement of the beam quality characteristics. The dose rate is defined as the dose rate at the incident plane of the skin.

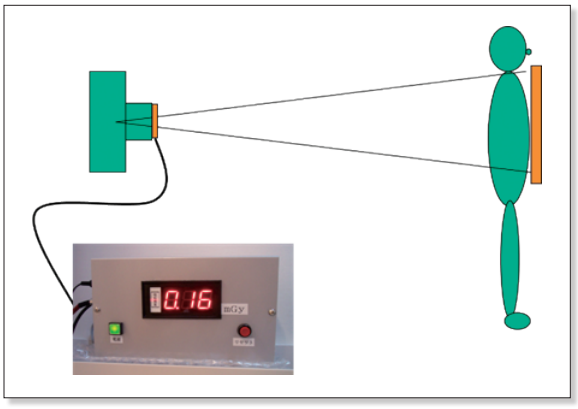

Fig.5 Schematic diagram of the layout

2.3 Clinical application of the custom-made dosimeter for chest radiography

2.3.1 Dosimetry by chest radiography dosimeters in health examinations

A schematic diagram of the arrangement is shown in Fig.5. The incident surface dose was measured at a chest thickness of 20 cm from the imaging top plate using an ionization chamber in front of the movable aperture and is indicated in units of absorbed dose (mGy).

This dosimeter for chest imaging is used in daily health checkups, and the absorbed dose values are currently recorded manually.

2.3.2 Analysis of exposure doses in medical examinations

The frequency of absorbed doses during medical examinations is shown in Fig.6. The male-female total and female mode are 0.18 mGy., while the mode for males was 0.22 mGy, which is approximately 22% higher. The median and mean for males and females combined are 0.23 and 0.25 mGy, respectively.

The relationship between the absorbed dose at the incident surface location and height, weight, abdominal circumference, and body mass index (BMI) was determined for the combined male and female data.

The correlation coefficient between absorbed dose and height was 0.3671, with correlation coefficients of 0.8349 for weight, 0.7882 for abdominal circumference, and 0.8386 for BMI. The correlation was weak for height but strong for BMI, weight, and abdominal circumference. Particularly, the correlation coefficients between BMI and weight wear close to 1.0, indicating a strong correlation.

However, since BMI is calculated through the

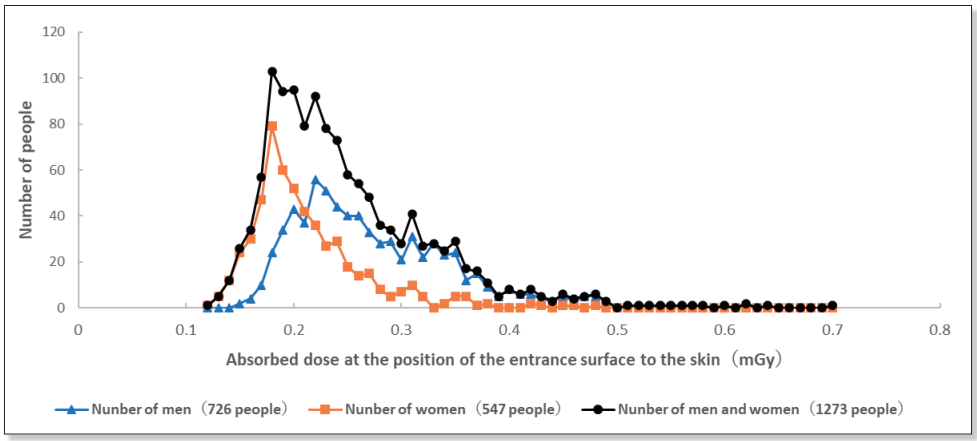

Fig.6　Frequency of the absorbed dose

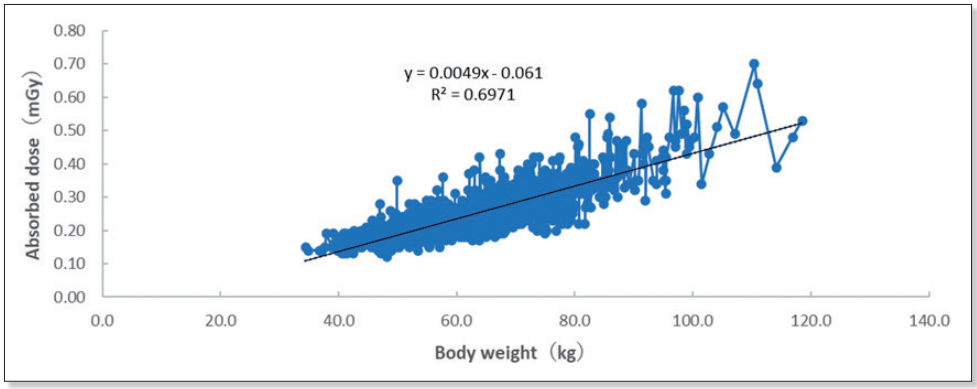

Fig.7　Relationship between the body weight and absorbed dose at the time of chest radiography

formula weight in kg / (height in m)^2, weight is easier to use; thus, weight was used for dose control in the other chest radiography rooms. Fig.7 shows the relationship between body weight and absorbed dose.

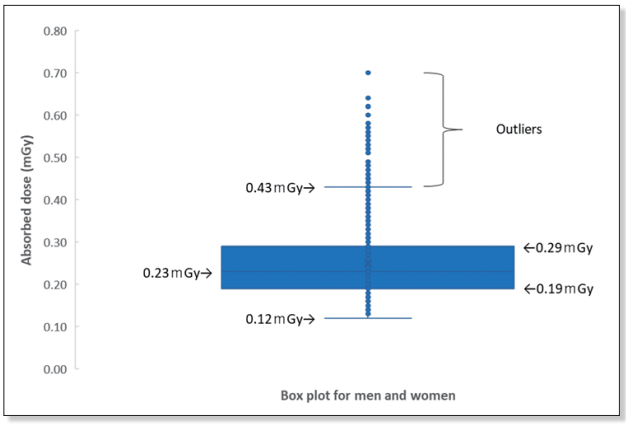

Fig.8　The box-and-whisker diagram

2.4　Dose control in other chest radiography rooms

The doses were measured using the custom-made dosimeter for chest radiography. The absorbed doses for the 1,273 male and female participants were statistically processed to produce box-and-whisker diagrams [4] as shown in Fig.8.

The lower part of the box had a 25th percentile tile value of 0.19 mGy. The upper part of the box has a 75th percentile tile value of 0.29 mGy. The median is 0.23 mGy, and the mean is 0.25 mGy. The lower "whiskers" are 0.12 mGy, and the upper "whiskers" are 0.43 mGy.

Therefore, the dose frequency is shown in Fig.9, using the dose frequency calculated by excluding the outliers in Fig.8 from the aforementioned dose frequency in Fig.6.

Fig.9 shows a median value of 0.23 mGy and

mean value of 0.24 mGy.

The difference between the median and mean values was small, and dose control was performed by assuming a normal distribution.

For dose control in the other chest radiography rooms, a lung field phantom (PBU-SS-2. Kyoto Scientific) was used under clinical conditions with a phototimer. The irradiation dose (μC/kg) under those imaging conditions was measured using the custom-made ionization chamber dosimeter (Roueiken type) [3] and multiplied by the backscatter coefficient and absorbed dose conversion coefficient to obtain the absorbed dose (mGy) at the incident surface position for 25 chest imaging rooms (vehicle-mounted: 22 rooms, facility-mounted: 3 rooms) (computed radiography [CR]: 2 rooms, flat panel detector [FPD]: 23 rooms). The absorbed doses ranged from 0.13 to 0.23 mGy.

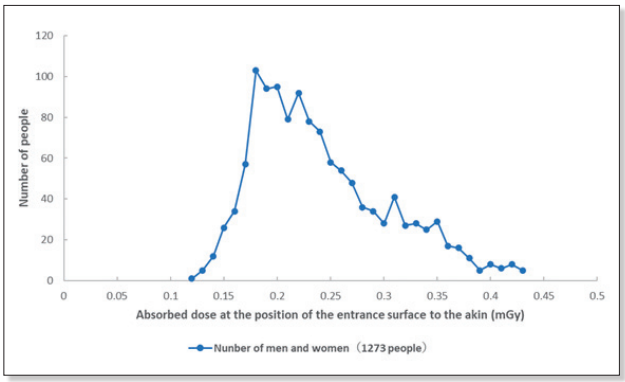

Fig.9 Frequency of the absorbed dose

3. Results

3.1 Overview of the custom-made dosimeter for chest radiography

The electrode in the center was covered with aluminum foil, which blocked the light-illuminated field. However, the area around it was made of polyester film; hence, taking pictures without any difficulty in positioning is possible.

3.2 Characterization of the custom-made dosimeter for chest radiography

3.2.1 Beam quality characteristics results

The measurement results at 80 to 130 kV are shown in Fig.10. The beam quality dependence is in the range +8% to -5%. Since chest imaging is almost exclusively performed at 120 kV, it can be said that there was no error.

3.2.2 Dose rate characteristic results

The results of measurements at dose rates from 144 to 300 (μC/kg)/s are shown in Fig. 11. The dose rate dependence is within -3%.

In chest imaging, dose control is possible with minimal dose quality or dose rate dependence.

3.3 Clinical application of the custom-made dosimeter for chest radiography

Since the correlation coefficient between the

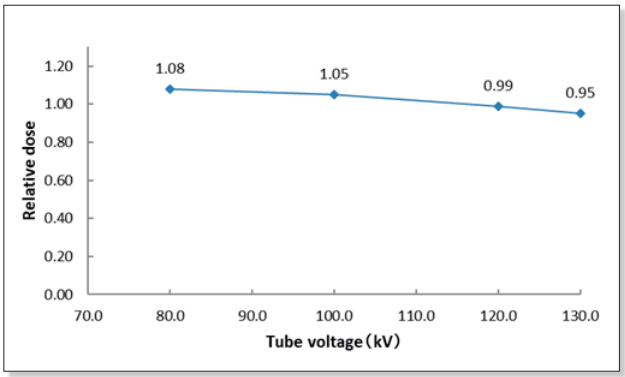

Fig.10 Beam quality dependence of an ionization chamber

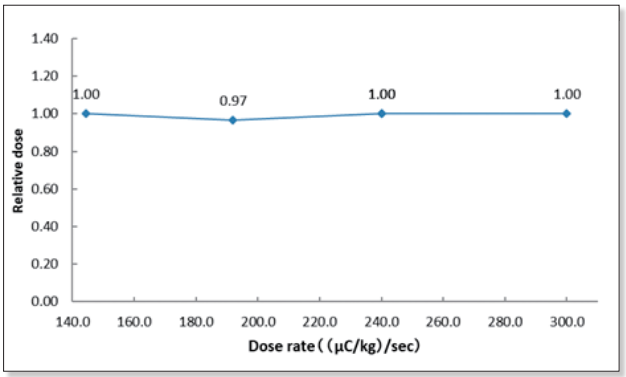

Fig.11 Dose rate dependence of an ionization chamber

absorbed dose and body weight for 1,273 male and female participants, whose data were taken with the custom-made dosimeter for chest radiography, showed a strong correlation, body weight was used to control doses in other chest radiography rooms.

3.4 Dose control in other chest radiography rooms

The regression equation between body weight and absorbed dose (y = 0.0049x - 0.061) in Fig. 7 was used for dose control in the other chest imaging rooms.

In the normal distribution, when the mean value is represented as μ and standard deviation as σ, 68.27% of the values are included in the $\mu \pm \sigma$ range. Therefore, the absorbed dose calculated by the regression equation is represented by one line in the middle and the σ range ($\pm$ 34%) by two lines. Fig.12 shows an example of the dose notation in another chest radiography room (absorbed dose: 0.15 mGy, vehicle-mounted type: FPD).

An example of a posting board in another chest radiography room (absorbed dose: 0.15 mGy, vehicle-mounted type: FPD) is shown in Fig.13. The notice was mounted next to the radiation room such that the radiation dose can be estimated based on body weight.

Examples of dose notations and postings for 0.15 mGy are shown here, but similar dose notations were used for all 25 chest radiography rooms with absorbed doses between 0.13 and 0.23 mGy, and postings were installed.

In addition, there were initially three rooms (0.23, 0.27, and 0.21 mGy) with equipment that exceeded the DRLs 2020 examination chest frontal incident surface dose of 0.2 mGy. The lung field phantoms were taken under reduced imaging conditions, and the images were eval-

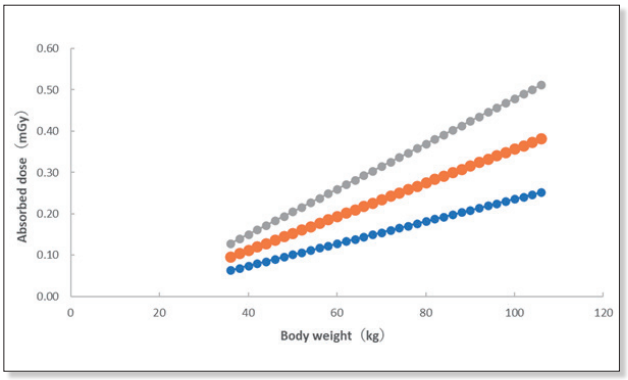

Fig.12 Relationship between the body weight and absorbed dose

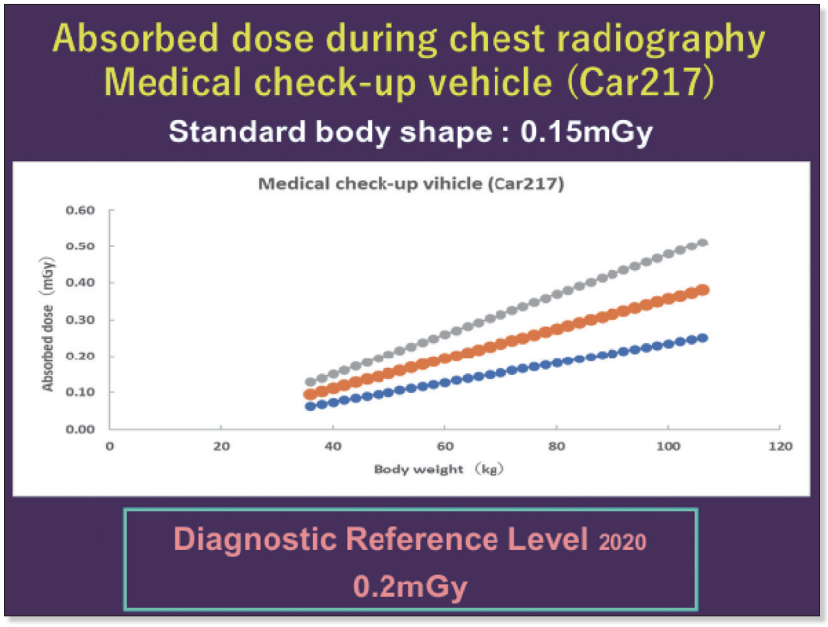

Fig.13 Postings for radiation dose control

uated by one doctor and six radiologists. Two rooms (0.27 mGy to 0.23 mGy and 0.21 mGy to 0.19 mGy) were able to reduce the dose.

Two rooms (0.23 mGy: two rooms) had equipment that exceeded 0.2 mGy of the DRLs 2020 examination chest frontal incident surface dose; however, all were vehicle-mounted and had been installed for 16 years, and the digital imaging equipment was CR equipment.

4. Considerations

In medical examinations, chest radiography requires the imaging of many examinees in a short period of time, and there is often insufficient time to consider individual exposure doses. Although installing dosimeters in all chest radiography equipment is desirable, it is difficult to do so in terms of cost and time. We also compared the results of computer software calculations and showed that they wear 10-20% lower.

Therefore, we used a simple method to estimate the absorbed dose at the incident surface location based on the body weight, which is strongly correlated with the absorbed dose of the examinee. A strong correlation between BMI and incident surface dose on chest radiography was observed [5]. It has also been reported that there was a strong correlation between BMI and incident surface dose in gastric radiography [6].

We also found similar results regarding the strong correlation with BMI and a similarly strong correlation with body weight; therefore, we decided to use the participant's weight for easier management.

5. Conclusion

A custom-made dosimeter for chest radiography was fabricated to control the exposure doses during chest radiography in health examinations in which many examinees wear examined.

The characteristics of the system were also confirmed to maintain sufficient accuracy, and the radiation dose during chest imaging was measured in a clinical setting. By analyzing and statistically processing the measurement results, a bulletin board was posted in each chest imaging room to enable the estimation of the dose from the weight of the examinee in the other chest imaging rooms. This enabled us to confirm the estimated doses of the examinees and establish a system to appropriately respond to inquiries from examinees regarding radiation exposure by providing them with the estimated doses and a separately prepared medical exposure Q&A (radiation exposure and effects on the human body, etc.).

Acknowledgements

We thank Prof. Toshioh Fujibuchi of the Department of Health Science, Faculty of Medical Sciences, Kyushu University for his guidance in calibrating the custom-made dosimeter. We also thank the members of the Department of Radiology, Department of Medical Technology, Kyushu University Hospital for allowing us to borrow the lung field phantom.

We would like to thank Editage (www.editage.com) for English language editing.

Ethics statement

Although we believe that this study needs to be reviewed by an ethics review committee because it includes the radiation dose, height, weight, abdominal circumference, and BMI of the examinees, our facility does not have an ethics review committee. Therefore, we consulted the "Medical Ethics Review Committee" of the Japanese Association of Radiological Technologists and conducted a full exchange of views with the facility manager (director). The study was then conducted based on the stipulation of the "Privacy Policy" of the facility's website such as the use of anonymous data

as sample data, including conference presentations, and obtaining the consent of the examinees on the examination forms.

Conflicts of interest

There are no conflicts of interest to disclose with respect to this study.

References

1) Eishu Shinkai: Patient dose control in X-ray examination. Japanese Journal of Radiological Technology, Vol.57, No.4, 377-387, 2001.
2) Eishu Shinkai, et al.: Property evaluation of newly developed patient double electrode ionization chamber for measuring patient exposure. Japanese Journal of Radiological Technology, Vol.52, No.5, 639-644, 1996.
3) Eishu Shinkai, et al.: Dosimetry in medical examinations - Characterisation of a custom-made ionization chamber dosimeter (Roueiken type) -. Annual meeting abstracts of the Kyushu Radiological Medical Technology, 109, 2012.
4) Hiroshi Hayama: Textbook of statistics for data analysis. Impress Co., Ltd, 1-252, 2018.
5) Yasuki Asada, et al.: BMI and incident surface dose analysis in general radiography. Japanese Society of Radiological Technology General Conference Abstracts, 2005.
6) Yoichi Ohta, et al.: Basic study of dosimetry in gastric X-ray examinations for lifestyle-related health check-ups. Journal of Gastrointestinal Cancer Screening, Vol.58, No.2, 83-92, 2020.

Received June 24, 2021; accepted February 15, 2022

Content analysis in the proceedings "Study Group on the Appropriate Management of Medical Radiation"

SAITO Hiroki, TOKUSHIGE Yumiko, MARUYAMA Sho, IWAI Tsugunori, KATOU Hideki, HOSHINO Syuhei

Gunma Paz University School of Radiological Sciences, Faculty of Medical Science and Technology

Note: This paper is secondary publication, the first paper was published in the JART, vol. 69 no. 837: 21-27, 2022.

Key words: Dose control, minutes, text mining, cluster analysis, correspondence analysis

【Abstract】

In April 2020, a ministerial ordinance was enforced to partially revise the Medical Care Act Enforcement Regulations. The amendment stipulates that the facility manager assigns a person in charge of the safety management system related to radiation medical care, formulates guidelines, trains staff, and manages and records patient doses. The Ministry of Health, Labor and Welfare (MHLW) has established the "Study Group on the Appropriate Management of Medical Radiation" and the minutes of the meeting are available as text data on the MHLW website.

In this study, the minutes of the review meeting were subjected to content analysis (cluster analysis and correspondence analysis) using KHcoder3. In the cluster analysis, 10 clusters were set up so that the keywords of the ministerial amendment, "record," "training," and "responsibility," would not be in the same cluster. Each Cluster appeared depending on the number of meetings. Each Cluster appeared depending on the number of meetings. Correspondence analysis was conducted on "record" and "responsibility" to clarify their relationship with other "words". The "record" was to facilitate the UNSCEAR Global Survey, and the "responsibility" was to promote the WHO/IAEA International Plan of Action on Patient Protection.

In this study group, the relevant laws and regulations were explained in the 1st meeting, the necessity of dose recording and the subjects of training in the safety management system were discussed in the 3rd, 4th, and 5th meetings, and the 6th, 7th, and 8th meetings. Regarding the guidelines for the safety management system, the rules regarding the person in charge, records, training, etc. were discussed.

1. Introduction

In April 2020, a ministerial ordinance partially amending the Ordinance for Enforcement of the Medical Care Act went into effect (Ordinance of the Ministry of Health, Labor and Welfare, (MHLW), No. 21 of 2019)[1]. This ordinance indicated that the medical facility administrator is responsible for the safety management system related to radiological treatment, and required to establish guidelines, provide staff training, and control and record patient doses. To date, radiation control to reduce radiation doses to the general public and workers has implied the use of radiation protection standards in facilities and structures and dose limits for those entering them in accordance with the Medical Service Act and related laws/ordinances. In contrast, the medical exposure to patients has not been controlled through dose limits even if X-ray examinations are performed at the lowest possible dose according to the International Commission on Radiological Protection (ICRP) "*as low as reasonably achievable*" principle[2]. These trends in radiation protection are based on the research of the United Nations Scientific Committee on the Effects of Atomic Radiation (UNSCEAR), the ICRP's recommendations on radiation protection, and the International Atomic Energy Agency (IAEA)'s guidelines. In particular, the IAEA compiled these recommendations into safety principles, requirements, and guidelines, which have been incorporated into the legal systems of various countries[3]. This has enabled us to implement radiation control in accordance with

international standards. The revision follows the same trend, and in April 2017, the MHLW launched the "Study Group on the Proper Management of Medical Radiation" and after eight meetings, the ministerial ordinance was revised[4]. However, there is little information on this revision of the ministerial ordinance, just an introduction to dose management software[5] and a preface by Yonekura[6]. Fortunately, the minutes of the study meeting are available as text data on the MHLW website.

Content analysis using text data has been long applied in research[7, 8]. Further, the widespread use of analysis software, such as KHcoder3[9], has allowed quantitative text data analysis. For instance, in sociology, Watabe's case study of hierarchical cluster analysis[10] and Kuwahata's case study of co-occurrence network analysis[11] used KHcoder3 and data from the proceedings of the Diet. In the field of radiology, Tokushige et al. reported a quantitative analysis of a questionnaire survey of medical radiology technician training schools[12].

This study aimed to clarify the process leading to the establishment of patient dose records and safety management systems by text analyzing the minutes of the review meeting using KHcoder3.

2. Materials and Methods

A KHcoder3 Windows version including ChaSen (WinCha 2000 R2), MySQL 5.6, Perl 5.14, R 3.1, and ggplot2 2.1[13] was used for analysis.

2.1 Preprocessing of text data

The minutes (.docx) of the 1st through 8th meetings of the "Study Group on the Proper Management of Medical Radiation" were downloaded from the MHLW website. At the beginning of each meeting, the secretary introduces the attendees; then, the chairperson gives their opening statement, followed by the explanation of materials by the secretary, and a question-and-answer (Q&A) session. Only the agenda items related to this proper management were subjected to text mining. Text data was created in Excel format (.xlsx).

The agenda is marked by the speaker, followed by what was said. The first line of the Excel worksheet had a header including <Text>, <Part>, and <Chapter>, and the agenda item was entered on the second line. The actual proceedings were entered in <Text>, the numbers in <Part>, the secretary's explanation as "1," and the Q&A as "2" in <Chapter>; the Chair's greeting was omitted. As the second agenda item was just a title change, it was excluded from this analysis. Next, a KHcoder3 project was registered and <preprocessing> was performed to check the text data.

As both "Diagnostic Reference Levels (DRL)" and "diagnostic reference level" were found in the minutes, to detect them as a single term, we specified both in <Select Terms> and performed <Preprocessing> and <Execute Preprocessing>. Then, the program z1_edit_words3.pm (https://github.com/ko-ichi-h/khcoder/issues/101), which absorbs the two terms, was installed in the Plugin_jp folder and <plugin> and <distortion of notation> were executed.

This way, we obtained the number of sentences and paragraphs to be analyzed, the extracted words, and their frequency.

2.2 Cluster analysis

Cluster analysis was performed to confirm the pattern of occurrence of the extracted words and phrases. KHcoder3 uses a <Hierarchical Cluster Analysis> as default, but to consider the location information of words with small number of occurrences[14], a csv data file was created using <export> and <"extracted words x context vector" table>. For the extraction, the minimum number of occurrences was set to 55 (default value), csv data was output, R was initiated to read the csv data, and hierarchical cluster analysis was performed using the hclust function. The distance between clusters

was specified as ward.D2.

2.3 Bubble plots for meeting number and each cluster

Coding rules were developed to check the frequency of occurrence of the extracted words in each cluster of the meeting numbers. The words extracted in each cluster specified in the text data (.txt) are shown in Table 1. Finally, a bubble plot of meeting numbers and clusters was created based on the cross-tabulation table (<Tools>, <Coding>, and <Cross-tabulation table>).

2.4 Correspondence analysis of the characteristic words "record" and "responsibility"

In terms of proper management, the key points of the revision of the ministerial ordinance are the recording of patient doses and the establishment of a safety management system. In 3.1, "record" is included in Cluster 1 and "responsibility" in Cluster 10. In 3.2, Cluster 1 appeared at high frequency in the 3rd, 4th, and 5th times, and Cluster 10 in the 6th, 7th, and 8th times. Therefore, a correspondence analysis was conducted to confirm the relationship between these words and meeting number. Texts of the 3rd, 4th, and 5th meetings containing "record" were extracted from the text data of the minutes and a correspondence analysis (<tool>, <extracted word>, <correspondence analysis>) was performed setting the minimum number of occurrences to 5 (default value). Similarly, texts from the 6th, 7th, and 8th meetings containing "responsibility" were extracted and analyzed for correspondence.

Table 1 Coding rules

Cluster	Words
1	examination, CT, dose, record, exposure, appropriate
2	actual, patient, receive, use, just now, need, say, extremely, now, think, see, problem, appear, impact, data, year, Japan, DRL
3	concrete, correspondence, case, protection, standard, define
4	future, study, discussion, administrative, teacher, opinion, page, documents, explanation
5	optimum, justifiable, training, implementation, partial, basic, consider, at this time, form, viewpoint, each, regulation, do, radiation, medical treatment
6	facilities, hospital, equipment, medical, institutions
7	treatment, devices, irradiation
8	pharmaceuticals, radiation, target, RI, hazard, regulatory, relation
9	doctor, technologist
10	responsibility, system, management, safety

3. Results

3.1 Preprocessing and cluster analysis

After preprocessing, there were 1,890 sentences, 907 paragraphs, and 76,829 total extracted words (e.g., medical: 587 occurrences, radiation: 478). Figure 1 shows the results of the cluster analysis. Words found near each other in a sentence formed a hierarchy. As the number of clusters can be determined arbitrarily, to avoid that the keywords "record," "training," and "responsibility" of the revised ministerial ordinance were all clustered together, we defined 10 clusters with a height of 2.68 (see Table 1). The number of extracted words were 6, 18, 6, 9, 15, 5, 3, 7, 2, and 4 for Clusters 1–10, respectively (Fig.1).

3.2 Bubble plots for meeting number and each cluster

Table 2 shows a cross table of which meetings the Clusters containing the words created by the coding rules appeared in. χ^2 represents the χ^2 test result, with $p<0.05$ indicating the threshold for significance. Figure 2 shows the percentage of each cluster in each meeting based on this cross-tabulation table. The percentage of occurrence was calculated by dividing the frequency in each meeting number by the total number of occurrences (e.g., 51/252 for Cluster 1) and is shown as the square size. The colors represent standardized residuals: Pearson rsd (√mean × (frequency - mean)/

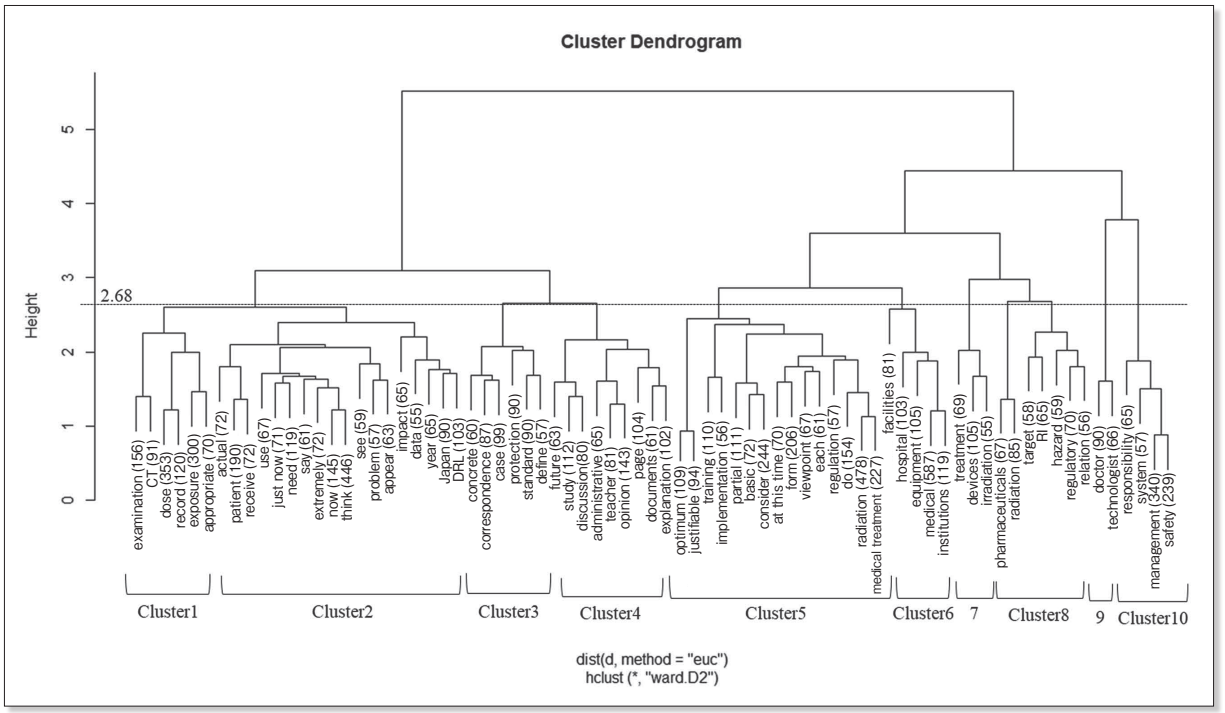

Fig.1 Cluster analysis

mean value), indicating the meeting in which the cluster appears more (or less) often, with warmer colors indicating more frequent appearance. The mean value corresponds to the number of current entries relative to the total number of sentences.

Cluster 1 appeared frequently in the 3rd, 4th, and 5th meetings, showing large standardized residuals. Clusters 2 and 5 often appeared in all meetings; standardized residuals were positive in the 3rd meeting for Cluster 2 and in the 6th and 7th meetings for Cluster 5. Cluster 3 appeared predominantly in the 7th meeting, although not so often, and showed large standardized residuals. Cluster 4 and 6 were moderately frequent but tended to appear in the 6th and 7th meetings. Cluster 7 and 8 did not occur often, but had large first standardized residuals. Cluster 9 and 10 did not occur very often, but showed large standardized residuals for the 6th, 7th, and 8th meetings.

Table 2 Cross-accumulation table of number of meetings held and clusters

Meeting Number	Cluster										n
	1	2	3	4	5	6	7	8	9	10	
1	51	149	81	108	143	104	51	95	5	63	252
3	59	93	33	39	60	46	13	9	3	5	106
4	63	79	24	51	68	47	9	12	3	28	99
5	90	115	35	52	97	56	16	9	4	24	146
6	34	89	30	66	99	70	10	26	20	59	123
7	43	68	46	56	78	46	10	18	16	33	93
8	17	47	19	37	60	31	4	30	15	37	88
sum	357	640	268	409	605	400	113	199	66	249	907
χ^2	128.95	52.66	26.43	22.97	39.25	15.34	22.73	82.52	61.41	75.61	
p<0.05	6.94E-30	3.97E-13	2.74E-07	1.65E-06	3.73E-10	9.00E-05	1.86E-06	1.05E-19	4.63E-15	3.45E-18	

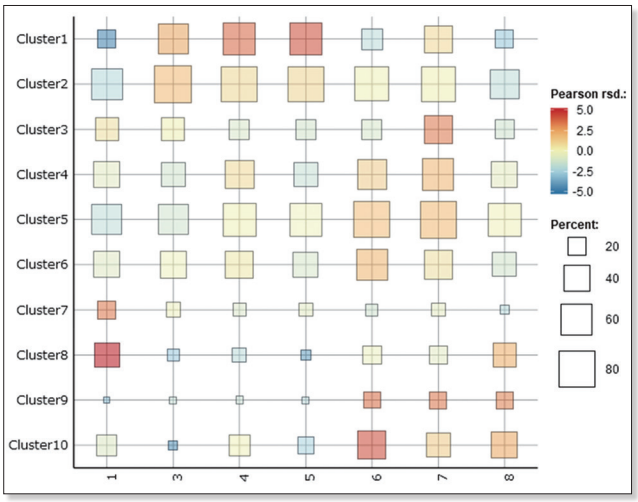

Fig.2 Bubble plot of meeting numbers and clusters

3.3 Correspondence analysis of the feature terms "record" and "responsibility"

Figure 3 shows the results of the correspondence analysis for the feature word "record." The number of target words was 73. The total number of words was 1,870 in the 3rd, 1,934 in the 4th, and 1,944 in the 5th meeting. Correspondence analysis is based on a 3×73 cross-tabulation table, with the proportion of occurrences (profile) between each word or meeting number determined by χ^2 distance [15]. The x-axis (component 1) represents the first dimension result of the word or conference number, and the y-axis (component 2) represents the second dimension result of the word or conference number, simultaneously distributed in a scatter plot. The values (0.2777, 61.33%) on the axes are contribution rates; the cumulative contribution rate of components 1 and 2 was 100%.

The origin (0, 0) represents the coordinates of the average profile; the closer to the origin, the more evenly distributed the words in every meeting. "Dose," "exposure," "medical," "irradiation," and etc., are some of these words. The feature word (the one appearing only once) appears on a straight line from the origin to the meeting number mark and outside of that mark. The 4th and 5th meetings appear on the right side of the x-axis, and many words commonly appeared. From the beginning, there were characteristic words such as "Japan," "IAEA," and "difficult" in the 3rd meeting, "hospital," "on-site," and "burden" in the 4th meeting, and "EU," "appropriate," and "training" in the 5th meeting. Several words followed a linear distribution between the third "IAEA" to the fourth "hospital," the fourth to the fifth "training," and the third "IAEA" to the fifth "training."

Figure 4 shows the results of the correspondence analysis of the feature word "responsibility." The number of target words was 43. The total number of words was 2,176 for the 6th, 982 for the 7th, and 1,285 for the 8th meeting. The correspondence analysis showed that the cumulative contribution of components 1 and 2 was 100% in a 3×43 cross-tabulation table. The 6th and 7th meetings were located to the left side of the x-axis.

"Responsibility," "management," "record," and "system" were distributed around the origin (0, 0). From there, there were characteristic words such as "hospital" and "occupation" in the 6th, "explanation" and "consider" in the 7th, and "regulation" and "pertaining to" in the 8th meeting. There were clusters of "technologist," "doctor," "dental," "justifiable," and "qualifica-

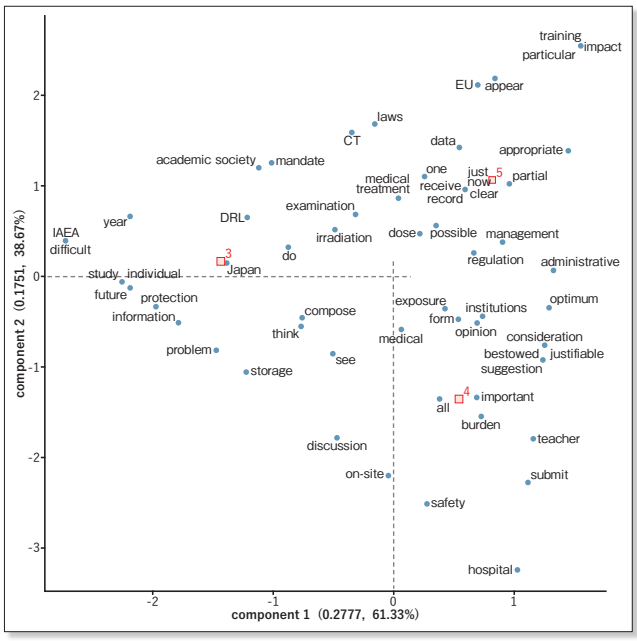

Fig.3 Correspondence analysis: record

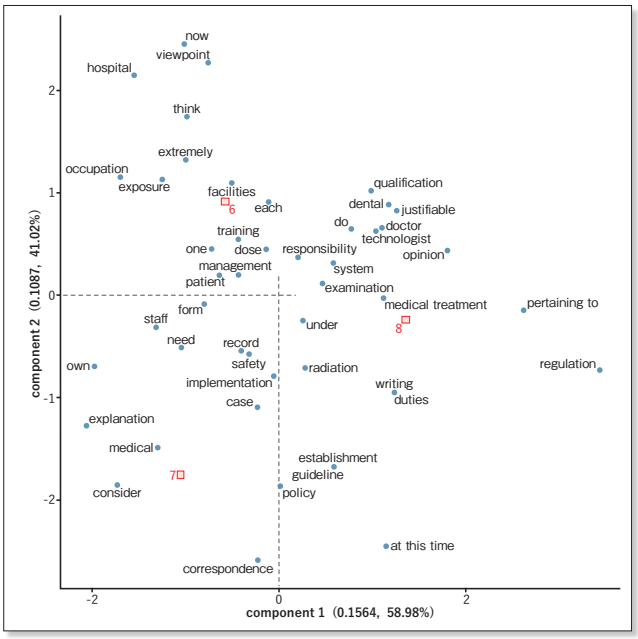

Fig.4 Correspondence analysis: responsibility

tion" in the 6th and 8th meetings, and of "policy," "guideline," and "establishment" in the 7th and 8th meetings. Some words were linearly distributed between "hospital" in the 6th and " consider" in the 7th, but not between the 7th and 8th, nor between the 6th and 8th.

4. Discussion

The revision of the ministerial ordinance made it mandatory for the first time to record patient doses and required the establishment of a dose control system. We were asked for public comment two years prior to the announcement of the revision of the ministerial ordinance (from January 9, 2019 to February 7, 2019), and in March 2019, we received a notice from the Director General (Medical Policy Bulletin No. 0312 No. 7). Therefore, text mining of the minutes of these proceedings was conducted to analyze the content.

4.1 Relationship between cluster analysis and meeting number

In cluster analysis, the words are clustered according to their close positions of occurrence. This time, we have subjectively determined 10 clusters according to the key words of the revised ministerial ordinance. This method is common in cluster analysis [16]. If the distance (Height = 2.68) increases, the clusters are aggregated to 6 and each cluster contains more words, while if the distance decreases, the number of words in each cluster is extremely small. Although the analysis results may change depending on clustering rules, consideration was given to the keywords in the ministerial ordinance revision.

Cluster 1 includes "dose," "record," and "exposure" and Cluster 2 includes "DRL;" Clusters 1 and 2 contain the key terms of the revision of the ministerial ordinance. They appeared in the 3rd, 4th, and 5th meetings, suggesting that patient dose control was conducted using DRL and that discussions were held on recording. Cluster 3 includes "protection" and "standard," Cluster 9 includes "doctor" and " technologist," and Cluster 10 includes "responsibility" and "system," suggesting that the discussions on the person responsible for the safety management system took place in the 6th–8th meetings. Clusters 4–6 include words such as "page," "documents," "basic," "consider," "medical," and "institutions," mentioned when the secretary explained the meeting, as well as words for medical facilities and equipment central to the meeting agenda, which generally appeared in all meetings. Clusters 7 and 8 were the first in which radiation-related laws such as the Law Concerning Regulation of Radioactive Isotopes were explained. Since this meeting included non-experts in radiation, the first half of the meeting served to explain trends in radiation control and the second to discuss how to develop a control system.

4.2 Correspondence analysis of "record" and "responsibility"

Although most text mining methods analyze and evaluate the subject matter of a text using the number of frequently occurring words as an indicator, we believe that it is difficult to

capture the background of the subject matter. The advantage of KHcoder3 is that the analyst can extract and analyze words independently. Through the cluster analysis described above, the author chose "record" from Cluster 1 to focus on patient dose records and "responsibility" from Cluster 10 to focus on the exclusive responsibility for the safety management system.

4.2.1 Feature word "record"

One of the major points of the revision of the ministerial ordinance is the recording of patient doses. The target equipment are CT, IVR, SPECT, and PET, which have high exposure doses. To manage patient doses easily, management software use has become widespread in clinical practice [17].

The 3rd meeting was the "IAEA." According to the minutes, international trends were introduced at the 3rd meeting. In the report, during UNSCEAR's global survey [18], Japan is struggling to collect dose data. On the other hand, at the IAEA, it was introduced that doses are managed by patient IDs through the smart card project [19]. The goal of the government is to establish a system to record and track medical exposure history (smart card project), as is being worked on by the IAEA, with the goal of reducing medical exposure. The company expressed its ambition to make good use of its my number card for this history tracking. There was a "burden" in the 4th meeting. This was a concern about the "on-site" "burden" of conducting "record." They also asked for opinions on how to make the "record" data easier to get out. Thus, better performance of medical equipment and equipment capable of recording patient dose information in the radiology information system, irradiation and electronic medical records might decrease the burden on the site of treatment allowing implementation. Since 2000, the International Electrotechnical Commission has been displaying radiation doses on equipment, including computed tomography dose index and dose length product for X-ray CT systems [20], and the reference air kerma rate, integrated reference air kerma, and integrated area dose at the patient entrance reference point are displayed on IVR systems [21]. The information is centrally managed by dose management software via the DICOM Radiation Dose Structured Report. However, clinical sites are struggling due to the lack of test protocol names, etc. [22]. Therefore, it is important to standardize the medical information to facilitate dose control and to easily obtain representative Japanese values in each examination site. The 5th meeting included "training." It was stated by the secretary that this can be properly managed to justify and optimize radiation protection by "training" and "record" of doses to radiation practitioners.

Based on the above, from the 3rd to the 5th meetings, proper management of radiological practice was agreed to be carried out through dose recording and training.

4.2.2 Feature word "responsibility"

There was "occupation" in the 6th meeting. The responsible person can be a doctor, dentist, or radiology technologist who can irradiate the human body (i.e., can press a button on a radiation device) but who is not responsible for the need of radiological treatment, but can be a radiology technician because he/she establishes guidelines and systems. An "explanation" was provided at the 7th meeting. Despite the opinion that nurses could provide explanations to patients to lower the burden on physicians, it was determined that medical treatment and explanation belong together, as required by the World Health Organization, the IAEA [23], and others [24, 25]. The 8th meeting, held in response to public comments, referred to "regulations." It was noted that there were many comments regarding the regulations for safety managers. The secretary proposed that a radiological technologist can be a safety manager only when the system is justified by a doctor or

dentist and can give instructions to the radiological technologist. The role of the responsible person is the justification of radiological inspections but the establishment of a safety management system, including the formulation of guidelines and the implementation of training.

Accordingly, the 6th–8th meetings served to discuss the selection of the responsible person and the establishment of a management system.

Conclusion

In the "Study Group on the Proper Management of Medical Radiation" the 1st meeting explained the relevant laws and regulations, the 3rd, 4th, and 5th meetings discussed the necessity of dose records and the subjects of training in the safety management system, and the 6th, 7th, and 8th meetings discussed the guidelines for the safety management system, including regulations on the responsible person, records, training, etc.

The present text mining analysis of the minutes of the "Study Group on the Proper Management of Medical Radiation" revealed the establishment of patient dose control and safety management systems based on international trends to properly manage justification and optimization in radiological practice.

References

1) Japanese Society of Nuclear Medicine: Enforcement of the Ministerial Ordinance Partially Revising the Ordinance for Enforcement of the Medical Care Act, etc., http://jsnm.sakura.ne.jp/wp_jsnm/wp-content/uploads/2019/03/0b991eb1e78fb147b7db007c53e1d308.pdf (March 31, 2021).
2) ICRP: Recommendations of the International Commission on Radiological Protection, ICRP Publication 26, Ann. ICRP, 1 (1977).
3) Yasuhito SASAKI: Considerations as a former member of the International Commission on Radiological Protection (ICRP), Trends in the sciences, 25.3: 12-18, 2020.
4) Ministry of Health, Labour and Welfare: Study Group on Appropriate Management of Medical Radiation, https://www.mhlw.go.jp/stf/shingi/other-isei_436723.html (March 28, 2021).
5) Defeng CHEN, et al.: Development of Patient Dose Management System FINO.XManage, Konica Minolta technology report, 17: 71-75, 2020.
6) Yoshiharu YONEKURA: International Framework for Radiation Protection and Safety Management, Journal of the Japanese Society of Radiation Safety Management, 19.2: 69-69, 2020.
7) Speed, John Gilmer: Do newspapers now give the news?, Forum, Vol. 15, 1893.
8) MATHEWS, Byron C. A study of a New York daily, Independent, 68, 82-86. 1910.
9) Koichi HIGUCHI: Quantitative Analysis of Textual Data: Differentiation and Coordination of Two Approaches, Sociological Theory and Methods, 19.1: 101-115, 2004.
10) Haruka WATANABE: Investigation of the themes of public policy based on text analysis: Case of the discussion on public theatres in local councils and committees, The Society of Socio-Informatics, 9.1: 1-15, 2020.
11) Yoichiro KUWAHATA: A Study on the Policy Making Process about Disease: Quantitative Text Analysis of Meeting Minutes of "HTLV-I Control Promotion Council", Meikou College University Thesis, 50: 48-70, 2017.
12) Yumiko TOKUSHIGE, et al.: Survey of the implementation status of clinical practice in radiological technologist education, The Japan Association of Radiological Technologists, 68.4: 369-376, 2021.
13) KHcoder 3: Required Software/Hardware, https://khcoder.net/spec.html (April 18, 2021).
14) Koichi HIGUCHI: Quantitative Text Analysis for Social Research, 42-43, Nakanishiya Publishing Co., 2020.
15) Michael Greennacre: Theory and Practice of Response Analysis, 33-40, Ohmsha, 2020.
16) H. C. Romesburg: Cluster analysis for researchers. 28, Uchida rokakuho, 1992.
17) Kiminobu EGAWA: Advantages of Introducing the Cloud-based Dose Management System "MINCADI" at Group Hospitals, 35.10: 54-55, 2020.
18) Reiko KANDA, et al.: Report on "International Activities on Occupational Exposure Dosimetry", Japanese Journal of Health Physics, 52.3: 212-217, 2017.
19) IAEA Smart Card/SmartRadTrack Project: https://www.iaea.org/resources/rpop/resources/smart-card (April 18, 2021).
20) JIS Z 4751-2-44: Medical electrical equipment-Part 2-44: Particular requirements for the basic safety and

essential performance of X-ray equipment for computed tomography.
21) JIS Z 4751-2-43: Medical electrical equipment–Part 2-43: Particular requirements for the basic safety and essential performance of X-ray equipment for interventional procedures.
22) Masahiko KONNO, et al.: “Radimetrics” Everywhere ～Dose information in a flash, INNERVISION, 35.10: 56-57, 2020.
23) WHO/IAEA: BONN CALL FOR ACTION 10 Actions to Improve Radiation Protection in Medicine in the Next Decade, https://www.iaea.org/sites/default/files/17/12/bonn-call-for-action.pdf (April 18, 2021).
24) The Japanese Society of Radiation Public Safety: A Guide for Medical Institutions and Local Medical Administrations on the Appropriate Management of Medical Radiation, http://www2.jart.jp/news/ib0rgt0000006cgw.html (March 21, 2023).
25) Japan Radiological Society: Guidelines for Safety Management System for Medical Radiation, http://www.radiology.jp/content/files/20191004_01.pdf (April 18, 2021).

Received December 24, 2021; accepted May 16, 2022

Student issues based on the results of clinical training of radiological technologists

MUTO Hiroe, NAKAYA Koji, MATSUURA Kanae

Department of Radiological Technology, Faculty of Health Science, Suzuka University of Medical Science

Note: This paper is secondary publication, the first paper was published in the JART, vol. 69 no. 842: 16-23, 2022.

Key words: Clinical training education, radiological technologist, student assignments, COVID-19

【Abstract】
The purpose of this study was to analyze the results from a 3-year clinical training evaluation conducted at the authors' university and to identify problematic issues in training education for students who aim to become radiological technologists. Participants were 325 university students who were in their fourth year of clinical radiological technologist training between 2019 and 2021. The clinical training evaluations of these students comprise a series of items and sub-items. We asked clinical training instructors to grade each item. Students had little knowledge about the cost of radiological examinations, and some students were unable to write training reports sufficiently. An analysis of clinical training evaluations indicated that some radiological technologist students had little knowledge about the cost of radiological examinations and showed poor report writing ability. Future clinical training should seek to strengthen the guidance offered to students on these topics in pre-education before conducting clinical training. We believe our findings can help facilitate further improvements in the development of clinical training.

Introduction

University training for radiological technologists in Japan follows a four-year curriculum. In those four years, students acquire the specialized knowledge necessary for practicing as a radiological technologist. In addition to classroom lectures, university education involves clinical skills training to prepare radiological technologists to work at a hospital. X-ray photography education, moreover, is continuously advancing, and thus clinical training education is indispensable for the production of aspiring radiological technologists[1]. At our university, clinical training is provided in the first half of the fourth year; during this training phase, students are taught by radiological technologists working in hospitals. The clinical training is conducted in a general hospital, and our aim is for students to acquire the clinical skills for the modality in which a given radiological technologist practitioner is engaged: general radiography, computed radiography, magnetic resonance imaging, angiography, ultrasonography, nuclear medicine, and radiotherapy. The Department of Radiation Technology Science at our university attracts more than 100 students from all over Japan every year. Therefore, because it is impossible to provide clinical training in a hospital near the university for all the students, we ask students to conduct their clinical practice at their local hospital. In the past, clinical training centered on the tour type has been conducted. However, in recent years, participatory clinical training has begun to be adopted to help students acquire more clinical skills[2]. At this point in their training, students do not yet have a radiological technologist license; therefore, they are not allowed to irradiate patients, although they have acquired other clinical skills through clinical training (e.g., patient treatment, image analysis processing, and understanding of examination content).

As part of our clinical training grade

evaluations, hospital-based clinical training instructors engaged in student guidance are asked to rate the grade evaluations created by our university. On the basis of the grade evaluations provided by the clinical instructors, the credits for clinical training are approved or rejected. However, we realized the potential usefulness for clinical training development (and thus for students) of identifying potentially problematic issues from among the grade evaluation data. Therefore, the purpose of this study was to analyze the past 3 years' grade evaluations for clinical training at our institution in Japan and to identify problems in clinical training education for students.

Materials and Methods

Targets

A total of 325 participants comprised: 100 students (69 male, 31 female) who underwent their fourth-year university clinical training in 2019; 108 students (61 male, 47 female) who underwent their fourth-year university clinical training in 2020; and 117 students (69 male, 48 female) who underwent their fourth-year university clinical training in 2021. The prescribed duration for clinical training set by our university is 57 days (training time per day is 8 hours). However, in 2020 and 2021, the clinical training period for some students was shortened owing to the response of the local hospital in which they were training to the effects of coronavirus disease 2019 (COVID-19) infection. This study was approved by our University's Conflict of Interest Management Committee and its Clinical Research Ethics Review Committee.

Grade evaluations for clinical training

Table 1 shows the items that comprise the clinical training evaluation for our university. The main items used for evaluation are as follows: item 1 evaluates the acquisition of basic practical radiological technologist skills; item 2 evaluates the development of knowledge about and analytical ability for operating the hospital radiation department; item 3 evaluates the ability to respond appropriately to patients; and item 4 evaluates the development of responsibility and awareness as a member of the medical team. To assess the topics covered in the main items in more detail, seven sub-items were set for each main item, as shown in Table 1. After clinical training is completed, the clinical training instructor evaluates all the sub-items for each student on a 4-point scale (1 point: inferior, 2 points: standard, 3 points: good, 4 points: excellence). From FY2019 to FY2021 the clinical training evaluations were conducted using the same method described above. The setting and evaluation method for these clinical training evaluation items were created by the university's clinical training instructor and have been used for 3 years to evaluate the university's clinical training program.

Comparison of clinical training evaluation scores (comparison of sub-items)

The sub-item scores (average value ± standard deviation (SD)) for the clinical training evaluation for all students (total students from 2019 to 2021) were calculated. The score for each sub-item (average value ± SD) was calculated for each year, and a comparison was made to see if there were differences in each sub-item score in each year.

Comparison of clinical training evaluation scores (comparison of main items)

The average values ± SDs of the main items were calculated from the average sub-item values for all students, and the overall scores for each main item were compared. The average values ± SDs of the main items for each year were calculated from the average value of the sub-items for each year, and

Table 1 Main and sub-items for clinical training evaluation

Items for grade evaluation in clinical training
Main item 1: Acquire basic practical skills as a radiological technologist
Sub-item 1-1. You can work on pre-learning and take part in practical training.
Sub-item 1-2. You can record what you experienced in training in the report and use it in future training.
Sub-item 1-3. You can clarify your own tasks from daily reports and study to gain knowledge that you lack.
Sub-item 1-4. You can work on the tasks you have been instructed to do and give feedback on the next day's training.
Sub-item 1-5. You know the structure and installation of the hospital that considers patient safety (including infection prevention and accident prevention) and comfort, and you can explain these in the report.
Sub-item 1-6. You understand the structure and installation of hospitals with staff safety (including infection prevention and accident prevention) and comfort in mind, and you can write down their characteristics in a report.
Sub-item 1-7. You can correlate and analyze the knowledge and theory learned in the classroom with the experience and situations in clinical practice.
Main item 2: Develop knowledge about and analytical skills for the operation of the hospital radiation department
Sub-item 2-1. You comply with the rules set by the training facility.
Sub-item 2-2. You do not view electronic medical records without the permission of the leader.
Sub-item 2-3. You do not record any personally identifiable information in the report.
Sub-item 2-4. During training, you do not leave your records or belongings on the desk in the imaging room or elsewhere.
Sub-item 2-5. You understand the functions and roles of the Radiology Department members (chief radiological technologist, sub-chief radiological technologist, chief radiological technologist of each modality, etc.).
Sub-item 2-6. You understand the role of the chief for each modality.
Sub-item 2-7. You understand the medical fees that are required for each radiological examination.
Main item 3: Learn how to respond appropriately to patients
Sub-item 3-1. Your appearance is suitable for medical personnel, and you can perform clinical training.
Sub-item 3-2. You can greet patients, staff, and leaders, etc.
Sub-item 3-3. You use polite language, such as using honorifics, when talking to patients.
Sub-item 3-4. You give an honorific title to your surname when you call a patient.
Sub-item 3-5. You try to read the patient's emotions in their facial expressions and wording.
Sub-item 3-6. You can respond to the patient with a clear and easy-to-hear voice.
Sub-item 3-7. You can flexibly adapt to children and elderly patients.
Main item 4: Develop responsibility and awareness as a member of the medical team
Sub-item 4-1. You are not late for clinical training.
Sub-item 4-2. You can keep the time you have promised to your teacher or clinical practice leader.
Sub-item 4-3. You reveal your whereabouts to the clinical practice leader and act (i.e., do not take a break without permission).
Sub-item 4-4. You can meet deadlines for submitting clinical training reports and other assignments.
Sub-item 4-5. You strive to improve what has been noted by clinical practice leaders and teachers.
Sub-item 4-6. You take care of your own health.
Sub-item 4-7. If you have any questions, you ask or consult with the medical team leader.

the overall scores for the main items were compared to identify differences.

Statistical analysis

The Kruskal-Wallis test of one-way ANOVA was used to test for significance. The significance level was set to $p<0.05$. The P-value used a two-sided test. When a significant difference was observed between groups, the p-value-corrected Dann-Bonferroni test was used to determine which group differed significantly. Again, the significance level was $p<0.05$. We used Statistical Package for the Social Sciences (SPSS), version 26.0 (SPSS Inc., Chicago, IL, USA) for these analyses.

Results

Comparison of clinical training evaluation scores (comparison of sub-items)

Figure 1 shows the results of the clinical training evaluation scores for each sub-item for all students (total students from 2019 to 2021). The scores for each sub-item were as follows: 1-1 was 3.13 ± 0.62, 1-2 was 3.23 ± 0.60, 1-3 was 3.15 ± 0.60, 1-4 was 3.23 ± 0.59, 1-5 was 3.07 ± 0.53, 1-6 was 3.05 ± 0.53, 1-7 was 3.04 ± 0.57, 2-1 was 3.55 ± 0.54, 2-2 was 3.68 ± 0.50, 2-3 was 3.67 ± 0.47, 2-4 was 3.44 ± 0.55,

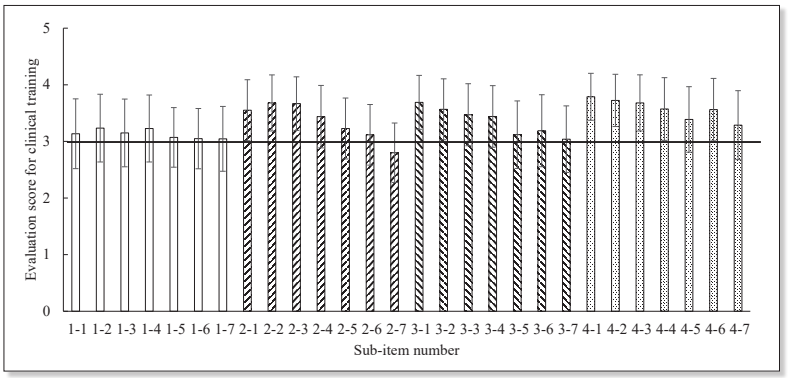

Figure 1 Scores for sub-items in the clinical training evaluations for all students (total students from 2019 to 2021). The horizontal black line indicates the average score of 3 points (good).

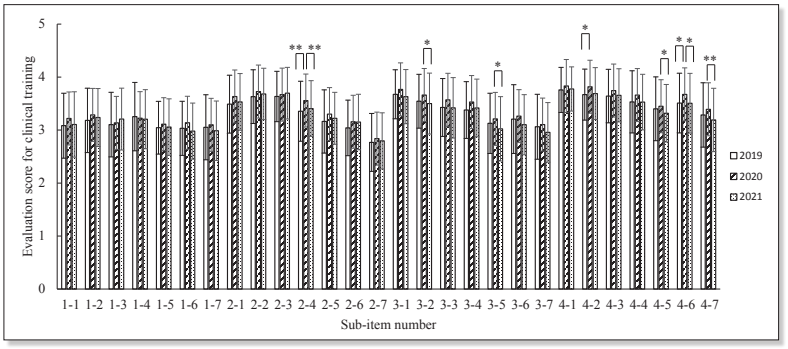

Figure 2 Scores for sub-items in the clinical training evaluations for each year. The Kruskal-Wallis test was used to test for significant differences between other groups. The significance level was set to P<0.05. When a significant difference was found, the P-value-corrected Dann-Bonferroni test was used to determine which group differed significantly.
*P<0.05, **P<0.01.

2-5 was 3.23 ± 0.54, 2-6 was 3.12 ± 0.54, 2-7 was 2.80 ± 0.52, 3-1 was 3.69 ± 0.48, 3-2 was 3.57 ± 0.54, 3-3 was 3.47 ± 0.55, 3-4 was 3.44 ± 0.54, 3-5 was 3.12 ± 0.60, 3-6 was 3.19 ± 0.64, 3-7 was 3.04 ± 0.59, 4-1 was 3.79 ± 0.41, 4-2 was 3.72 ± 0.46, 4-3 was 3.68 ± 0.50, 4-4 was 3.57 ± 0.55, 4-5 was 3.39 ± 0.58, 4-6 was 3.56 ± 0.55, and 4-7 was 3.29 ± 0.61.

Figure 2 shows a graph comparing each sub-item of the clinical training evaluation classified in 2019–2021. The Kruskal-Wallis test revealed significant differences between the years for the sub-items 2-4, 3-2, 3-5, 4-2, 4-5, 4-6, and 4-7 (sub-items 3-2, 3-5, 4-2, and 4-5 were $p<0.05$, and sub-items 2-4, 4-6, and 4-7 were $p<0.01$). The results of the Dann-Bonferroni test were as follows: $p<0.05$ was seen between 2020 and 2021 in 3-2, between 2020 and 2021 in 3-5, between 2019 and 2020 in 4-2, between 2020 and 2021 in 4-5, between 2019 and 2020 in 4-6, and between 2020 and 2021 in 4-6. We observed $p<0.01$ between 2019 and 2020 in 2-4, between 2020 and 2021 in 2-4, and between 2020 and 2021 in 4-7.

Comparison of clinical training evaluation scores (comparison of main items)

Figure 3 shows the scores for each of the main items for all students; they were: 3.13 ± 0.08 for 1, 3.35 ± 0.32 for 2, 3.36 ± 0.25 for 3, and 3.57 ± 0.18 for 4. The Kruskal-Wallis test showed a significant difference between groups ($p<0.05$). The Dann-Bonferroni test showed a significant difference between main items 1 and 4 ($p<0.01$).

Figure 4 shows a graph comparing each main item in the clinical training evaluation classified in 2019–2021. Scores for main item 1 were: 3.11 ± 0.08 in 2019, 3.17 ± 0.07 in 2020, and 3.11 ± 0.11 in 2021. Scores for main item 2 were: 3.30 ± 0.32 in 2019, 3.41 ± 0.33 in 2020, and 3.36 ± 0.32 in 2021. Scores for main item 3 were: 3.35 ± 0.22 in 2019, 3.44 ± 0.25 in 2020, and 3.29 ± 0.26 in 2021. Finally, scores for main item 4 were: 3.54 ± 0.26 in 2019, 3.65 ± 0.17 in 2020, and 3.52 ± 0.21 in 2021. The Kruskal-Wallis test showed no significant difference between the years in any of the major items (n.s.).

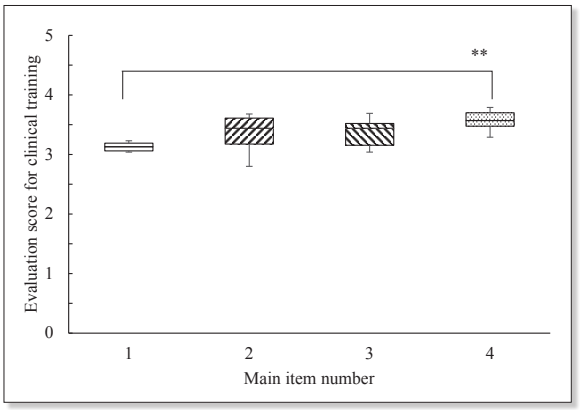

Figure 3 Scores for main items in the clinical training evaluations for all students (total students from 2019 to 2021). The Kruskal-Wallis test was used to test for significant differences between other groups. The significance level was set to $P<0.05$. When a significant difference was found, the P-value-corrected Dann-Bonferroni test was used to determine which group differed significantly.
**$P<0.01$.

Discussion

The purpose of this study was to analyze the grade evaluations for clinical training for the past three years at our institution and to identify problems in clinical training education for students. For students who aim to become medical professionals, clinical training education can give them the necessary skills for clinical practice. Therefore, this research attempts to identify and highlight problematic issues in students' clinical training to inform and facilitate the further development and improvement of clinical training education.

First, the method used for clinical training evaluation will be mentioned. The Likert scale is used for the clinical training evaluation of this study. In order to easily evaluate the comparison of clinical training evaluation items and the comparison of each year, the analysis was performed by quantifying the Likert scale. In addition, we asked clinical

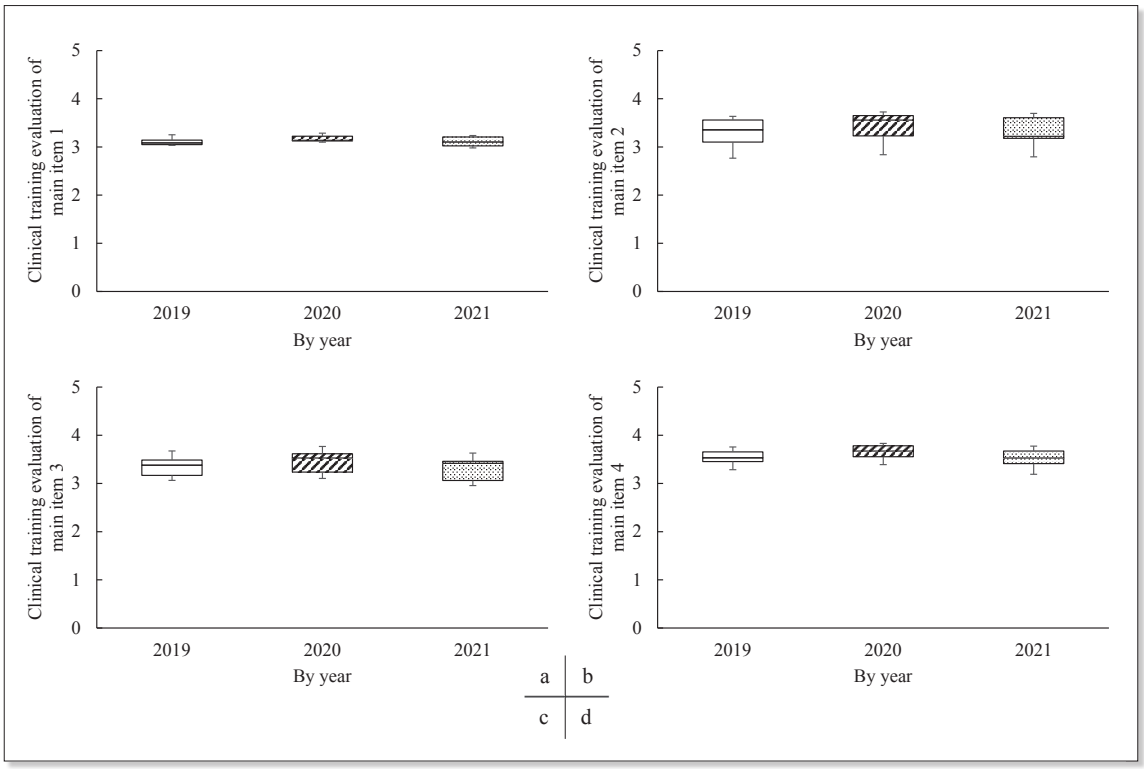

Figure 4 Scores for main items in the clinical training evaluations for each year. (a) Main item 1 score. (b) Main item 2 score. (c) Main item 3 score. (d) Main item 4 score. The Kruskal-Wallis test was used for the significance test between other groups. The significance level was set to $P<0.05$. No significant difference was found in any of the Main items (n.s.).

training instructors to evaluate the Likert scale in four stages without using the median. This is because the absence of an intermediate value makes it possible to remarkably evaluate the quality of each item of students and facilitate future student guidance.

The first notable outcome from this study is the consistently satisfactory average scores for the clinical training results among all students across all 3 years. The average score for most of the sub-items was 3.0 or higher, which indicates that students were able to perform clinical training well in the areas and topics covered by the evaluation items. Only sub-item 2-7 had an average score of less than 3. This item addresses medical fees. Clinical training instructors mainly provide information and direction about how to handle medical devices and how to communicate with patients during clinical work. While some clinical training instructors also inform students about medical fees, most do not. Additionally, even in university classes, there are no official lectures that explain medical fees for each type of medical examination. This can help explain why these students' understanding of this item was the poorest, and the associated scores the lowest. However, when a student becomes a radiological technologist and works at a hospital, knowledge about medical fees is always essential. Patients often ask medical staff about the cost of their tests. Therefore, it is necessary to introduce classes to improve students' knowledge about medical fees.

The second outcome to underscore is the higher grades observed for some of the sub-items in 2020 compared with other years. Furthermore, no differences were observed in the average scores for the sub-items in 2019 and 2021. In 2020 and 2021, students' clinical training underwent changes influenced by the COVID-19 pandemic. Recent clinical training education has shifted to address COVID-19 infections[3]. More specifically, the clinical training curriculum was unexpectedly changed in some cases, and/or the clinical training period shortened, to prevent students from contracting COVID-19, and to protect students' mental health[4, 5]. Moreover, students whose clinical training period was shortened were also expected to study independently when they were not engaged in clinical training. Thus, although many facilities were forced to change some aspects of their clinical training teaching methods, some of the evaluation items were scored the same or better than before the changes were enacted. Currently, to improve clinical training, workshops are also held to further educate clinical training instructors. Some reports indicate that clinical training instructors have low participation rates in these workshops[6], despite bearing all the responsibility for their students during the clinical training period[1]. In addition, the quality of the instructor's teaching ability has a substantial impact on student learning[6-9]. Therefore, in Japan, to improve the leadership skills of clinical training instructors who train radiological technologists, the number of facilities participating in these workshop is increasing. Furthermore, university faculty members continue to work well with students and hospital-based clinical training instructors to improve clinical training. Therefore, even during the period of restricted clinical training owing to COVID-19, the students were able to receive high-quality clinical training education. The reasons why we were able to carry out sufficient clinical training even with COVID-19 disasters are "sufficient guidance on infection control in pre-education of clinical training", "thoroughness not to go out unnecessarily", "students will be on standby at home from 2 weeks before the start of clinical training", and "Students and clinical training instructors and faculty members will be in close contact", etc. In addition, the students themselves kept a high awareness of infection prevention, and they wanted to acquire clinical techniques, so we think that they were successful in the

clinical training during the prevalence of COVID-19.

Here, we will describe the attendance of student education guidance in order to improve the leadership of clinical training instructors. On September 30, 2021, the Ministry of Health, Labor and Welfare of Japan revised the guidelines for guidance at radiological technologist training centers. As part of the amendment, it is stated that hospitals that conduct clinical training should have radiological technologists who have completed the radiological training instructor training course[10]. Improving the leadership of clinical training instructors is a very important item, and we hope that this revision will lead to the further development of clinical training education.

A comparison of the main items for all grades showed that the acquisition of basic practical abilities as a radiological technologist was the lowest scoring item. This main item was, moreover, considerably lower than the item that addresses fostering responsibility and awareness as a member of the medical team; its content deals mainly with sub-items that evaluate the technological knowledge required to complete a report. The clinical training instructor requires students to write their own thoughts in their own words in their reports, including their experiences and activities on a given day of clinical training. However, some students find it difficult to express in their own words what they were involved in during medical examinations on the day. Such students rather describe the contents of the textbook as if it were their report. Therefore, we would like to offer proper guidance on how to write a report through pre-education in clinical training.

In our comparison of main items in the clinical training evaluations for each student cohort, we used the same evaluations for each year. While some sub-items differed considerably across cohorts, a comprehensive assessment of the main items indicated there were no differences in evaluations across cohorts.

On the basis of the foregoing analyses, we noted that students lacked knowledge about medical fees and that some students could not write reports well. To improve these aspects in future, we would like to enhance the relevant instructions in pre-education courses and in-person clinical training. Clinical training education is necessary for preparing students to play active roles as radiological technologists. We want students to be at the forefront of the medical field when they become radiological technologists and engage in clinical work. Thus, the problems identified in this research can facilitate improvements in those areas to produce higher quality radiological technologists.

One limitation of this study is that the clinical training evaluation we analyzed was only a four-stage evaluation (i.e., 1 point: inferior, 2 points: standard, 3 points: good, 4 points: excellent). If the evaluation stages were extended, differences may appear in other items. Therefore, in the future, we would like to review the scoring criteria for evaluations. A further limitation is the absence of evaluation for each modality in the clinical training evaluation we studied; rather, it is an evaluation of the entire clinical training process. Importantly, students have likes and dislikes and various weaknesses in different modalities. Therefore, a separate assessment should be conducted for each modality's clinical training evaluation. Additionally, reports indicate that remote lectures have been adopted in various school settings in response to the spread of COVID-19, and that they have had a positive educational effect for students[11-14]. Furthermore, education that incorporates e-learning into existing lessons has been shown to be effective[5, 15, 16]. The e-learning system is not introduced in this research. we would like to create an e-learning

program for distance learners whose clinical training has been interrupted or shortened because of COVID-19. Finally, another study reported on the creation and effective use of a video recording of a radiological technologist's work for student education[17]. We wish to contribute to the further development of clinical training education by incorporating the trials of those previous reports.

Conclusion

The findings from our analysis of the grade evaluations for clinical training for the past three years at our institution show that some students' knowledge about medical fees was weak and their reports poorly written. It is, therefore, essential to improve students' knowledge and skills in the areas in which they are weakest by including a pre-education phase for clinical training and by enhancing the future development of clinical training education.

Acknowledgments

We would like to express our deep gratitude to all the radiological technologists at the hospital who were involved in the clinical training of our students. We thank Anita Harman, PhD, from Edanz (https://jp.edanz.com/ac) for editing a draft of this manuscript.

Conflicts of Interest / Funding Statement

The authors declare no conflicts of interest associated with this manuscript.

References

1) A. England, et al.: Clinical radiography education across Europe. Radiography (Lond), 23; Suppl 1:S7-S15, 2017.
2) H. Muto: Educational contents for introducing clinical participatory training -What should be taught at the university before clinical training begins in order to shift to clinical participatory practices? -. The japan Society of Education for Radiological Technologists, 10; 12-16, 2018 (in Japanese).
3) L. A. Rainford, et al.: The impact of COVID-19 upon student radiographers and clinical training. Radiography (Lond), 27; 464-474, 2021.
4) Y. X. Tay, et al.: Clinical placements for undergraduate diagnostic radiography students amidst the COVID-19 pandemic in Singapore: Preparation, challenges and strategies for safe resumption. J Med Imaging Radiat Sci, 51; 560-566, 2020.
5) L. W. Teo, et al.: Coping with COVID-19: Perspectives of Student Radiographers. J Med Imaging Radiat Sci, 51; 358-360, 2020.
6) K. J. Rye, et al.: Respiratory care clinical education: a needs assessment for preceptor training. Respir Care, 54; 868-77, 2009.
7) K. A. Laugaland, et al.: Improving quality in clinical placement studies in nursing homes (QUALinCLINstud): the study protocol of a participatory mixed-methods multiple case study design. BMJ Open, 10, e040491, 2020.
8) L. Newton, et al.: Experiences of registered nurses who supervise international nursing students in the clinical and classroom setting: an integrative literature review. J Clin Nurs, 25; 1486-1500, 2016.
9) K. Immonen, et al.: Assessment of nursing students' competence in clinical practice: a systematic review of reviews. Int J Nurs Stud, 100; 103414, 2019.
10) About revision of "the guidelines for guidance at radiological technologist training centers". Issued by Director of Medical Affairs Bureau, Ministry of Health, Labour and Welfare. Medical administration 0930 No. 13.
11) A. E. Seymour-Walsh, et al.: Pedagogical foundations to online lectures in health professions education. Rural Remote Health, 20; 6038, 2020.
12) K. Nakaya, et al.: Educational effect of remote lectures for students aiming to become radiologic technologists: Questionnaire on nuclear medicine examinations. J Nucl Med Technol, 49; 164-169, 2021.
13) K. Nakaya, et al.: Changing methods of education during a pandemic: questionnaire survey about examinations for nuclear medicine technology at educational institutions in Japan. J Nucl Med Technol, 50; 60-65, 2022.
14) T. E. Shim, et al.: College students' experience of emergency remote teaching due to COVID-19. Child Youth Serv Rev, 119; 105578, 2020.
15) R. Sadeghi, et al.: Comparison of the effect of lecture and blended teaching methods on students' learning and satisfaction. J Adv Med Educ Prof, 2; 146-150, 2014.
16) T. Haslerud, et al.: E-learning for medical imaging specialists: introducing blended learning in a nuclear medicine specialist course. Acta Radiol Open, 6; 2058460117720858, 2017.
17) S. Giordano, et al.: Using athletic training clinical education standards in radiography. Radiol Technol, 83; 218-225, 2012.

Received January 18, 2021; accepted May 26, 2021

The effects of electrical muscle stimulation on facial muscles: Volume change of facial muscles measured with magnetic resonance imaging

NAKAYA Koji[1)], MUTO Hiroe[1)], MATSUURA Kanae[1)], SUDO Shu[2)], YAMANAKA Aya[2)]

1) Department of Radiological Technology, Faculty of Health Science, Suzuka University of Medical Science
2) Research Dept. Mikimoto Pharmaceutical CO., LTD.

Note: This paper is secondary publication, the first paper was published in the JART, vol. 69 no. 831: 40-47, 2022.

Key words: electrical muscle stimulation, buccinator muscle, masseter muscle, slimming effect on the face

【Abstract】
Purpose: Electrical muscle stimulation (EMS) delivers a low-intensity stimulus to the nerves in the muscle to cause muscle contraction, and can result in a cosmetic effect. In this study, we measured volume changes of facial muscles before and after using EMS facial equipment via magnetic resonance imaging, and investigated the effects of EMS facial equipment on facial muscles.
Methods: Eight sessions of facial treatment were performed on healthy volunteers using EMS facial equipment. T_2-weighted images were acquired before and after using the EMS facial equipment, and volume changes in the buccinator and masseter muscles before and after using EMS facial equipment were measured from the images.
Results: The use of EMS facial equipment caused a decrease in masseter muscle volume in magnetic resonance images.
Conclusion: The results suggested that the use of EMS facial equipment had a clear effect on facial muscles, and that a facial treatment effect could be obtained even with short-term use.

1. Introduction

Human skin shows the effects of aging over time[1)]. Many women use cosmetics and medicines to prevent skin aging and rejuvenate the skin[1, 2)]. In recent years, the market for beauty appliances has grown rapidly and demand is increasing[3)]. In addition, many beauty salons offer treatments that attempt to prevent skin aging using beauty equipment. In recent years, beauty appliances and esthetic salons have developed and utilized facial equipment using electrical muscle stimulation (EMS). EMS involves the application of a low-intensity electrical stimulus to the nerves in the muscle, causing contraction of the muscle[4-6)] resulting in a cosmetic effect. EMS is also used as an exercise device for muscle training in the sports industry[6)]. Furthermore, it has been reported that EMS is effective for dieting[7)]. Facial EMS is now widely used for skin anti-aging and dieting purposes, providing a facial treatment that stimulates facial muscles and promotes facial muscle movement[8)]. It contracts the muscles of the face and gives a slimming effect on the face.

In the current study, we examined the effects of EMS on facial muscles. Many people regularly perform EMS on their face, reporting beneficial effects on their appearance[9)]. However, the extent to which EMS affects facial muscles is currently unclear. There are no reports quantifying the effects of EMS as a facial treatment. Therefore, we sought to clarify the effect of EMS by using the volume change of facial muscles. Imaging of facial muscles can be taken by computed tomography (CT) and magnetic resonance imaging (MRI), etc. MRI has better contrast resolution than CT[10)]. Muscles with a small area can be evaluated more accurately from MR images. Therefore, we thought that the facial treatment effect of EMS

could be evaluated if the muscles were activated by EMS and the degree of muscle contraction could be captured by MR images. In addition, there is T_2-weighted imaging (T_2WI) in the MR sequence. It has been reported that this sequence is anatomically easy to see and provides good contrast[11]. Therefore, we would like to adopt T_2WI for the MR sequence that images facial muscles. In the current study, we measured changes in the volume of facial muscles before and after using EMS facial equipment via T_2WI of MRI, and investigated the effects of EMS facial equipment on facial muscles.

2. Materials and Methods

2-1. Subjects

The subjects were 10 healthy women, aged 21 to 22 years (mean 21.7 ± 0.5 years), who volunteered to take part. This study was carried out with the approval of the Ethics Committee of Suzuka University of Medical Sciences.

2-2. Use of EMS facial equipment

PEARL FACE ESTHE Sonic EX (ITO CO., LTD., Saitama, Japan) was used as the EMS facial equipment. The method of using the EMS facial equipment is shown in Fig.1. When using the EMS facial equipment, pearly sonic gel (Mikimoto Pharmaceutical CO., LTD., Mie, Japan) was applied to the tip of the probe. The electromagnetic waves of EMS used medium frequencies that affect muscles. Electromagnetic wave output was performed at 13 out of 40 stages. EMS facial equipment was used for 20 minutes per person, and was used twice a

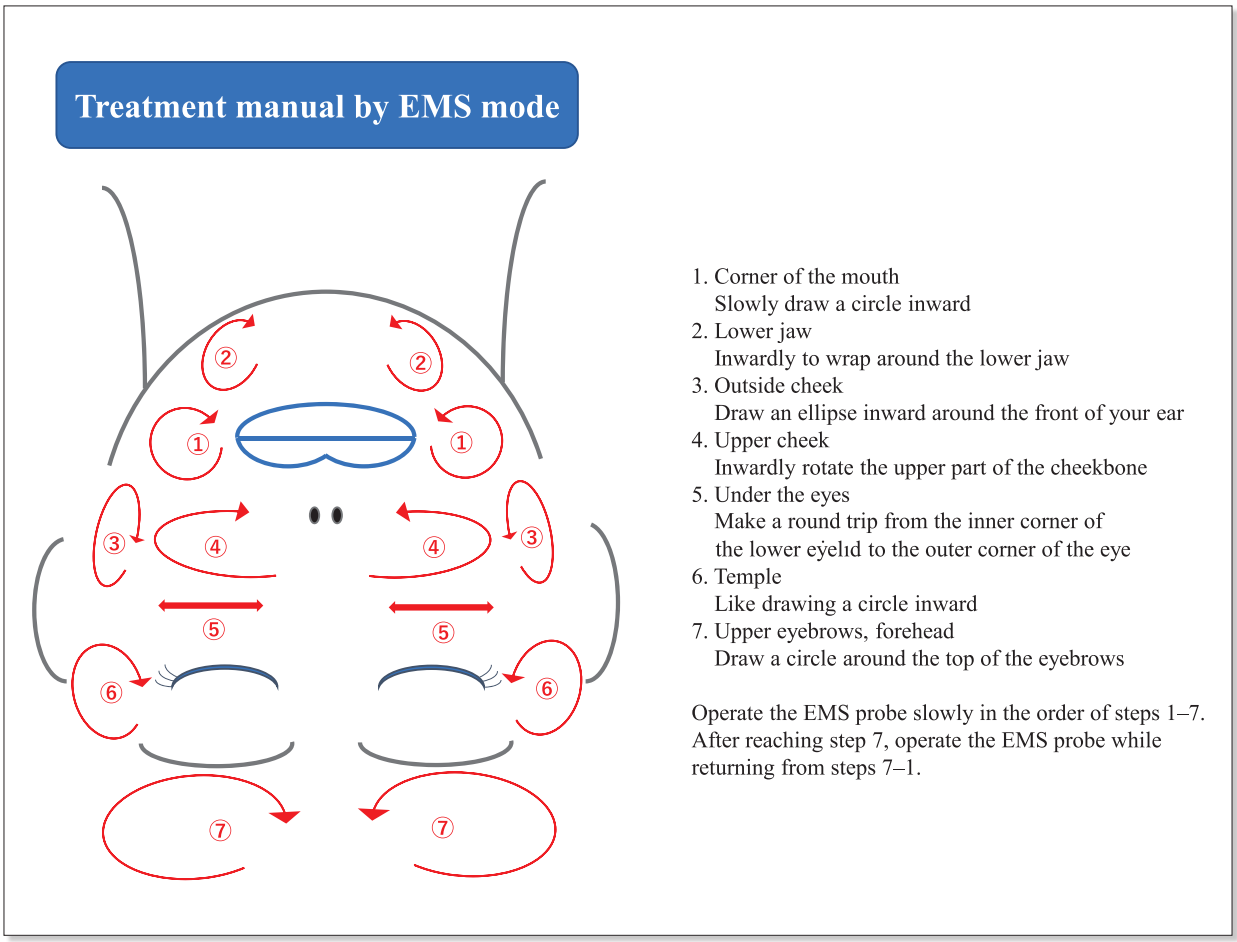

Fig.1 How to use electrical muscle stimulation facial equipment.
Instructions provided by Mikimoto Pharmaceutical CO., LTD.

week. In total, subjects underwent eight treatment sessions from September 2020 to October 2020. Subjects practiced using the EMS facial equipment, and, after securing an environment in which to do so, operated the EMS facial equipment themselves.

2-3. Acquisition of magnetic resonance imaging

MRI was performed before the use of the EMS facial equipment and within 2 to 3 days after the last day of use. An ECHELON 1.5T scanner (Hitachi, Ltd., Ibaraki, Japan) was used as the MRI device. A head coil was used as the receiving coil. T_2WI was used as the imaging sequence, and the imaging conditions for the T_2WI are shown in Table 1. The imaging cross-section was set so that a cross-section perpendicular to the long axis of the cheek could be obtained.

2-4. Comparison of facial muscle volume before and after using EMS facial equipment

The muscles used for volume measurement were the buccinator muscle, which is involved in facial expression, and the masseter muscle, which is involved in jaw movement and mastication. The masseter muscle is used to open and close the mouth and is also an important muscle for facial expression[12, 13]. Also, these muscles are the parts where the EMS probe is in close contact, and it was the subject of evaluation. For measuring the volume of both muscles, the region of interest (ROI) tool attached to the workstation of the MR device was used. MR images were acquired by 2-demensional scan (3 mm slices at 3 mm intervals). The ROI was surrounded by both muscles in all slice cross-sections where both muscles were depicted (Fig.2). Add up the muscle areas of all cross sections, and the volumes of both left and right muscles were measured. Volumes of the buccinator and masseter muscles were compared before and after the use of the EMS facial equipment. The ROI was set by a radiological technologist with 10 years of experience in MRI work.

Table 1 Imaging conditions for T_2-weighted images

Parameters	
TR (ms)	3,000
TE (ms)	84
FOV (mm)	200
Matrix	320 × 320
FA	90
IR Pulse	off
Thickness (mm)	3
Interval	3
Multi slice	40
E. Factor	12
NSA	2
Bandwidth (Hz/pixel)	147.5

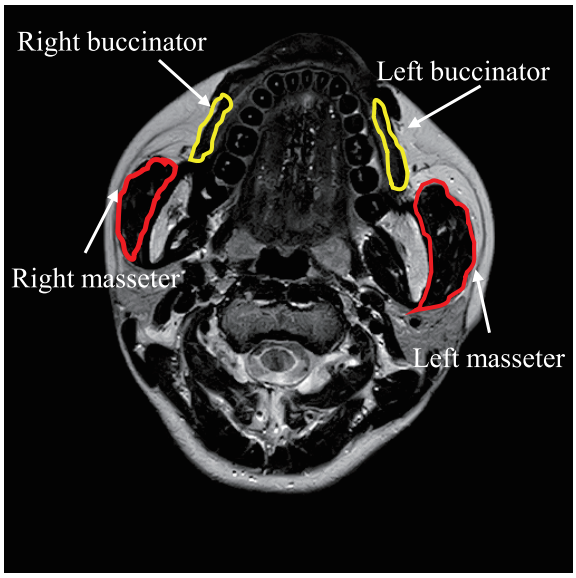

Fig.2 Buccinator and masseter muscles region of interest settings

2-5. Statistical analysis

Wilcoxon signed-rank test was used for statistical analysis of volume changes in the buccinator and masseter muscles before and after use of the EMS facial equipment. Statistical significance was defined as a P-value < 0.05.

We analyzed using Statistical Package for the Social Sciences (SPSS), version 26.0 (SPSS Inc., Chicago, IL, USA) for statistical analysis.

3. Results

3-1. Volume change of buccinator muscle

Fig.3 shows the volume of the right buccinator muscle before and after using the EMS facial equipment. The volume of the right buccinator muscle before and after using the EMS facial equipment was 1.15 ± 0.43 cm^3 and 1.03 ± 0.27 cm^3, respectively. There was no significant difference in the volume of the right buccinator muscle before and after using the EMS facial device (P = 0.508). Fig.4 shows the volume of the left buccinator muscle before and after using the EMS facial equipment. The left buccinator muscle volumes before and after using the EMS facial equipment were 1.04 ± 0.45 cm^3 and 0.88 ± 0.36 cm^3, respectively. There was no significant difference in the volume of the left buccinator muscle before and after using the EMS facial equipment (P =

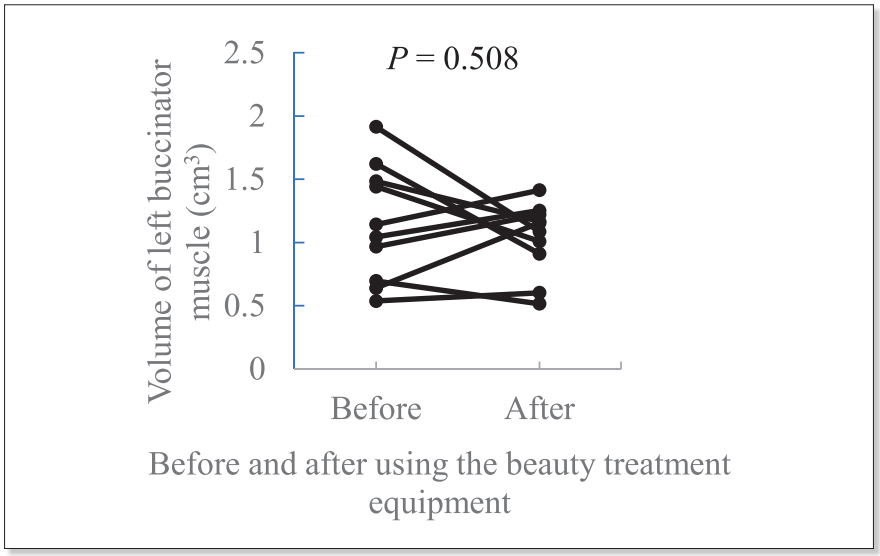

Fig.3 Volume of the right buccinator muscle before and after using electrical muscle stimulation facial equipment

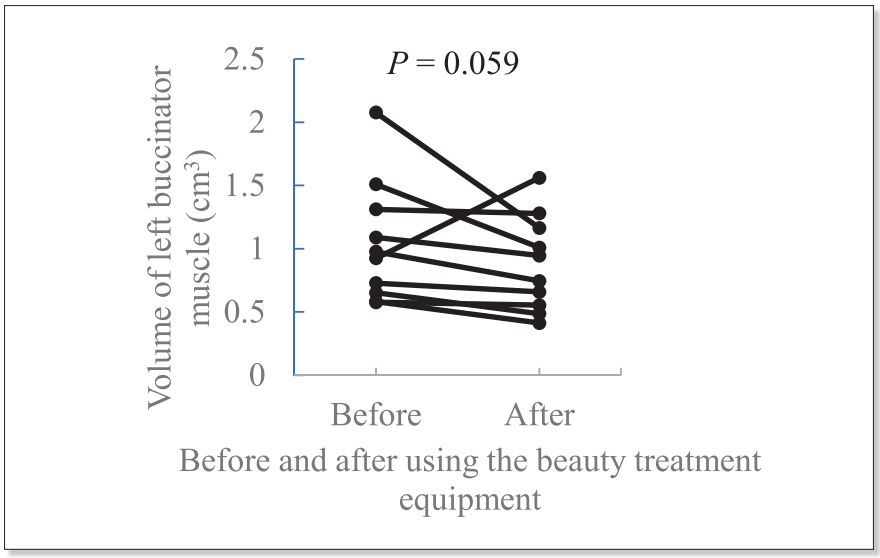

Fig.4 Volume of the left buccinator muscle before and after using electrical muscle stimulation facial equipment

0.059).

3-2. Volume change of masseter muscle

Fig.5 shows the volume of the right masseter muscle before and after using the EMS facial equipment. The volume of the right masseter muscle before and after using the EMS facial equipment was 19.70 ± 5.86 cm^3 and 18.13 ± 4.73 cm^3, respectively. There was a significant decrease in the volume of the right masseter muscle after the use of the EMS facial device compared with before ($P < 0.05$). Fig.6 shows the volume of the left masseter muscle before and after using the EMS facial equipment. The left masseter muscle volume before and after using the EMS facial equipment was 20.44 ± 6.26 cm^3 and 19.06 ± 6.04 cm^3, respectively. There was a significant decrease in the volume of the left masseter muscle after the use of the EMS facial device compared with before ($P < 0.05$).

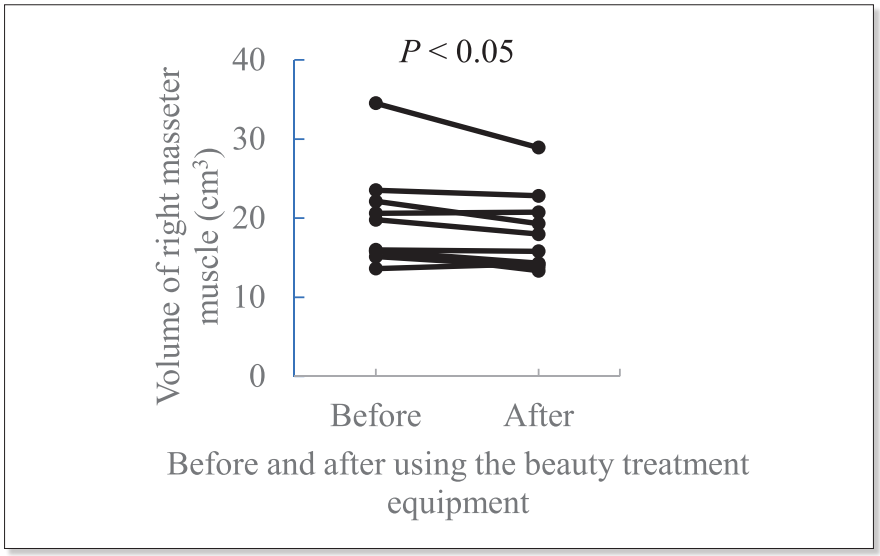

Fig.5 Volume of the right masseter muscle before and after using electrical muscle stimulation facial equipment

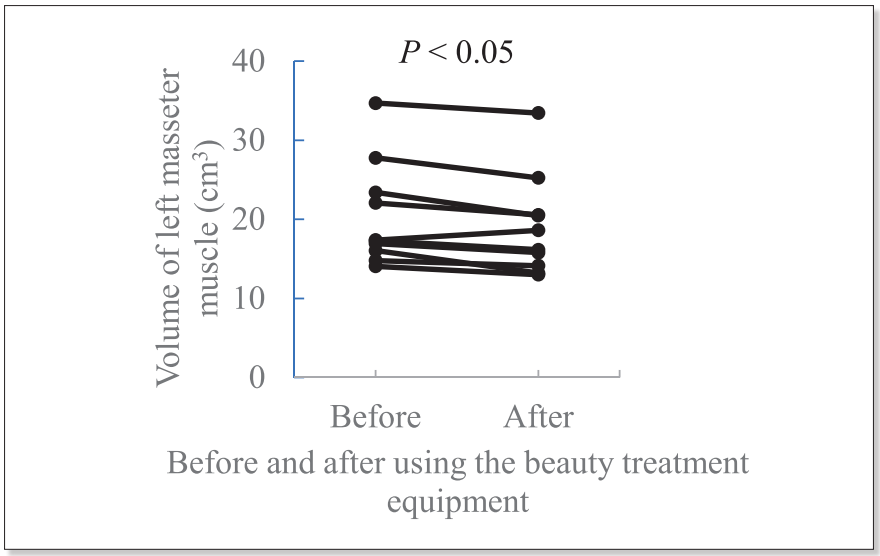

Fig.6 Volume of the left masseter muscle before and after using electrical muscle stimulation facial equipment

4. Discussion

We measured the volume change of facial muscles from T_2WI of MRI before and after using the EMS facial equipment, and examined the effects of the EMS facial equipment on the facial muscles.

In the current study, the buccinator and masseter muscles were targeted to induce changes in the volume of facial muscles. The buccinator and masseter muscles were selected because they provided suitable contact with EMS facial equipment, and it was relatively easy to set an effective ROI than other muscles in the MRI images. Regarding the buccinator muscle, there were no changes in the volume of the left and right buccinator muscles following the use of EMS facial equipment. This finding may have occurred for several reasons. First, the volume of the buccinator muscle is small, and no significant volume change was observed. Furthermore, the EMS facial equipment was used by the subjects themselves. Using the EMS facial equipment took exactly 20 minutes. However, because the procedure was performed by the subjects themselves, there were individual differences in the effects, and some subjects did not exhibit an effect on the buccinator muscle, which has a small volume. In addition, there may have been limited reproducibility, because the ROI for measuring volume was set manually. However, the average volume decreased after using the EMS facial equipment. Thus, the results suggest that a significant decrease in volume may be obtained by continuing to use the EMS facial equipment. In contrast, there was a marked effect of the EMS facial equipment on the masseter muscle, with the volume of the left and right masseter muscles significantly decreasing after using the EMS facial equipment. The masseter muscle has a larger volume than the buccinator muscle and came into contact with the EMS facial equipment more often. Therefore, the masseter muscle volume was significantly reduced, even though the equipment was controlled by the subjects themselves. However, there were cases in which the volume of the masseter muscles after EMS did not decrease. As with the buccinator muscle, the cause of the cases where the volume reduction was not obtained after EMS was that the subjects themselves used EMS. Therefore, it is considered that there were cases in which the probe could not stimulate the muscles well and the facial treatment effect could not be obtained. In the future, we would like to implement it after sufficient training on how to use the probe. Thus, only the masseter muscle gained volume reduction after using EMS. The muscle that most closely adheres to the skin and the largest of the facial muscles is the masseter muscle. The reduction in masseter volume after using EMS makes the face slimmer. Therefore, it is considered that the use of EMS provided a facial treatment effect. In addition, the loss of muscle volume after EMS is not a loss of muscle mass itself. As mentioned in the introduction, EMS promotes muscle movement and contracts muscles. Muscle activation also has the benefit of enriching facial expressions. Therefore, although the muscle volume is reduced, there is no health problem in using EMS and it can be used for beauty.

In this study, the EMS facial equipment was used only eight times in total. The volume of the masseter muscle was reduced with this relatively small number of uses, suggesting that this EMS facial equipment may be suitable for use as a cosmetic device, inducing facial treatment effects in a relatively short period of time. However, when use of the EMS facial equipment is discontinued, muscle contraction is likely to return to its original state, leading to the disappearance of the facial treatment effect. Thus, it is likely to be necessary to use the EMS facial equipment on a regular basis to continue the facial treatment effect. Importantly, some facial muscle rollers, cosmetics, and pharmaceuticals have been reported to affect

facial expression. One previous study reported that the use of facial muscle roller devices must consider the facial muscles, and that training is required for safe use[12]. In addition, rough skin and other side effects are induced by some cosmetics and pharmaceuticals. Because the EMS facial equipment does not have a risk of these negative effects, facial treatment effects can be obtained efficiently.

Overall, the current results revealed that the EMS facial treatment device induced a facial treatment effect in a relatively short period of time. We describe future research topics below. The number of subjects in this study is 10 cases. Since the number of cases is small in this study, we would like to increase the number of cases and obtain credible data when conducting further research. In addition, the volume data used this time is the one that sets the ROI for one person. Originally, it is appropriate to evaluate with a few people and perform calculation of intra-class correlation coefficient. However, it was too difficult to set the ROI for muscles, so the ROI setting was for one person. We would like to create a manual for muscle ROI setting and build a system that can be evaluated by multiple people. In addition, there is also fat in the muscle. EMS may also be given the ability to burn fat. Therefore, we would like to pursue a method that can evaluate facial treatment from the viewpoint of fat using short TI inversion recovery images. The current study targeted young women in their twenties. In the future, we plan to evaluate whether the treatment effect varies across age groups. In addition, we plan to investigate changes in the thickness of facial muscles using an ultrasonic device, and to measure changes in muscle hardness using shear wave elastography. At the end, in this study, one EMS device is used for evaluation. However, other manufacturers are also developing devices with EMS function. Since the principle of EMS effect is the same even if the device is different and the treatment procedure is different, it is considered that the same facial treatment effect can be obtained. It is also necessary to examine the effects of facial treatments on various devices.

5. Conclusion

The use of EMS facial equipment induced a decrease in masseter muscle volume measured using T_2WI of MRI. Therefore, it was suggested that the use of EMS facial equipment promotes the movement of facial muscles, reduces muscle mass, and has the effect of slimming the face. In addition, a facial treatment effect could be obtained even with short-term use.

Acknowledgments

We would like to express our deep gratitude to Soichi Tatsutani of Hitachi, Ltd. Health care Chubu/Hokuriku Branch, Nobuyuki Arai of Suzuka University of Medical Science, students of Muto Laboratory, and volunteers for their cooperation in this research. We thank Benjamin Knight, MSc., from Edanz Group (https://en-author-services.edanz.com/ac) for editing a draft of this manuscript.

Conflicts of Interest

This research was supported by joint research funding from Mikimoto Pharmaceutical CO., LTD.

References

1) S. Zhang, et al.: Fighting against Skin Aging: The Way from Bench to Bedside. Cell Transplant, 27; 729-738, 2018.
2) A. Kazanci, et al.: Analyses of changes on skin by aging. Skin Res Technol, 23; 48-60, 2016.
3) T. Kaneko, et al.: Effect of Improving Skin Quality by Facial Equipment Using Radio Waves. Shinryo to Shinyaku (Med Cons New-Remed), 55; 787-793, 2018.
4) V. Esteve, et al.: The effect of neuromuscular electrical stimulation on muscle strength, functional capacity and body composition in haemodialysis patients. Nefrologia, 37; 68-77, 2017.
5) N. A. Maffiuletti, et al.: Neuromuscular adaptations to electrostimulation resistance training. Am J Phys Med Rehabil, 85; 167-175, 2006.
6) General incorporated foundation Institute of Japan Therapeutic Apparatus. http://nihondenshi.xsrv.jp/hp/?page_id=964. Accessed November 15, 2020.
7) E. J. Choi, et al.: Effects of Electrical Muscle Stimulation on Waist Circumstance in Adults with Adbominal Obesity: A Randomized, Double-blind, Sham-Controlled Trial. JNMA J Nepal Med Assoc, 56; 904-911, 2018.
8) ITO CO., LTD. Instruction manual for PEARL FACE ESTHE Sonic EX.
9) Beauty Eos Inc. Kireinosennsei. https://kireinosensei.com/1300113/. Accessed January 12, 2021.
10) K. Yamada, et al.: Difference of the Contrast between CT and MRI: the Selection of the Alternative Imaging. Journal of Animal Clinical Research Foundation, 12; 27-29, 2003.
11) K. Yamada, et al.: Technical parameters affecting image characteristics in in vivo MR microscopy of the mouse. Vet Radiol Ultrasound, 43; 518-527, 2002.
12) R. Nishime, et al.: Effects on Face Caused by the Face Roller. Bulletin of Nagoya Future Culture College, 43; 13-19, 2018.
13) Y. Matsuoka: HYOJOKIMMASSAJI SEJUTSU TEKUNIKKU. 46-58, FRAGRANCE JOURNAL LTD., 2011.

Received July 7, 2021; accepted November 7, 2021

Dementia disease classification of the statistical analysis images of cerebral blood flow SPECT using deep learning

YAMAMOTO Yasushi[1], SHIRAI Masato[2], KATSUBE Takashi[1], YOSHIZAKO Takeshi[1], UWABE Hoshio[3], MIYAHARA Yoshinori[3], KITAGAKI Hajime[4]

1) Department of Radiology, Faculty of Medicine, Shimane University
2) Interdisciplinary Faculty of Science and Engineering, Shimane University
3) Department of Radiology, Shimane University Hospital
4) Kobe City Nishi-Kobe Medical Center

Note: This paper is secondary publication, the first paper was published in the JART, vol. 69 no. 837: 36-42, 2022.

Key words: GoogLeNet, AlexNet, Artificial intelligence, Grad-CAM, 3D-SSP

【Summary】
Using the original deep learning model, we attempted to classify the following disease: AD, DLB, and normal cognition, from the cerebral blood flow SPECT 3D-SSP images. Then we compared it with the transfer learning of GoogLeNet and AlexNet that was previously reported. Furthermore, we tried to visualize the accuracy of each analysis by Grad-CAM. The accuracy was low in AD for AlexNet, and in DLB for GoogLeNet. We obtained stable results in the original model. There were differences between the position and the size of the feature areas captured in each model from the Grad-CAM images. The original model captured the hypovolemic region precisely.

Introduction

Recently, in the field of radiographic images, the clinical application of Artificial Intelligence (AI) has been rapidly growing, and many of them are reported in papers. Typical examples are the detection of brain haemorrhage by head CT scans [1], the detection of unruptured aneurysms on the MRA [2], applications of noise reduction technologies [3], or reconstruction technologies [4] on Computed Tomography (CT) or Magnetic resonance imaging (MRI). As we have shown, AI technology is used in many ways. In 2019, the software, which allows us to detect a cerebral aneurysm on Magnetic resonance angiography (MRA), received regulatory approval for the first time in Japan. Turning to the field of nuclear medicine, it is reported that an attempt to make images of CT scans from Positron computed tomography (PET) images and to use them for attenuation correction [5]. Iizuka and others classified dementia disease from Three-dimensional stereotactic surface projection (3D-SSP) [6] images made from cerebral blood flow Single photon emission computed tomography (SPECT) with deep learning (DL), then they reported the scientific validity from the perspective of visualizations of the specific hypovolemic regions [7]. We, our group, have been attempting the classification of dementia disease by our original deep learning model with 3D-SSP images made from cerebral blood flow SPECT images [8]. Moreover, with an application of the notion of simulation training data stated by Uwabe [9], we have verified and reported the classification of dementia disease [12, 13] by well-recognised AlexNet (A.N) [10] and GoogLeNet (G.N) [11]. This time, we assessed the results of identification accuracy calculations by O.N from data groups which are the same as the reports from by A.N and G.N. Additionally, using Gradient-weighted Class Activation Mapping (Grad-CAM) [14]; one of technologies for visualizing Convolutional neu-

ral network (CNN), we compared O.N with G.N and A.N to clarify their differences by Grad-CAM heat map images.

1. Methods

1-1 Used Models (A.N, G.N, O.N)

O.N is composed of 4 layers of CNN and 3 layers of Pooling. We showed detailed settings in Fig.1. We utilised Matlab 2019b (Mathworks Company), Deep learning toolbox, Image Processing Toolbox, Computer vision toolbox, and Parallel computing toolbox in the analysis. We also described the details of G.N and A.N as comparison objects in References [10, 11].

1-2 Making image data

The images we utilised in the analysis are 3D-SSP Z-score maps gained from N-Isopropyl-p-[^{123}I] Iodoamphetamine (^{123}I-IMP) 167 MBq cerebral blood flow test. Moreover, we also utilised Discovery NM/CT 670pro, 3D-OS-EM methods (subsets 10, iterations 6) for image reconstruction, Dual energy window methods, CT based Attenuation correction methods. For 3D-SSP analysis, we utilised the Normal Database of Shimane University. We showed the standard output images from 3D-SSP in Fig.2 (C). They were images of a human brain taken from eight different directions: the anterior surface, the posterior surface, the left lateral surface, the right lateral surface, the left medial surface, and the right medial surface. The original sizes were 890 × 660 pixels. However, we adjusted the sizes for 224 × 224 pixels in order to assess with G.N and A.N. (Supplementary information: the size- 224 × 224 pixels is the same size for A.N. The size for G.N is 227 × 227 pixels.) Then in order to avoid loss of detection accuracy by image reduction in the hypovolemic regions (Z-score description regions) as targets, we chose the images from 4 different directions (the left and right lateral-medial surface sides) from the images from 8 directions as shown in Fig.2 (D). Why we chose these images is it is important to discern the

(A)

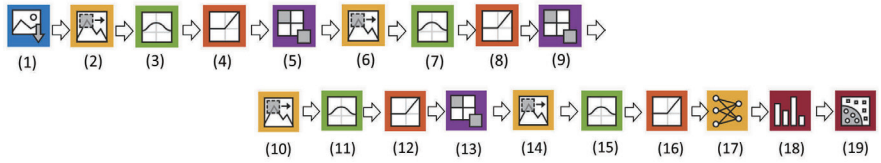

(B)

Image input layer(1)		**Convolution 2Dlayer(6)**	
Input Size	[224,224,3]	Channels	16
Convolution 2Dlayer(2)		**Batch normalization layer(7)(11)(15)**	
Filter Size	[3,3]	**Convolution 2Dlayer(10)**	
Channels	8	Channels	32
Stride	[1,1]	**Convolution 2Dlayer(14)**	
Padding	zero padding	Channels	64
WeightsInitializer	Xavier	**Full connected layer(17)**	
Batch normalization layer(3)(7)		InputSize	50176
ReLU layer(4)(8)(12)(16)		OutputSize	3
Max pooling 2Dlayer(5)(9)(13)		Bias	[-0.04;-0.02;0.06]
PoolSize	[2,2]	WeightsInitializer	Xavier
Stride	[2,2]		

Fig.1 Configuration diagram and parameters of the original model.

It comprises 4 convolution layers and 3 pooling layers. (A: Configuration diagram created with deep network designer in matlab.)

typical hypovolemic regions for Alzheimer's disease (AD) or Dementia with Lewy bodies (DLB). Moreover, we regenerated all these images to ensure that they are placed on the same coordinates. To analyse, we need three data groups: Training, Validation and Test. About Training, we utilise 3D-SS images made from the simulation data of SPECT imitating the specific hypovolemic of AD, DLB as well as the report from Uwabe [8]. The SPECT data used as the basis for the simulation data were ^{123}I-IMP healthy data collected in 2013 for the Normal database (28 subjects (15 males: 67.7 ± 6.2 years, 13 females: 68.1 ± 5.7 years)), which were transformed into Montreal neurological institute (MNI) brain coordinates using statistical parametric mapping 8 (SPM8) [15]. The results of this study were used to determine the neurological volume of interest (VOI) in the brain, and the neurological VOI was estimated using the Voxel-based analysis-stereotactic extraction estimation (vbSEE) [16] Level3 after conversion to Montreal neurological institute (MNI) brain coordinates using SPM8. The neurological VOI regions were utilised, including the angular gyrus, superior parietal lobule, inferior parietal lobule and superior marginal gyrus, which are located in the left and right parietal lobule regions, plus six regions of the posterior cingulate gyrus and precuneus in AD, and the superior occipital, middle and inferior occipital gyri, which are located in the occipital lobe region, plus the wedge, which is the primary visual cortex, and the cuneus in DLB. Masked images were generated by multiplying the base image with masked data in which the counts in each mask were progressively reduced to 35%, 30%, 25% and 20%, to generate various patterns of dementia SPECT data. We set the threshold value of the Z-score (Fig.2 (C)

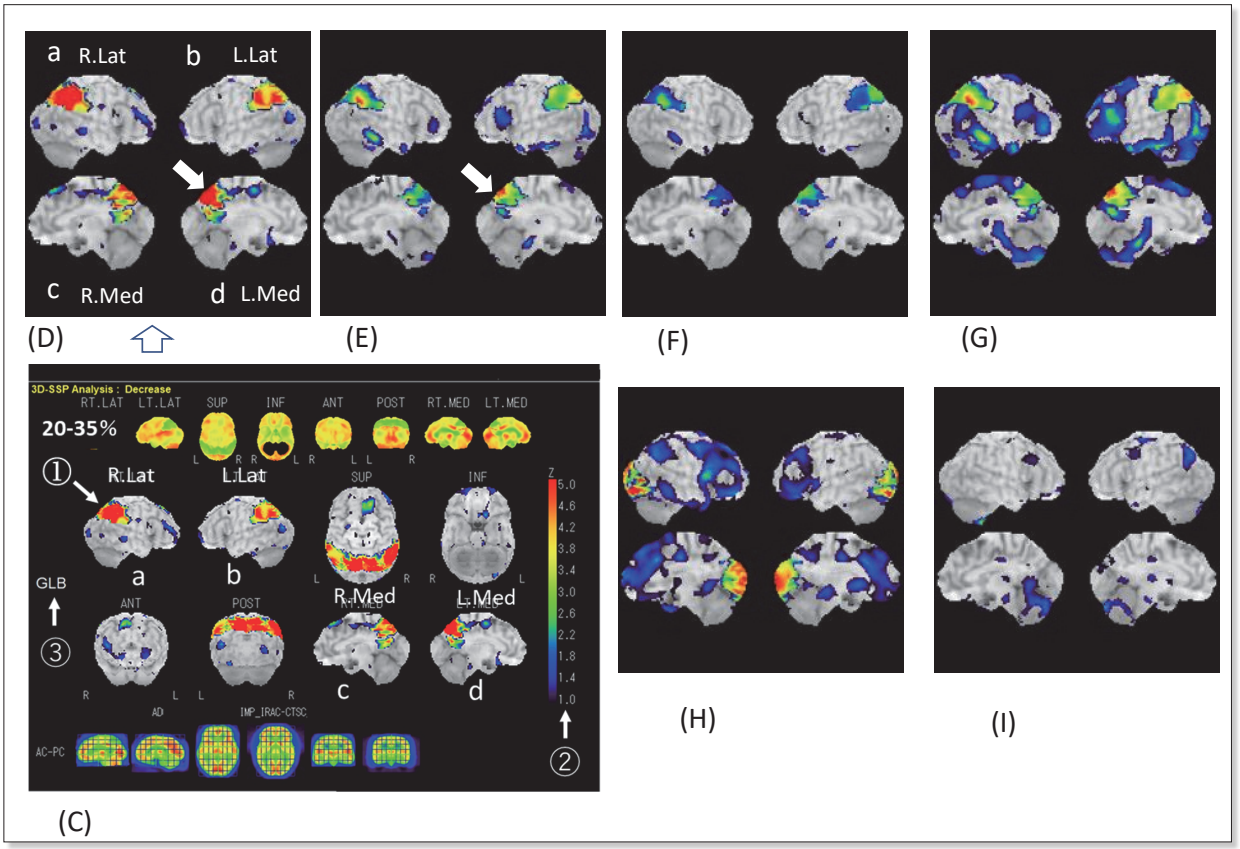

Fig.2 AD and DLB simulation images and the NC image used for the training.

(C) Original image of 3D-SSP, (D) AD simulation data created from C (⇨:-35%), (E) Simulation image of AD (⇨:-20%), (F) Simulation image of AD (Changed reference region from GLB to THL), (G) Simulation image of AD (Changed Z-score threshold), (H) Simulation image of DLB, (I) NC image.

②) from the Z-score map of each hypovolemia gained from these 3D-SSP analyses. Then, we made a simulated Z-score map of each 341 cases of AD, and DLB to make normalised site setting (whole brain: GLB, thalamus: THL, pons: PNS, cerebellum: CBL③) and the setting of threshold value we have stated before variable in each image. About (D) (①), we reduced 35% of the count of a specific hypovolemic region of AD, and additionally, made it by extracting 4 directions. For (E), we reduced 20% of counts for a specific hypovolemic region. In the case of (F), a reference area was changed from GLB to THL. Moreover, (G) shows a case of each Training in which its threshold value setting of (E) was changed. In that way we have written, we multiplied simulated Training of AD, and DLB to 341 cases from the 28 cases of healthy ones. Now we must mention that we excluded the reference area which hardly detected AD, and DLB even though they were seen by Diagnostic Radiologist with more than 20 years of experiences who were good at diagnosing dementia disease. We showed the detailed data breakdowns in the references [10]. Fig.2 (H) shows one case of DLB, and (I) shows one case of Training of N.C. For the Test, we chose 20 cases with each disease: AD, DLB, and NC which were diagnosed by Diagnostic Radiologist from patients' Z-score maps made from patients' data who were taken ^{123}I-IMP cerebral blood flow SPECT. Additionally, we adopted 2 images which were best seen from normalised sites. Finally, we adopted 40 cases. Patients' background; diagnosed with AD, Age (y); 72.3 ± 3.8, M/F; 15/5, DLB 80.5 ± 7.3, M/F; 10/10, NC 67.8 ± 15.4, M/F; 6/14. For Validation, we utilised 28 cases by fixation analysis. In these 28 cases; a reference area is GLB set from Training of AD, DLB, NC, a lower threshold limit setting is 1.0, and an upper threshold limit setting is 5.0.

1-3 Evaluation & Assessment

For diagnosis with AD, DLB, or NC, postulated that diagnosis by Diagnostic Radiologist is correct, we assessed it in the 4 sections; Accuracy (the rate of the correct data), Precision (the rate of true positive in the total positives), Recall (that shows sensitivity and statistical power), and F-measure (that means overall indicate value.) If we calculate them by these factors: True Positive (TP), False Positive (FP), False Negative (FN), and True Negative (TN), they are Accuracy = TP + TN/Total, Precision = TP/TP + FP, Recall = TP/TP + FN, F-measure = 2 × (Precision × Recall)/(Precision + Recall). We assessed each indicator value by mean value of 20 times' trials and standard deviation. Subsequently, we also visually assessed how the hypovolemic regions determined the classifications, by heat map images made by Grad-CAM. Furthermore, we conducted this research after gaining the approval from Ethics Committee at Shimane University, Faculty of Medicine.

2. Results

Fig.3 is a candlestick chart that shows Recall by pathological types in G.N and A.N from the already submitted reports [10, 11] with added the results of O.N. From Fig.3 and Table 1, the results of AD's recall are O.N (0.83 ± 0.09) > G.N (0.82 ± 0.12) > A.N (0.52 ± 0.12), the results of DLB's are O.N (0.85 ± 0.05) > A.N (0.74 ± 0.09) > G.N (0.42 ± 0.12), in the case of NC, they are O.N (0.86 ± 0.06) > G.N (0.78 ± 0.08) > A.N (0.76 ± 0.06). In the case of AD, there are no significant differences between G.N and O.N. However, others show a great value of O.N with significant differences, additionally, in the sections of Training and Validation of O.N, many index values were 1.0. Fig.4 shows the data that are Grad-CAM heat map images of A.N and G.N quoted from References [11] and their images are added with the results of O.N. There are differences between the size of regions or the shape of the distribution that is "heat-mapped" by each analysis model. In each model of AD (J, K, L), bilateral

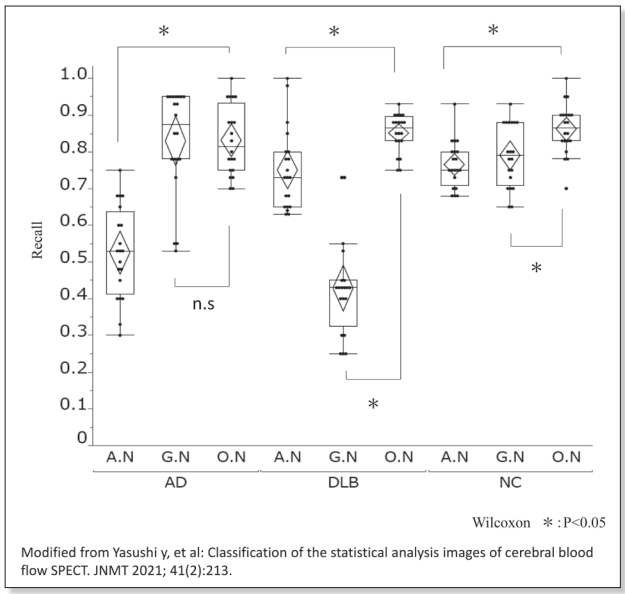

Modified from Yasushi y, et al: Classification of the statistical analysis images of cerebral blood flow SPECT. JNMT 2021; 41(2):213.

Fig.3 The graph shows the recall in each model by disease type.

In the AD group, G.N and O.N showed high values, and there was no significant difference in them. In the DLB group, O.N showed the highest value, which was significantly different from those of G.N and A.N. Additionally, O.N was high in NC, and it differed from A.N and G.N.

posterior cingulate gyrus, precuneus, temporal regions, and parietal lobe were heat-mapped. In the models of DLB (M, N, O), bilateral temporalis and occipital lobe were heat-mapped. Lastly, in the case of NC (P, Q, R), non-hypovolemic regions were.

3. Consideration

First, we will state some things for the simulated training data of O.N; Accuracy of Training in Table 1 is all types of disease 1.0 and it consists of the different images pattern (different feature images) from AD and DLB. Furthermore, seen from the results of Validation, we can state it can precisely classify the disease by 3D-SSP images if these images are typical patterns of them. As we stated, we determined that these training data groups were appropriate for this research. From AD's heat map in Fig.4 (J, K, L), in A.N and G.N, the regions whose Z-scores are high are correctly captured. However, there are some cases which are not correctly classified; the cases which the heat map was widely spread (J) and extended into the occipital lobe which the specific hypovolemic regions for DLB like R.Med. Or the cases that parietal lobe was weakly heat-mapped like L.Lat (K). Given these cases, we could assume that the two conditions in order to correctly classify; Z-score description areas are limited to the specific areas of AD and DLB. Furthermore, Z-scores are high. To classify the given diseases properly, these two conditions must be fulfilled. If we take a look at the occipital lobe of DLB in Fig.4 (M, N, O), in O.N, A.N, and G.N, they were strongly heat-mapped

Table 1 Recall, Precision, and F-measure in O.N analysis method were calculated separately for AD, DLB, and NC.

Data type	Evaluation method	AD	DLB	NC	Accuracy
Test	Recall	0.83 ± 0.09	0.85 ± 0.05	0.86 ± 0.06	0.84 ± 0.02
	Precision	0.84 ± 0.05	0.83 ± 0.06	0.87 ± 0.06	
	F- measure	0.83 ± 0.04	0.83 ± 0.04	0.86 ± 0.03	
Training	Recall	1.00	1.00	1.00	1.00
	Precision	1.00	1.00	1.00	
	F- measure	1.00	1.00	1.00	
Validation	Recall	1.00	1.00	0.98 ± 0.02	0.99 ± 0.01
	Precision	0.98 ± 0.02	1.00	1.00	
	F- measure	0.99 ± 0.01	1.00	1.00	

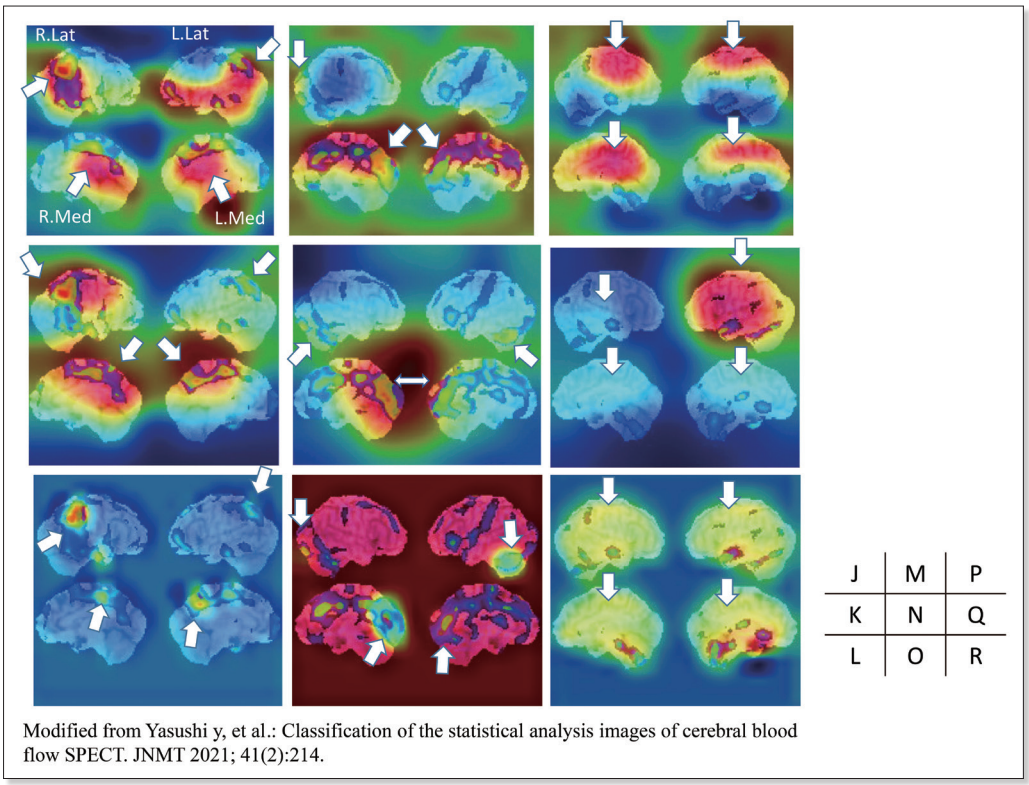

Fig.4 Heat map of A.N, G.N, and O.N analysis images classified as AD, DLB, and NC by matching with the radiologist's reading results.

Heat map of images classified as (J) AD, (M) DLB, and (P) NC by A.N. Heat map of images in which the same image is classified as (K) AD, (N) DLB, and (Q) NC by G.N. Heat map of images in which the same image is classified as (L) AD, (O) DLB, and (R) NC by O.N. (⇨) indicates a heat map region that correctly recognizes the specific blood flow reduction region in AD and DLB, and NC heat map region without blood flow reduction.

in R.Med, additionally, they were weakly done in L.Med. For these facts, we can assume that the "High" and "Low" of the Z-score are recognised as one of the features as well as (K) L.Lat. Also, in (N) of G.N, the left and right occipital lobes were captured as one large region. So that made the centre of the heat map not located in the images. We can also see some other cases which have the same tendencies that we stated, so we couldn't carry out the feature detections that were limited in the regions of Z-score by the transfer learning whose configuration conditions were not changed for the analysis model. For NC in Fig.4 (P, Q, R), they didn't have any specific hypovolemic regions, so we can determine these images are the ones in which the entire images are heat-mapped, and we cannot find the feature regions. Fig.5 (S, U, X) shows the images of each model whose classifications differ from the diagnosis by Diagnostic Radiologist. (S) is the case DLB was classified as AD by A.N. Heat map extended to the occipital lobe (⇨) which is the hypovolemic region of DLB. That made the classification wrong. Then we researched the images of AD Training in A.N, there were images which were heat-mapped in Z-score lower than the hypovolemic regions shown in (M). In order to distinguish it from DLB, we need to reconsider the addition of the training data which are with the feature of AD and low Z-score exists in the occipital lobe. (U) is the case in which DLB was classified as AD by G.N, the occipital lobe is weakly heat-mapped, and the cingulate gyrus regions were strongly captured. (V) shows one of the cases of DLB Training in G.N. As well as in Fig.4 (N), it was widely heat-mapped with the occipital lobe of

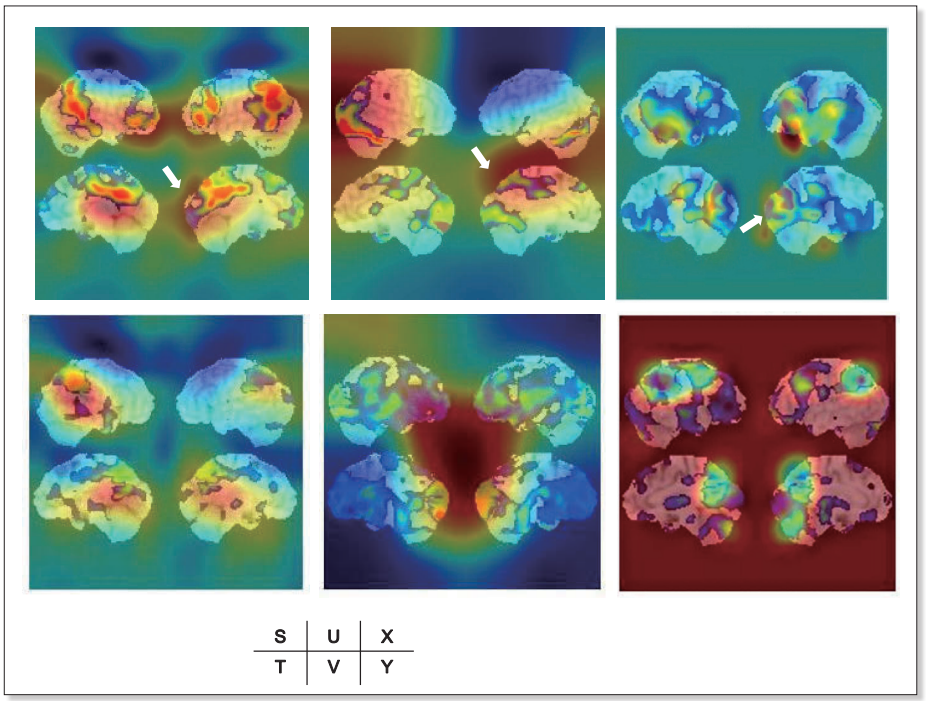

Fig.5 Heat map of images in which the radiologist's reading results and classification results did not match.
(S) In A.N, AD was erroneously classified as DLB. (U) In G.N, DLB was erroneously classified as AD. (X) In O.N, DLB was erroneously classified as AD. (⇨) indicates the heat map area that caused the erroneous classification of AD and DLB. (T) AD in A.N (V) DLB in G.N (Y) AD in O.N, heat map area of each train data.

R.Lat and L.Lat as one of the features. For this, we need to add the data on which one side of the Z-score (not bilateral symmetry) is low for Training. (X) is the case in which AD was classified as DLB by O.N; blood flow was strongly reduced in the cingulate gyrus. Diagnostic Radiologist could recognise that was because of the effects of a high Z-score. However, O.N could not. (Y) shows one of the cases of AD Training of O.N. O.N can recognise slight Z-score and differences in position. So, we assume that we can correspond to it by the addition of training data like (X).

Generally speaking, given models which have deep layered like G.N have a lot of parameters for learning objectives, we need to verify it with an increase in the numbers of training data. A.N has one more convolutional layer compared to O.N. Each convolutional layer has many channels, so we need to give a lot of data for it as well as G.N. Also, we utilised Local Response Normalization for a normalisation process. However, in O.N, by use of Batch Normalization, we can keep the changes in the internal variable distribution small and reflect the learning results to the estimated results more precisely. In the case we have given in this research: a small variation in characteristics of training data, the number of classifications is small, less geometrical differences as the whole images, what difference are only Z-score's distribution geometry and Z-score itself, we could classify by simple models like O.N. However, if we enrich the training data and utilise parameters that it appropriates for each model, the results can differ.

4. Conclusion

By using deep learning, we tried the classifications of dementia disease by aspects from blood flow SPECT and 3D-SSP images. The Training data we use were 341 data made from simulations. Cases are each 40 data with AD, DLB, and no abnormality. We utilised 4 layers of CNN and O.N with 3 layers of Pooling layers

as analysis models. We could classify these diseases with more than 80% of accuracy against the diagnosis by Diagnostic Radiologist. It showed a better result than the transfer learnings of A.N and G.N that we previously reported. Compared to the visualizations of feature areas by Grad-CAM, O.N took more confined specific hypovolemic areas than A.N and G.N. In this case with a fewer number of classifications and the same kinds of images, D.L with a fewer layers are available for use. However, we need to prepare a lot of training data and compare it with each model.

Conflicts of Interest

There is no conflict of interest a first author and co-author have to disclose so far.

References

1) Chilamkurthy S, Ghosh R, Tanamala S, et al.: Deep learning algorithms for detection of critical findings in head CT scans: a retrospective study. Lancet, 392 (10162): 2388-2396, 2018.
2) Ueda D, Yamamoto A, Nishimori M, et al.: Deep Learning for MR Angiography: Automated Detection of Cerebral Aneurysms. Radiology, 290 (1): 187-194, 2019.
3) Tatsugami F, Higaki T, Nakamura Y, et al.: Deep learning-based image restoration algorithm for coronary CT angiography. Eur Radiol, 29 (10): 5322-5329.
4) Ryu K, Nam Y, Gho SM, et al.: Data-driven synthetic MRI FLAIR artifact correction via deep neural network. J Magn Reson Imaging, 50 (5): 1413-1423, 2019.
5) Fukui R, Fujii S, Ninomiya H, et al.: Generation of the Pseudo CT Image Based on the Deep Learning Technique Aimed for the Attenuation Correction of the PET Image. Jpan J.Radiol.Technol, 76 (11): 1152-1162, 2020.
6) Minoshima S, Robert A. Koeppe M. A, et al.: Anatomic standardization; Linear scaling and nonlinear warping of functional brain images. J Nucl Med, 35 (9): 1528-1537, 1994.
7) Iizuka T, Fukasawa M, Kameyama M: Deep-learning-based imaging-classification identified cingulate island sign in dementia with Lewy bodies. Sci Rep, 9 (1): 8944, 2019.
8) Yamamoto Y, Uwabe H, Yada N, et al.: Classification of the Statistical Analysis Images of Cerebral Blood Flow SPECT by Using the Deep Learning. Jpan J.Nucl Med.Technol, 40 (4): 407-412, 2020.
9) Uwabe H,Yamamoto Y,Yada N, et al.: Accuracy of Classification of Cerebral Blood Flow Reduction Patterns Using Statistical Analysis Images Generated with Simulated SPECT Datasets via Deep Learning. Jpan J.Radiol.Technol, 77 (6): 581-588, 2021.
10) Krizhevsky A, Sutskever I, Hinton G: ImageNet Classification with Deep Convolutional Neural Networks. Communications of the Acm, 60 (6): 84-90, 2017.
11) Szegedy C, Liu W, Jia Y, et al.: Going Deeper with Convolutions. 2015 IEEE Conference on Computer Vision and Pattern Recognition (CVPR), 7-12, 2015.
12) Yamamoto Y, Uwabe H, Yada N, et al.: Classification of the Statistical Analysis Images of Cerebral Blood Flow SPECT by Using the GoogLeNet. Jpan J.Radiol. Technol. 41 (2): 204-209, 2021.
13) Yamamoto Y, Uwabe H, Yada N, et al.: Classification of the Statistical Analysis Images of Cerebral Blood Flow SPECT by Using the Transfer Learning. Jpan J.Nucl Med.Technol, 41 (2): 210-215, 2021.
14) Selvaraju R, Cogswell M, Das A, et al.: Grad-CAM: Visual Explanations from Deep Networks via Gradient-Based Localization. International Journal of Computer Vision, 128 (2): 336-359, 2020.
15) Oda K, et al.: Base and application of the clinical analysis software in nuclear medicine. 1-3 SPM. series of publications, (28), 16-22, Japanese society of Radiological Technology. 2011.
16) Uruma G, Hashimoto K, Abo M.: A new method for evaluation of mild traumatic brain injury with neuropsychological impairment using statistical imaging analysis for Tc-ECD SPECT. Annals of Nuclear Medicine, 27 (3): 187-202, 2013.

Received May 23, 2021; accepted December 2, 2021

Research on eye lens exposure doses and exposure management for physicians involved in Interventional Radiology

ARAI Kazumasa[1)], WATANABE Hiroshi[2)], MEGURO Yasuhiro[3)], KITAYAMA Sanae[4)], YABE Satoshi[5)], SASAKI Takeshi[6)], HASEGAWA Takeshi[7)], FUKUZUMI Toru[8)], KAWASAKI Hideo[9)], SATO Yoichi[10)]

1) Department of Radiological Technology, Japanese Red Cross Musashino Hospital
2) Department of Radiological Sciences, Faculty of Health Science and Technology, Gunma Paz University
3) Department of Radiological Technology, Hokkaido Industrial Health Management Fund
4) Department of Radiological Technology, Japanese Red Cross Saitama Hospital
5) Department of Radiology, Central Medical Division, Koshigaya Municipal Hospital
6) Department of Radiological Technology, Ageo Central General Hospital
7) Department of Radiological Technology, Tsuchiura Kyodo General Hospital
8) Department of Radiology, Dokkyo Medical University Hospital
9) Department of Radiology, Juntendo University Hospital
10) Department of Radiological Technology, Kofu-Kyoritsu Hospital

Note: This paper is secondary publication, the first paper was published in the JART, vol. 69 no. 840: 32-41, 2022.

Key words: Medical exposure, Medical Law Enforcement Regulations, Radiation protection, Exposure management, Lens exposure dose

【Abstract】
The Ministry of Health, Labour and Welfare revised the "Regulation on Prevention of Ionizing Radiation Hazards," which was established based on the Industrial Safety and Health Act, and implemented from April 1, 2021, with particular emphasis on the reduction of the equivalent dose limits for eye lens exposure. A study group was formed to review the exposure limit for the eye lens in Japan; the report of the study group stated that many medical workers experience radiation exposure to the eye lens, and that appropriate individual exposure doses have not been measured. We conducted a fact-finding survey to investigate radiation exposure to physicians belonging to the interventional radiology department at different medical institutions. Our results clearly indicate that by considering the standards for lowering the dose limit, some physicians will be exposed to radiation exceeding the newly recommended dose limits, and that even currently, the exposure dose for physicians is not being measured correctly at medical institutions.

Introduction and Purpose

The partial revision of the Regulations for the Prevention of Ionizing Radiation Hazards in the Industrial Safety and Health Act was implemented from April 1, 2021. What emphasized here is to reduce the equivalent dose limit for the lens of the eye. The main points of the revised ministerial ordinance are (1) 3 mm dose equivalent dose of the lens equivalent dose was added to the conventional measurement of the 1 cm dose equivalent and the 70-micrometer dose for the measurement of the dose by external exposure, (2) the equivalent dose limit to the lens of the eye for medical staff and etc. engaged in work dealing with radiation was lowered to 50 mSv from 150 mSv per year, 100 mSv dose limit for each period divided into five-year periods was also added starting from April 1, 2021.

According to the Kunugita Document 3 of the Ministry of Health, Labour and Welfare's 2nd "Study Group on Lens Exposure Limit," medical professionals are the most common category of radiation workers who are subject to exceeding the dose limit with the revised dose limit values. Among the 511,499 radiation workers in the 2017 fiscal year, except for atomic, decontaminations and reactor decommissioning workers, the annual equivalent lens

dose for most of them was less than 20 mSv limit, but 2,236 were exposed to more than 20 mSv limit per year. Of the 364,740 medical staff employed in general healthcare in fiscal 2017, 2,221 were exposed more than 20 mSv equivalent dose to the lens of the eye, this number comprised 0.6% of the total [1]. (369 medical staff in general healthcare exceeded 50 mSv, 0.1% of the total). More than 99% exceeding 20 mSv are medical professionals, therefore the medical field is the most concerned to consider reducing of the equivalent dose limit for lens of the eye mandated by the revision of the law. In the Kunugita Document 5, the physicians exposed to more than 20 mSv to lens of eye are cardiologists, gastroenterologists/gastroenterological surgeons, radiologists, and orthopedic surgeons in the order of exposure dose from higher to lower, and for physicians those exposed to 50 mSv or more were gastroenterologists, orthopedists, neurosurgeons, and cardiologists as well [2]. Furthermore, in Kunugita Document 4 of the 6th Study Group on Lens Exposure, there are some cases where appropriate dosimetry was not performed [3]. In earlier literature, Meguro et al. pointed out that fluoroscopy doses in Interventional Radiology (IVR) are left to the determination and discretion of the physician, and it is not easy to evaluate excess exposure [4] in the study of the necessity of Ministerial Ordinance Guidelines for the Revision of the Enforcement of Regulations of the Medical Law to be enacted in 2020. After the implementation of the revised ministerial ordinance, it is expected that radiation exposure management for physicians who comply with the dose limits will become more difficult than before the implementation of the revised ordinance.

The purpose of this study was to clarify the current problems of medical institutions by investigating the number of physicians who are exposed to excess dose limit for lens of eye in accordance with the revised ministerial ordinance, the accurate exposure measurement status of physician personal dosimeters, the use of X-ray protective equipment of physicians involved in eye lens exposure reduction, the use and availability of X-ray protective glasses, the management status for the occupational exposure as well the patient exposure from the actual situation of radiation exposure management at hospitals nationwide.

1. Methodology

1-1 【Investigation】

We conducted a questionnaire survey by sending a survey request on eye lens exposure doses and exposure management of physicians involved in IVR by e-mail and obtaining responses through Google Form as the target of total of 308 medical institutions, covering 217 medical institutions to which members of the Japan Society of Radiation and Public Safety belong (excluding 12 Red Cross hospitals employing members of the Japan Society of Radiation and Public Safety) and 91 national Red Cross hospitals. The period was from October 1, 2020 to January 31, 2021.

The survey consisted of the facility name, the name and e-mail address of the respondents, the total annual eye lens exposure dose of physicians recorded at each medical institution for the one year of FY2019 and the total eye lens exposure dose in the period FY2015 to FY2019, the measures of personal dosimeters, the use/availability of lens dosimeters, the status of use of X-ray protective equipment, the number and use of X-ray protective glasses, and the arrangements at hospitals to manage patient and operator exposure.

1-2 Ethical Considerations

In September 2020, this research was approved as clinical research after an ethics review by the Clinical Research Ethics Review Committee of Musashino Red Cross Hospital (approval number: Musashi So. 698).

2. Results

2-1 【Basic Information】

2-1-1 Response rate and respondents

The response rate was 24% (74/308) from 74 facilities in Japan. The response rate was 17% (37/217) from facilities with members of the Japan Society of Radiation and Public Safety, and the response rate of Red Cross hospital facilities was 41% (37/91). There were 74 respondents, all radiological technologists: general managers and chief technicians 26% (19/74), section managers 24% (18/74), assistant managers 27% (20/74), and not in management position 23% (17/74).

2-1-2 Number of beds in the responding facilities

The numbers of beds in the responding facilities were as follows: 600 beds or more (24%, 18/74), 300~599 beds (47%, 35/74), 100~299 beds (16%, 12/74), and fewer than 100 beds (12%, 9/74) (Fig.1).

2-1-3 Survey of the number of physicians by department in the medical institutions

Physicians by department were classified into the following six departments with eye lens exposure dose based on previous literature [2]: cardiologists, radiologists, and neurosurgeons performing IVR; gastroenterologists, gastroenterological surgeons, and orthopedic surgeons mainly performing IVR in X-ray fluoroscopy room.

The survey results showed that the number of medical institutions and physicians employed as cardiologists was 459 at 58 medical institutions, 131 diagnostic radiologists at 47 institutions, and 184 neurosurgeons at 49 medical institutions. There were 456 gastroenterologists at 61 medical institutions, 388 gastroenterological surgeons at 59 medical institutions and 364 orthopedic surgeons at 58 medical institutions (Fig.2).

For surveys of the classification of physicians by department, the ratio (%) is shown using the number of medical institutions with the number of physicians as the denominator. For other questions unrelated to the classification of physicians by department, the ratios (%) are shown using the 74 of the valid facility responses as the denominator.

2-1-4 Percentage of full-time physicians at facilities by department

Figure 3 shows the ratio of physicians employed in each department at the responding facilities.

2-2 【Lens exposure】

Table 1 shows the results of a survey of the number of physicians who exceed the dose

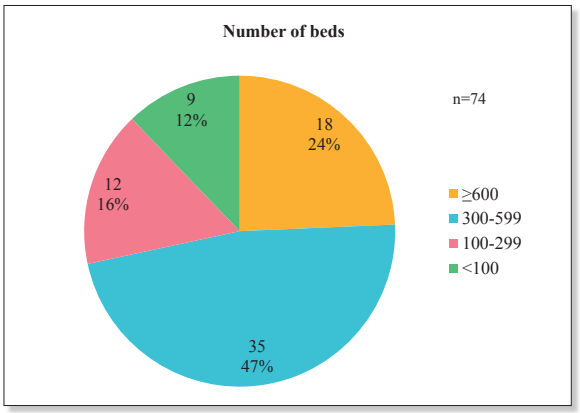

Fig.1 Number of beds in participating medical institutions

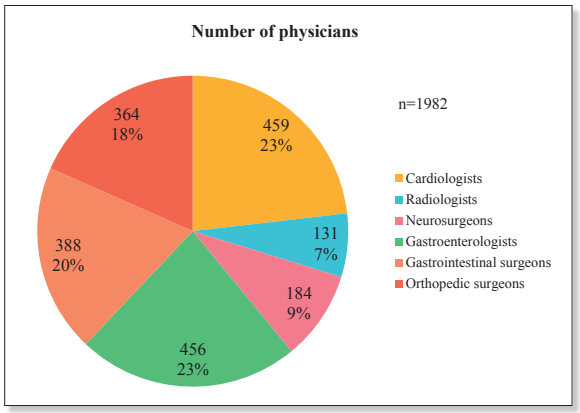

Fig.2 Number of physicians by specialty at participating medical institutions

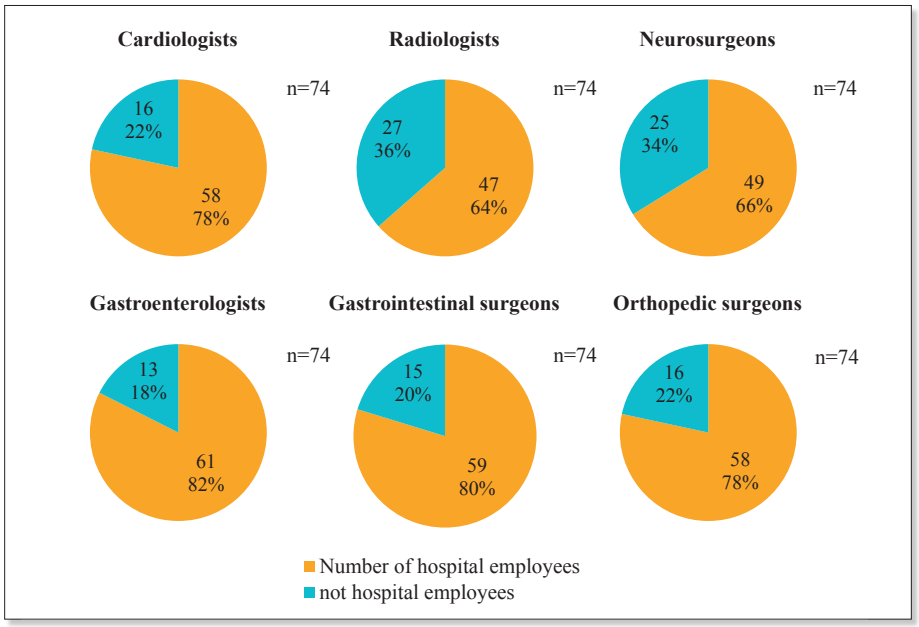

Fig.3　Percentage of medical institution specialists

Table 1　Exposure to eye lens of physicians

	Total number of physicians (n=1982)	Cardiologists (n=459)	Radiologists (n=131)	Neurosurgeons (n=184)	Gastroenterologists (n=456)	Gastrointestinal surgeons (n=388)	Orthopedic surgeons (n=364)
≥ 20 mSv within one year	69 (3.5)	43 (9.4)	3 (2.3)	0 (0.0)	14 (3.1)	5 (1.3)	4 (1.1)
≥ 100 mSv in a 5-year period	57 (2.9)	37 (8.1)	3 (2.3)	1 (0.5)	14 (3.1)	2 (0.5)	0 (0.0)

Unit：Number of physicians（%）

limit when the equivalent dose limit of exposure was reduced.

2-2-1　Table 1 shows the number of physicians exposed to equivalent eye lens exposure dose of 20 mSv or more in FY2019, and total eye lens eye exposure dose of 100 mSv or more in the 5 years from FY2015 to FY2019.

According to the results, 9% of cardiologists, 3% of gastroenterologists and 2% of radiologists had exposed more than 20 mSv equivalent eye lens exposure dose for one year. In addition, 8% of cardiologists, 3% of gastroenterologists, and 2% of diagnostic radiologists had been exposed to high rates of total lens of the eye exposure more than 100 mSv of over 5 years.

2-3　【Management for personal dosimeters】

Appropriate use of personal dosimeters enables accurate exposure evaluation. Table 2 shows the results of surveys on the measurement status of non-uniform exposures, the actual use of personal dosimeters and the measurement positions of personal dosimeters.

2-3-1　Survey of the distribution of personal dosimeters to physicians by department at each medical institution (response to non-uniform exposures)

Table 2 shows the results of the distribution of personal dosimeters to physicians by department. The distribution of personal dosimeters was surveyed by dividing the facilities into the following three categories: facilities that distribute two dosimeters that can measure non-uniform exposures, one for the head and neck and the other for the chest and abdomen, facilities that distribute only one dosimeter that

Table 2 Use of personal dosimeters

	Cardiologists	Radiologists	Neurosurgeons	Gastroenterologists	Gastrointestinal surgeons	Orthopedic surgeons
Number of physicians	(n=459)	(n=131)	(n=184)	(n=456)	(n=388)	(n=364)
Number of medical institutions	(n=58)	(n=47)	(n=49)	(n=61)	(n=59)	(n=58)
Dosimetry use of uneven exposure in medical institutions						
Personal dosimeter measure in 2 places	53 (91)	42 (89)	44 (90)	55 (90)	37 (63)	41 (71)
Personal dosimeter measure in 1 place	4 (7)	5 (11)	4 (8)	5 (8)	14 (24)	14 (24)
No personal dosimeter	1 (2)	0 (0)	1 (2)	1 (2)	8 (14)	3 (5)
						Unit：Number of medical institutions (%)
Percentage of dosimetry performed by physicians using personal dosimeters						
≥ 80% used	311 (68)	118 (90)	113 (61)	241 (53)	141 (36)	163 (45)
≥ 50 − < 80% used	35 (7)	2 (2)	15 (8)	68 (15)	30 (8)	48 (13)
< 50% used	63 (14)	3 (2)	47 (26)	110 (24)	146 (38)	100 (27)
unknown	50 (11)	8 (6)	9 (5)	37 (8)	71 (18)	53 (15)
Percentage of accurate dosimetry by physicians						
accurate measurements	374 (82)	121 (92)	128 (70)	283 (62)	180 (46)	201 (55)
wrong measurements	11 (2)	0 (0)	4 (2)	25 (6)	37 (10)	26 (7)
unknown	74 (16)	10 (8)	52 (28)	148 (32)	171 (44)	137 (38)
						Unit：Number of physicians (%)

cannot measure non-uniform exposures and facilities that do not distribute dosimeters.

When non-uniform exposures could not be measured, accurate measurement of eye lens exposure would be impossible. Based on this, when the results are summarized by physician and department, about 10% of facilities are unable to measure non-uniform exposures about cardiologists, diagnostic radiologists, neurosurgeons and gastroenterologists. Approximately 30% of facilities with only one distribution arrangement and those without distribution were unable to measure non-uniform exposures. It was shown that the proportion of physicians who performed procedures in the X-ray fluoroscopy room was higher in facilities where non-uniform exposures could not be measured.

2-3-2 Survey on the actual use of personal dosimeters by physician and department (actual usage of personal dosimeters)

Table 2 shows the results of a survey on the use of personal dosimeters by physicians in each department. The survey was conducted by dividing each department into three categories depending of the ratio of the number of physicians during the IVR treatment and examination: more than 80% of physicians wears personal dosimeters, from 50% or more to less than 80% wears and less than 50% wears.

These results suggest that personal dosimeters are not worn in the working environment where they should be worn. The percentages of physicians wearing personal dosimeters by each department are as follows: diagnostic radiologists (≥ 90%), gastroenterologists (36%), orthopedic surgeons (45%), gastroenterologists (53%), neurosurgeons (61%) and cardiologists (68%). These showed that the measured radiation values with personal dosimeters were inaccurate and underestimated.

2-3-3 Survey of the mounting position of personal dosimeters for the head and neck for physicians by department

Table 2 shows the results of a survey of the mounting position of the personal head and neck dosimeters for physicians by department. Physicians were classified into three catego-

ries: physicians wearing head and neck dosimeters in the correct position, physicians wearing the dosimeters in the wrong positions, and physicians with the position unknown.

The percentages of physicians wearing personal dosimeters in the wrong positions by each department are as follows: gastroenterological surgeons (10%), orthopedic surgeons (7%), gastroenterologists (6%), neurosurgeons (2%), cardiologists (2%), and radiologists (0%). This shows that the physicians who perform the procedures in the X-ray fluoroscopy room often make mistakes in the mounting position of the dosimeters.

2-3-4 Survey of the wrong measurement positions of personal dosimeters for the head and neck (measurement positions of personal dosimeters)

A survey of the wrong measurement positions of personal dosimeters for the head and neck was conducted. The total number of responses was 19 cases. The most common position was the chest pocket inside the X-ray protective clothing (47%, 9/19), followed by outside on the chest of the X-ray protective clothing (21%, 4/19), outside on the back of the X-ray protective clothing (16%, 3/19), on the back of the headpiece of the hat (5%, 1/19), reversed wearing from head and neck to chest and abdomen and vice versa (5%, 1/19), and wearing for chest and abdomen but not on the head-neck (5%, 1 /19).

2-3-5 Survey on the use of special eye lens dosimeters

A survey of the use of special eye lens dosimeters was conducted.

Nine percent (7 of 74) of facilities used special eye lens dosimeters and 91% (67/74) did not (Fig.4). At present, many facilities do not use special eye lens dosimeters.

2-4 【X-ray protection】

The use of X-ray shielding plates, protective cloth and X-ray protective glasses is important for reducing the eye lens exposure dose. Fig.5 shows the results of a survey on the use of X-ray protection in each facility.

2-4-1 Survey on the use of ceiling shielding plates in angiography rooms for different clinical procedures

To reduce the exposure to physicians, we surveyed the use of ceiling shielding plates used in angiography rooms for the following five procedures: transcatheter arterial chemoembolization of hepatic artery (TACE), percutaneous coronary intervention (PCI), peripheral angioplasty (endovascular treatment: EVT), catheter

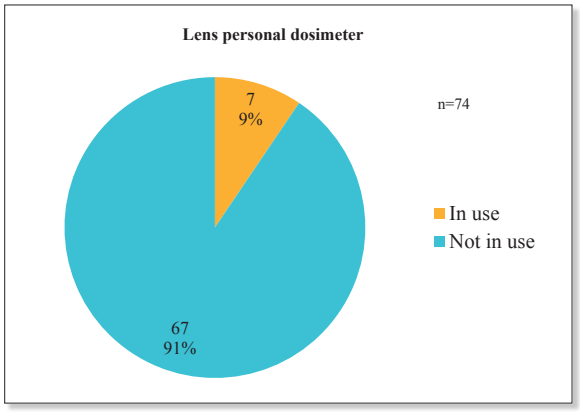

Fig.4 Use of dosimeters for the eye lens exposure at participating medical institutions

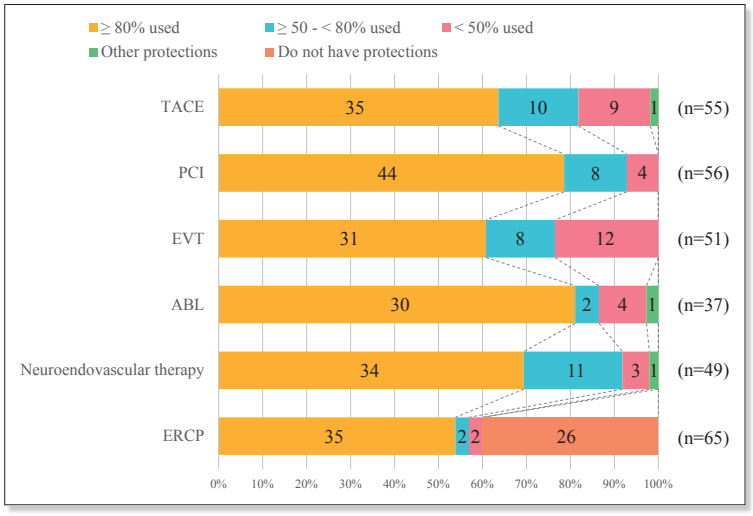

Fig.5 Usage of X-ray protective equipment

myocardial ablation (radiofrequency catheter ablation: ABL i.e. shortened form of RFCA), and cerebrovascular treatment (cerebral aneurysm coil embolization, arteriovenous malformation embolization etc.). The survey results are shown in Fig.5. The use of ceiling shielding plates was divided into four frequencies: used in more than 80% of procedures in all treatments, used in 50% to 80% of procedures in all treatments, used in below 50% of procedures in all treatments, and shielded by another shielding method such as a shielding box.

The procedures where the use of ceiling shielding plates was below 50% were as follows: EVT (23%), TACE (16%), and PCI (7%). When we compared the facilities in which the cardiologists were exposed to 100 mSv or more with the facilities where the ceiling shielding plates use in PCI, EVT, and ABL was 50% to 80% and below 50%, 33% (4/12 facilities) were the same facilities. Similarly, we compared the facilities where the diagnostic radiologists were exposed to 100 mSv or more with the facilities where the ceiling shielding plates use in TACE was 50% to 80% and below 50%, and 33% (1 of 3 facilities) was the same facilities.

2-4-2 Investigation of the use of X-ray protective cloths when performing endoscopic retrograde cholangiopancreatography (ERCP) including crushing gallstones endoscopically and lithotripsy

To reduce the exposure to physicians, we surveyed the use of X-ray protective cloths during ERCP (treatment and contrast examination). The survey results are shown in Fig.5. The use of X-ray protective cloths during ERCP was classified into four frequencies: used in more than 80% of procedures in all treatments and contrast examinations, 50% to 80%, below 50%, and zero X-ray protective cloths. About half (47%) of facilities with ERCP have X-ray protection for physicians, but 40% of facilities do not offer X-ray protection measures for physicians because they have no X-ray protective cloths. When we compared the facilities that did not have X-ray protective cloths with the facilities where the gastroenterologists were exposed to 100 mSv or more, 43% (3/7 facilities) were the same facilities.

2-4-3 Survey about the availability of X-ray protective glasses in each radiological rooms of respective facilities

To reduce the eye lens exposure to physicians, we surveyed the availability of X-ray protective glasses in the imaging facility. The number of X-ray protective glasses for physicians managed by hospitals was the number of glasses shared with other professions and glasses purchased by individuals. Table 3 shows the results of the survey on the availability of X-ray protective glasses in the angiography rooms and X-ray fluoroscopy rooms. The average number of X-ray protective glasses per section was 5 for angiography and 2 for X-ray fluoroscopy rooms. There were more X-ray protective glasses in the angiography

Table 3 Availability of X-ray protective glasses in institutions

	Number of X-ray protective glasses	Number of rooms	Number of glasses per room
Angiography room	288	62	5
X-ray fluoroscopy room	120	72	2

Table 4 Wearing rate of X-ray protective glasses by specialty

	Cardiologists	Radiologists	Neurosurgeons	Gastroenterologists	Gastrointestinal surgeons	Orthopedic surgeons
≥ 80	40 (70)	29 (64)	26 (55)	18 (29)	2 (4)	4 (7)
≥ 50 – < 80	14 (25)	9 (20)	12 (26)	23 (38)	13 (24)	14 (26)
< 50	3 (5)	7 (16)	9 (19)	20 (33)	38 (72)	36 (67)

Unit : Number of medical institutions (%)

rooms than X-ray fluoroscopy rooms.

2-4-4 Survey on the Wear of X-ray protective glasses by clinical department

The X-ray protective glasses can reduce the eye lens exposure of physicians. Table 4 shows the results of a survey of facilities where it was possible to respond to the use of X-ray protective glasses worn by physicians of the respective departments. The use of X-ray protective glasses was classified into three categories: X-ray protective glasses are used in more than 80% of procedures (glasses are used in more than 80% of treatments and examinations), more than 50% and less than 80% of procedures (glasses are used in more than 50% and less than 80% of treatments and examinations), and less than 50% of procedures (glasses are used in less than 50% of treatments and examinations).

The percentages of physicians wearing X-ray protective glasses by clinical department are as follows: cardiologists (70%), diagnostic radiologists (64%), neurosurgeons (55%), gastroenterologists (29%), gastroenterological surgeons (4%), and orthopedic surgeons (7%). Compared to physicians who worked in angiography facilities, physicians who worked X-ray fluoroscopy rooms less wear the X-ray protective glasses.

2-4-5 Survey of reasons for physicians not wearing X-ray protective glasses by clinical department

The reasons for not wearing X-ray protective glasses were that the glasses made it difficult to see the screen during the procedure (53%, 39/74 facilities), they caused trouble due to the two layered glasses (35%, 26/74), fogging of X-ray protective glasses (26%, 19/74), unnecessity for X-ray protective glasses (26%, 19/74), the glasses were heavy (23%, 17/74), distorted vision due to wearing the glasses (15%, 11/74), the eye lens exposure dose is less than 20 mSv per year (11%, 8/74), headache when using the glasses (5% 4/74), absence of glasses (4%, 3/74), and using protective cloths and shielding plates (3%, 2/74).

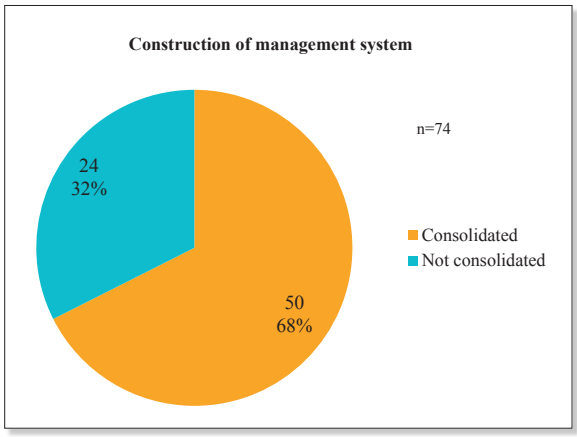

Fig.6 Status of committees established to manage exposure at medical institutions

2-5 【Radiation exposure management at medical institutions】

To control patient and operator radiation exposure in medical institutions, each medical institution needs to take the initiative in exposure control. For this reason, we surveyed the status of the establishment of committees to control patient and operator exposure in hospitals.

2-5-1 Survey of management status to control patient and operator exposure

We surveyed if the participating institutions have established the management system in the hospital structure (in charge of dose management, manual availability, protection education, etc.) such as institutional committees to control patient and operator exposure including the eye lens exposure. The survey results showed that 68% of facilities (50/74) had such management arrangements, and 32% (24/74) had no such arrangements (Fig.6).

3. Discussion

Reduction of exposure to the equivalent dose limit for the lens of the eye of medical staff was mandated by the revision of the Regulations for the Prevention of Ionizing Radia-

tion Hazards in the Industrial Safety and Health Act. To respond to this revision, we surveyed the following issues about physicians: agenda of those who exceed the dose limit for lens exposure, status of accurate measurement of personal dosimetries, the use of X-ray protective equipment, the use and availability of X-ray protective glasses, and management arrangements to control patient and operator exposures in medical institutions.

3-1 【Eye lens exposure】

The results of this survey showed that the proportion of physicians exceeding the dose limit is higher than in a previous study [2]. The problems that exposure to the eye lens of physicians exceeds the dose limit will be discussed for each clinical department. The highest percentage of physicians exposed to more than 20 mSv in a year and more than 100 mSv for a 5-year total for eye lenses is cardiologists. When we compared the facilities where the physicians were exposed to 100 mSv or more in 5 years with the facilities where the physicians were exposedz to 20 mSv or more in one year, all (n=12) cardiologists, four of seven gastroenterologists, one of three diagnostic radiologists, and one of two gastroenterological surgeons were in the same facilities. This suggests that they are constantly exposed to radiation at these same facilities.

There are 43 physicians of 17 facilities exceeding 20 mSv per year. Despite the fact that the more than 80% facilities used ceiling shielding plates for radiation protection during PCI, EVT, and ABL procedures, the increase in the number of PCI and EVT procedures for chronic occlusions which require longer durations of fluoroscopy and more frequent imaging could be the reasons for the higher eye lens exposure doses to physicians. The most effective way to reduce the exposure to physicians is to reduce fluoroscopy and radiography doses from angiography equipment. As shown in the "2020 Report on Reference Doses from Equipment in FY2020" by the Japan Accreditation Organization for Radiological Technologists Specializing in Angiography and Interventions (as of April 11, 2021), there are variations in doses at medical facilities nationwide [5].

For the future, the standardization of the fluoroscopy and imaging doses of angiography equipment would be expected in Japan. Physicians who were subject to the second most radiation exposures to eye lenses were gastroenterologists. In this present survey, the number of physicians exposed to 20 mSv or more per year was 14 at 10 facilities. The results of the survey showed that more than 80% of the facilities used X-ray protective cloths for radiation protection during ERCP. The reason for the high eye lens exposure to physicians may be because it is difficult to perform puncture procedures such as PTCD when using X-ray protective cloths. The same approach to this issue as described above can be applied to the reduction of radiation exposure. The reductions of fluoroscopy and radiography doses from X-ray monitoring equipment can still contribute to the reduction of the exposure to the eye lenses of physicians.

Two reasons may explain why diagnostic radiologists and neurosurgeons, who perform endovascular treatment in the same way as cardiologists, are less likely to exceed the eye lens exposure dose limit than cardiologists. One reason may be the difference in the number of treatments. The other reason may be that the distance between the surgeon and the X-ray source tube changes depending on differences in techniques. For example, in neurovascular treatment, exposure to the surgeon is reduced because the surgeon can stand at a greater distance from the X-ray tube than in PCI. The differences in the percentage exceeding the dose limit of gastroenterologists, gastrointestinal surgeons, and orthopedic surgeons could be due to the differences in the number of procedures performed and the number of patients treated.

3-2 【Management of personal dosimeters】

If exposure is not accurately measured, the evaluation of dose limits will be inaccurate. This makes it impossible to evaluate the influence of radiation exposure on radiation workers. For this reason, exposure measurements are very important to protect the health of physicians. This section discusses the status of measurements of non-uniform exposures and the use of personal dosimeters in different clinical department.

3-2-1 Measurement of uneven exposure

The measurement of non-uniform exposure to physicians is clearly stated in the "2021 Revised Guidelines on Radiation Exposure in Cardiovascular Care (as of April 11, 2021) [6] by the Japanese Circulation Society. Descriptions for non-uniform exposures control are in the recommended class I, Evidence Level A of the guidelines. Based on the results of the survey in this study, for cardiologists, diagnostic radiologists, neurosurgeons, and gastroenterologists, approximately 10% of facilities underestimated the eye lens exposure doses of physicians because the accurate non-uniform exposures were not measured in those facilities. For gastroenterological surgeons and orthopedic surgeons, 37% and 29% of those facilities underestimated the eye lens exposure doses. The distribution of individual dosimeters among institutions may differ because the cost of measurement equipment is borne by the hospitals. To reduce this difference among facilities, it is necessary for Japanese administrative agencies to provide medical institutions with auditing guidance on non-uniform exposures measurements and to offer subsidies for radiation dosimetry.

3-2-2 Use of personal dosimeters

The most important aspect for the eye lens exposure to physicians is to promote exposure reduction measures so that the eye lens exposure dose does not exceed the dose limit. When introducing exposure reduction measures, if the eye lens exposure dose is not accurately measured to determine whether it is high or low, the overall exposure may be significantly underestimated. The results of the present study showed that the use of personal dosimeters varied widely among physicians in different clinical departments. Among diagnostic radiologists who mainly perform endovascular treatment, 90% were able to accurately measure exposure by using personal dosimeters. However, cardiologists and neurosurgeons reported less accurate measurements at 68% and 61%. Furthermore, the measurement accuracies of gastroenterologists, orthopedic surgeons, and gastroenterological surgeons performing procedures in the X-ray fluoroscopy room were only 53%, 45%, and 36%. These results suggest that physicians except for diagnostic radiologists greatly underestimate the eye lens exposure doses. To improve on this situation, information of the necessity of radiation dosimetry should be provided by professional societies, providing education and guidance on individual dosimetry at medical institutions. Further, government agencies may need to provide administrative guidance by conducting secret surveys without publicizing the results. In addition, according to the report by Kunugita Document 7 of the 2nd Study Group on Lens Exposure, all physicians wore personal dosimeters when the radiological technologists "encouraged" physicians to wear personal dosimeters [7]. This suggests that efforts by radiological technologists in clinical settings can also lead to improvement of wearing dosimetry.

3-2-3 Incorrect position of head and neck dosimeters

There were commonly reported errors in the placement of the head and neck dosimeters by gastroenterological surgeons, orthopedic surgeons, and gastroenterologists, who mainly perform procedures in X-ray fluoroscopy room. It may be necessary to provide educa-

tion and guidance on personal dosimetry to solve this problem.

3-2-4 Introduction of special eye lens dosimeters

Only 9% (7/74) of the facilities used eye lens dosimeters. Currently, many facilities measure eye lens exposure doses using two dosimeters to measure non-uniform exposures. The dose values do not take into account the use of X-ray protective glasses. Even if these dose values exceed 20 mSv per year, it will result in overestimated dose values if X-ray protective glasses are used. Therefore, it would be more economical to limit the use of eye lens dosimeters to physicians subject to 20 mSv or more annual lens equivalent dose in the current non-uniform exposure measurements. It would be realistic way to minimize the management costs.

3-3 【X-ray protection】

It is widely known that the effective use of X-ray protective equipment enables reductions in the exposure to the eye lenses of physicians, but such equipment is not fully used. Here, we discuss various types of X-ray protective equipment.

3-3-1 Use of ceiling shielding plates and X-ray protective cloths

The results showed that at facilities where ceiling shielding plates are not commonly used during endovascular treatment, physicians are at the risk of exceeding the eye lens exposure dose limits, although the number of such facilities is small. The reason for the low use of ceiling shielding plates and X-ray protective cloths may be the presence of physicians with low awareness of the importance of protection against radiation exposure to the physicians. To improve this situation, it is necessary to create a workplace culture that increases the number of physicians with a high awareness of radiation protection. Providing radiation protection education and guidance in clinical settings as well as educational support from related academic societies is important to create a workplace culture of high protection awareness. Another factor for the low use of these protective tools is the interference between the ceiling shielding plates and the C-arm or vascular puncture route of angiography devices, which may interfere with the procedure, resulting in the absence of the shielding plates use. Further studies are needed to increase the awareness of the need for protection among physicians and to develop shielding plates that will not interfere with the procedures.

3-3-2 X-ray protective glasses

It is well known that X-ray protective glasses can reduce the eye lens exposure to physicians. Problems based on this survey show that the availability of X-ray protective glasses and use of the X-ray protective glasses differs greatly from angiography room to X-ray fluoroscopy room.

Angiography rooms have more protective glasses and a higher percentage of physicians wearing X-ray protective glasses. Clearly, physicians who perform procedures in angiography rooms have a higher awareness of exposure protection. This may be because many academic societies provide information on radiation protection during endovascular treatment. Many educational lectures on radiation protection for physicians are held at related conferences such as the Japanese Circulation Society, the Japanese Association of Cardiovascular Intervention and Therapeutics, the Japan Radiological Society, Japanese Society of Interventional Radiology, and the Japanese Society for Neuroendovascular Therapy.

There were also many presentations on radiation protection by radiological technologists, offering opportunities to share information on radiation protection issues with physicians. From here on, it is desirable for the relevant academic societies involved in medical treatment using X-ray fluoroscopy rooms to publish guidelines on radiation exposure pro-

cedures and issues. Many of the reasons for not wearing X-ray protective glasses are related to the performance with X-ray protective glasses, such as difficulties with seeing the screen during procedures, inconvenience of wearing overglasses, fogging of X-ray protective glasses, not feeling of the necessities for X-ray protective glasses, heavy X-ray protective glasses, and distortion of vision due to wearing X-ray protective glasses. These are in agreement with the opinion of physicians [8] reported in the Kunugita Document 2 of the 5th Study Group on Lens Exposure, and the development of X-ray protective glasses that are lightweight, have good visibility, and do not fog up is desirable.

3-4 【Radiation exposure management arrangements at medical institutions】

The Kunugita Document 4 of the 3rd Study Group on Lens Exposure stated that administrative staff of hospitals need to establish occupational health management arrangements where health managers and industrial physicians play central roles to promote occupational health measures. The document also reported that it is necessary to manage the workplace environment, workers, and their health comprehensively with a proper understanding of occupational health activities through occupational health education [9]. It is reported that radiation protection is effectively managed by an occupational health and safety management system with clear control methods to achieve the goals. To introduce such occupational health and safety management arrangements, every medical institution needs to have a committee to control radiation exposure. In this survey, only 68% of the medical institutions had established a committee to control radiation exposure. It is recommended that every medical institution should introduce radiation exposure control system for radiation workers by utilizing such management arrangements. In 2020, the Ministry of Health, Labour and Welfare started a project to support the introduction of an occupational health and safety management arrangement for radiation exposure as their commissioned project. We expect the government to provide continual support in the future.

4. Conclusions

The findings of this survey showed that there are many physicians who do not accurately measure the radiation exposures to their eye lens and there are also many facilities with inadequate protection equipment for physicians to protect against radiation exposure. To improve the radiation exposure control for radiation workers, it is recommended that occupational health and safety management arrangements should be introduced and that hospitals need to comprehensively manage radiation exposure for radiation workers. Hospital administrators, medical radiation safety managers, industrial physicians, clinical physicians, nurses, and radiological technologists must work as a team to protect the health of radiation workers. In the hospitals that have difficulties in ensuring the proper use of personal dosimeters and X-ray shielding plates, it is important for radiological technologists to take the initiative to improve the workplace environment.

5. Conflicts of interest

There are no conflicts of interest to be disclosed in relation to this study.

Acknowledgements

We would like to express our sincere gratitude to the members of the Japanese Society of Radiation Public Safety and the radiological technologists of each Red Cross hospital who cooperated with the questionnaire survey of this research during their busy schedules.

Reference literature

1) The 2nd Study Group on the Revision of the Exposure Limits for the Lens of the Eye Submitted Material 3. (Accessed 2020.8.1).
https://www.mhlw.go.jp/content/11201000/000477102.pdf
2) The 2nd Study Group on the Revision of Exposure Limits for the Lens of the Eye Submitted Material 5. (Accessed 2020.8.1)
https://www.mhlw.go.jp/content/11201000/000477104.pdf
3) The 6th Study Group on the Revision of Exposure Limits for the Lens of the Eye Submitted material 4. (Accessed 2020.8.1)
https://www.mhlw.go.jp/content/11201000/000534350.pdf
4) Yasuhiro Meguro, Hiroshi Watanabe, et al.: Necessity of a revised ministerial ordinance guide for medical institutions and local government agencies. Nippon Journal of Japanese Games, vol.67, no.817, 2020.
http://www.jart.jp/activity/ib0rgt0000006kex-att/2020-11_paper2.pdf
5) Japan Angiography and Intervention Radiological Technologist Accreditation Organization: [Source] Report on the reference dose of the device in FY2020. (Accessed 2021.4.11)
http://ivr-rt.kenkyuukai.jp/special/?id=18190
6) Japan Cardiovascular Society: 2021 Revised Guidelines for Radiation Exposure in Cardiovascular Practice. (Accessed 2021.4.11)
https://www.j-circ.or.jp/cms/wp-content/uploads/2021/03/JCS2021_Kozuma.pdf
7) The 2nd Study Group on Revision of Exposure Limits for the Lens of the Eye Submitted Material 7. (Accessed 2020.8.1)
https://www.mhlw.go.jp/content/11201000/000477751.pdf
8) The 5th Study Group on the Revision of Exposure Limits for the Lens of the Eye Submitted Material 2. (Accessed 2020.8.1)
https://www.mhlw.go.jp/content/11201000/000519683.pdf
9) The 3rd Study Group on the Revision of Exposure Limits for the Lens of the Eye Submitted material 4. (Accessed 2020.8.1)
https://www.mhlw.go.jp/content/11201000/000490657.pdf

Regulations and Requirements for Submissions to the Journal of the Japan Association of Radiological Technologists

Submission Regulations

Revised: April 1, 2013
October 30, 2013
February 20, 2016
April 20, 2019
October 3, 2020
July 9, 2022
December 3, 2022

Objective

Article 1. These regulations are based on the operations defined in Article 4 of the articles on the incorporation of the Japan Association of Radiological Technologists (hereafter "the Association"). They stipulate the criteria for submissions to the Journal and informational magazines published by the Association (hereafter "the Journal, etc.").

Eligibility

Article 2.

2-1. Only members of this association are allowed to submit articles to the association's journal, etc.

2-2. However, the following requirements must be met in order to submit articles:

(1) Students of radiologic technology schools who have a member of this association as a co-author.

(2) Individuals with a foreign nationality who hold a radiologic technologist license.

(3) Non-members other than the above may submit articles by paying half of the association membership fee per article as a submission fee.

2-3. The submission fee stated in the preceding paragraph 3 will not be refunded regardless of whether the article is accepted or not.

2-4. Co-authors do not need to pay the submission fee.

Copyright

Article 3. The copyright of the published manuscript is based on rules regarding the management of the works of the Society.

Obligations

Article 4.

4-1. The topic of submitted manuscripts must belong to a relevant domain to technologies for prevention, diagnosis, and treatment related to radiation therapy, and manuscripts must be unpublished.

4-2. Submitted papers, whether for fundamental or applied research, must sufficiently consider bioethics, and authors must bear the ultimate responsibility for their content.

4-3. Fabrication, forgery, plagiarism, violation of the law, and other forms of wrongdoing are not allowed in submissions.

4-4. If the author has already reported similar content to that of the published manuscript or submitted it to another journal, the author is required to explain the difference from the manuscript in a separate document.

4-5. The author must disclose all information regarding conflicts of interest.

4-6. The author shall be held accountable for any misconduct regarding the content of the publication, and the Society shall not be involved at all.

Submissions

Article 5. The types of accepted submissions are categorized as follows:

(1) Original articles
Highly original research papers with clear objectives and conclusions.

(2) Review articles
Articles systematically summarizing a specific research domain from a particular perspective.

(3) Rapid communications
Reports of original research that must be published rapidly.

(4) Reports
Surveys of significance to the study of radiological technology or reports of interesting and

important cases.

(5) Notes

Articles on the development or evaluation of new equipment, techniques, products, etc.

(6) Technical material

Compilations of survey data or technical aspects, or anything that can serve as a reference for research and technology.

(7) Overview articles

A compilation of technologies, principles, or basic elements with reference to the literature. However, what was explained in the development and use of equipment and software constitutes a technical explanation.

(8) Miscellaneous

Other items approved by the editorial committee for publication, such as lecture transcripts, courses published as journal articles, and newspaper/magazine articles that were not published in Issues 1–7.

How to submit

Article 6.

6-1. Use the online posting system.

6-2. The author shall save the duplicate data of the submitted manuscript until the publication decision.

Formatting

Article 7. The explanation of the manuscript shall be provided according to the submission procedure specified separately.

Reception of submissions

Article 8. The reception date shall be the date on which the editorial board has determined to comply with this regulation.

Review

Article 9.

9-1. Received manuscripts will be reviewed carefully and impartially by peer-reviewers selected by the editorial committee.

9-2. Peer reviews are limited to two times. However, in the case of Article 5, items 7 and 8, in principle, peer review is not performed.

9-3. The acceptance or rejection of the manuscript will be decided by the editorial committee in consideration of the opinions of the reviewers, and the date will be the final acceptance date.

Corrections

Article 10.

10-1. In principle, the author must proofread the manuscript up to twice and return it by the designated date. If the deadline is breached, the school will be completed with the proofreading of the editorial board.

10-2. The correction of words and plates that were not included in the manuscript is not allowed.

Printing

Article 11.

11-1. 20 copies of the papers published in the Journal, etc., will be presented to their authors as an offprint.

11-2. The authors must bear the expenses of any additional offprints. If additional offprints are required, they must be requested by the time corrections are submitted.

Revision or repeal of regulations

Article 12.

12-1. This regulation will come into effect on April 1, 2012.

12-2. This regulation will come into effect on April 1, 2016.

12-3. This regulation will come into effect on April 20, 2019.

12-4. This regulation will come into effect on October 3, 2020.

12-5. This regulation will come into effect on July 9, 2022.

12-6. This regulation will come into effect on December 3, 2022.

Requirements for Submissions to the Journal of the Japan Association of Radiological Technologists

Revised: February 20, 2016
April 20, 2019
October 3, 2020

The formatting requirements for manuscripts specified in Article 7 of the submission regulations of the Journal of the Japan Association of Radiological Technologists are as follows:

1. How to write original articles, reviews, breaking news, reports, notes, materials, and explanations.

1) Title and abstract

Enter the following items in the online posting system.

①Enter the author's name, facility name, affiliation, occupation, and contact information, and select the specialized field.

②Select the type of post.

③Enter the title and co-author information in Japanese and English. Co-authors are limited to members of the Society. However, this does not apply if the co-author is not a radiological technologist.

④Summarize the abstract in Japanese and English within 300 characters (words).

⑤Enter the keywords in English. Keywords should be in noun forms and should be limited to five.

2) Text and figures/tables

For the text and figures/tables, create and post both a separate file and a file containing figures and tables within the text.

①The manuscript should be written in Japanese or English.

Create the manuscript using Word with a paper size set to the A4 size. The type and size of the fonts should be 12 points for both Japanese and English fonts, Mincho font, and Times. The line spacing should be 18 points. Leave a margin of 2 cm or more on the top, bottom, left, and right.

②The specified number of pages and excess page costs of the manuscript are as shown in the following table.

Type of submission	Number of pages (as published)	Fee for additional pages
Original articles	8	¥10,000 per page
Review articles	8	
Rapid communications	3	
Reports	3	
Notes	8	
Technical material	8	
Overview articles	8	
Technical overview articles	4–6	None
Miscellaneous	2 (strictly enforced)	

③As a general rule, academic terms should conform to Cabinet Notification No. 2 and JIS.

④The unit of quantity is the International System of Units (SI).

⑤Indicate the insertion position of the figure/table in red in the text created as a separate file from the figure/table.

⑥The figures and tables created as separate files from the main text are of higher resolution and can be subjected to secondary processing in production.

⑦For academic treatises, write the title and characters in the table in English.

⑧When reprinting figures/tables, specify the source and obtain permission.

⑨Attach the explanation of the figures and tables in Japanese in a separate file.

3) References

References should be listed in the order in which they appear, with the numbers in parentheses at the end of the referenced text.

The notation format is as follows.

①For magazines

Author names: Title (article title) Magazine name (abbreviation), volume, first-last page, year of publication.

②For a book

Author names: Book title, First-last page, publisher, year of publication.

③If there are two or more authors, enter only the first author and enter "other" and "et al."

4) Trademark name
If a trademark name is required, write the trademark name in both parentheses after the common name and add ®.

2. Submission of copyright transfer agreement
(1) The first author and co-authors must agree with the contents of the copyright transfer agreement stipulated in the copyright management regulations.
(2) The copyright transfer agreement shall be stipulated by the rules regarding copyright management, and the format specified on the Society's website should be used.
(3) The copyright transfer agreement must be signed by the first author and co-authors, and provided when the manuscript is submitted.

3. About secondary publication
(1) Obtain approval from the editorial departments of both the first and second journals.
(2) The period until the secondary publication should be decided through discussions between the editorial departments of both parties and the author.
(3) Secondary publications of treatises are intended for different types of readerships.
(4) The secondary publication of a treatise should faithfully reflect the content of the first treatise.
(5) Specify the source of the original treatise.
(6) Specify in the title that it is a secondary publication.

4. About technical commentary requested by the editorial board.
The composition of the text is as follows (1) to (9).
(1) Abstract (100-150 words in Japanese and English)
(2) Keywords (3 words)
(3) Introduction:
(4) Purpose of explanation (overview)
(5) Main paper
(6) Comparison and consideration with previous research (development technology)
(7) Clinical usefulness
(8) Conclusion
(9) References

Journal of JART
-English edition 2023-

June 16, 2023

Issuer: Ueda Katsuhiko
Publisher: The Japan Association of Radiological Technologists
22F Mita Kokusai Building. 1-4-28,
Mita, Minato-ku, Tokyo. 108-0073
TEL: +81-3-4226-2211　FAX: +81-50-3153-1519
https://www.jart.jp

・Published by The Japan Association of Radiological Technologists

The Japan Association of Radiological Technologists
https://www.jart.jp